ESA CONTRACT REPORT

Contract Report to the European Space Agency

The technical support for global validation of ERS wind and wave products at ECMWF (July 2008 – July 2011)

Authors: Saleh Abdalla,
Giovanna De Chiara and
Hans Hersbach

Final report for ESA contract 22025 CCN1

European Centre for Medium-Range Weather Forecasts
Europäisches Zentrum für mittelfristige Wettervorhersage
Centre européen pour les prévisions météorologiques à moyen terme

ECMWF

Series: ECMWF - ESA Contract Report

A full list of ECMWF Publications can be found on our web site under:

http://www.ecmwf.int/publications/

European Centre for Medium Range Weather Forecasts
Shinfield Park, Reading, RG2 9AX, England

Contract Report to the European Space Agency

The technical support for global validation of ERS wind and wave products at ECMWF (July 2008 – July 2011)

Authors: Saleh Abdalla, Giovanna De Chiara and Hans Hersbach

Final report for ESA contract 22025 CCN1

European Centre for Medium-Range Weather Forecasts
Shinfield Park, Reading, Berkshire, UK

December 2011
[Revised March 2012]

TABLE OF CONTENTS

Abbreviations

3D ..... 3-day repeat cycle
AMI ..... Active Microwave Instrument
AN ..... ECMWF ANalysis
AOCS ..... Attitude and Orbit Control System
ASAR ..... Advanced Synthetic Aperture Radar
ASCAT ..... Advanced SCATterometer
ASCII ..... American Standard Code for Information Interchange
ASPS ..... Advanced Scatterometer Processing System
BUFR ..... Binary Universal Form for the Representation of meteorological data
CERSAT ..... French ERS Processing and Archiving Facility (Centre ERS d'Archivage et de Traitement)
CMEDS ..... Canadian Marine Environmental Data Service
CMOD ..... C-band Geophysical MODel function
DES ..... Digital Earth Sensor
DNMI ..... (Det) Norwegian Meteorological Institute
EBM ..... Extra Back-up Mode
ECMWF ..... European Centre for Medium-range Weather Forecasts
ECWAM ..... ECMWF WAve Model (an enhanced version of WAM model)
ENVISAT ..... ENVIronmental SATellite
ERA-40 ..... ECMWF 40-Year Reanalysis
ERS ..... European Remote sensing Satellite
ESA ..... European Space Agency
ESACA ..... ERS Scatterometer Attitude Corrected Algorithm
ESOC ..... European Space Operations Centre
ESTEC ..... European Space research and TEchnology Centre
ESRIN ..... European Space Research INstitute
EUMETSAT ..... EUropean organization for the exploration of METeorological SATellites
FD ..... Fast Delivery product
FEEDBACK ..... data to which information on usage in the ECMWF assimilation system has been added
FG ..... ECMWF First Guess with a time resolution of 3 hours
FGAT ..... First Guess at Appropriate Time
GMF ..... scatterometer Geophysical Model Function
GTS ..... Global Telecommunication System
HRES ..... High RESolution
IDL ..... Interactive Data Language
IFREMER ..... French Research Institute for Exploitation of the Sea (Institut français de recherche pour l'exploitation de la mer)
IFS ..... ECMWF Integrated analysis and Forecast System
JPL ..... Jet Propulsion Laboratory
KNMI ..... Koninklijk Nederlands Meteorologisch Instituut
LRDPF ..... Low Rate Data Processing Facility

LBR ..... Low Bit Rate
MPI ..... Max-Planck-Institut for meteorology, Hamburg
NESDIS ..... National Environmental Satellite Data and Information Service
NDBC ..... U.S. National Data Buoy Center
NH ..... Northern Hemisphere
NRES ..... Nominal RESolution
NRT ..... Near-Real Time
NSCAT ..... NASA (National Aeronautics and Space Agency) Scatterometter
OPR ..... (ERS Radar Altimeter) Ocean PRoduct
QC ..... Quality Control
QSCAT-1 ..... QuikSCAT scatterometer geophysical model function
RA ..... Radar Altimeter
RA-2 ..... (ENVISAT) Radar Altimeter-2
RMSE ..... Root-Mean Square Error
SAR ..... Synthetic Aperture Radar
SH ..... Southern Hemisphere
SI ..... Scatter Index
STDV ..... STandard DeViation (of the Difference)
SWH ..... Significant Wave Height
UKMO ..... UK Met Office
URA ..... User FD Radar Altimeter product
UTC ..... Coordinated Universal Time
UWA ..... User FD SAR WAve product
UWI ..... User FD scatterometer WInd product
WAM ..... third-generation ocean-WAve Model
WVC ..... scatterometer Wind-Vector Cell (node)
WMO ..... World Meteorological Organization
YCM ..... Yaw Control Monitoring
ZGM ..... Zero-Gyro Mode

Abstract

Contracted by ESA/ESRIN, ECMWF is involved in the global validation and long-term performance monitoring of the wind and wave Fast Delivery products that are retrieved from the Radar Altimeter (RA) and the Active Microwave Instrument (AMI), on-board the ERS spacecraft. Their geophysical content is compared with corresponding parameters from the ECMWF atmospheric and wave model as well as in-situ observations (when possible). Also, tests on internal data consistency are performed.

An on-board failure in January 2001 degraded attitude control of ERS-2. It had a negative, though acceptable, effect on the quality of the RA and SAR related products; however, a detrimental effect on scatterometer winds. The problems in attitude control were gradually resolved, and since August 2003 the quality of all products is nominal. After 21 June 2003, ERS-2 lost its global coverage permanently due to the failure of both on-board tape recorders. However, the remaining coverage (North Atlantic and western coasts of North America and at a later stage the Southern Ocean, the coasts of East Asia, the north-eastern parts of the Indian Ocean and the southern coasts of Africa) provides valuable data for assimilation in atmospheric models.

Since the beginning of the mission ERS-2 has been operated in a 35-day repeat cycle. To meet the requirements of the cryosphere community, at the end of February 2011 the satellite was moved into a 3-day repeat cycle to reproduce the ERS-1 Ice Phases of 1992 and 1994. In July 2011 the satellite has been permanently switched off.

An overview evaluation of the wind and wave products from the entire ERS mission was carried out in previous reports (see Abdalla and Hersbach, 2006, 2007 and 2008) and here. The products involved are the fast delivery AMI scatterometer wind and SAR wave mode spectra and the off-line ocean product (OPR) wind and wave data from both ERS-1 and ERS-2 missions.

1. Introduction

The ERS mission has been a great opportunity for the meteorological and ocean-wave communities. The wind and wave products from ERS-1/2 provide an invaluable data set over more than 20 years. They form some kind of benchmarks against which model products can be validated. In addition, they are assimilated in the models to improve the predictions. On the other hand, consistent model products, especially first-guess products, can be used to validate and monitor the performance of the satellite products.

The European Centre for Medium-Range Weather Forecasts (ECMWF) has been collaborating with the European Space Agency (ESA) since the beginning of the ERS-1 mission in performing the global validation and long-term performance monitoring of the wind and wave products. These products are retrieved from three instruments, defining three Fast Delivery (FD) products that are received at ECMWF in BUFR format. Significant wave height and surface wind speed (URA product) are obtained from the Radar Altimeter (RA). Ocean image spectra (UWA product) are from the Synthetic Aperture Radar (SAR). Surface wind speed and direction (UWI product), finally, are retrieved from the Wind scatterometer. In-house developed monitoring tools are used for the comparison of these products with corresponding parameters from the ECMWF atmospheric (IFS) and wave (ECWAM) models (IFS Documentation, 2004). Whenever possible, these tools include a comparison with in-situ measurements. In addition, tests are performed on the internal consistency of the underlying observed quantities measured by the three instruments.

Findings from the monitoring activities described above have been summarized in monthly or cyclic (depending on the product) data quality and validation reports. These reports were regularly sent to ESRIN. Besides giving an overview on instrument performance and scientific interpretation, these reports also included recommendations to ESA for refinements of calibrations, further algorithm development and model tuning. Such recommendations were based on a long-term analysis of the relevant parameters.

In addition to these monitoring activities, dedicated studies on data quality and related scientific research have been carried out. These embrace, among others, collocation studies, algorithm development and the incorporation of ERS wind and wave data in the operational ECMWF assimilation system. As a result, ERS altimeter wave heights have been assimilated in the ECMWF wave model since 15 August 1993 (Janssen et al., 1997). It was replaced by ENVISAT Radar Altimeter-2 (RA-2) on 22 October 2003. Scatterometer winds were introduced in the atmospheric variational assimilation system on 30 January 1996 (for a description of its impact, see Isaksen and Janssen 2004). It was re-introduced on 8 March 2004 (Hersbach et al., 2004), after the suspension in January 2001. The assimilation of SAR wave mode spectra in the ECMWF wave model, on the other hand, was realised on 13 January 2003. ERS-2 SAR assimilation was replaced by ENVISAT Advanced Synthetic Aperture Radar (ASAR) Level 1b wave mode spectra on 1 February 2006. On 5 July 2011 the ERS-2 satellite was permanently switched off which meant the end of assimilation of scatterometer winds.

A review of the quality of the various products from both ERS-1 and ERS-2 satellites was already performed for the previous contracts in 2006, 2007 and 2008. Those products are the fast delivery (FD) scatterometer wind (UWI) product, FD SAR Wave Mode (UWA) product and both FD (URA) and the off-line OPR (Ocean Product) altimeter wind and wave products. The results of this exercise can be found in Abdalla and Hersbach (2006, 2007 and 2008). The ECMWF long-term reanalyses ERA-40 was used in that exercise. Here, the same exercise was repeated using better ECMWF reanalysis which is called ERA-Interim.

This document presents the final report of the present contract that covers also the last period of ERS-2 life. It provides a focus on the operational performance of the wind and wave products over the last few years of ERS-2 activities including the orbit change in February/March 2011. Furthermore, it also includes an overview assessment of wind and wave products from the ERS mission since the start of the mission.

In Section2, the performance of altimeter FD URA data in the North Atlantic will be considered. An overview of the performance of the SAR significant wave height in the North Atlantic will be presented in Section3, and of UWI wind data in Section4. In Section5, the results of the long-term monitoring of ERS-1/2 wind and wave products against ECMWF ERA-Interim product are presented. Finally, conclusions are formulated in Section 6, and the report ends with a list of ECMWF model changes since November 2000.

2. The Radar Altimeter URA Product

Each URA (User fast delivery Radar Altimeter) product is sampled at 7 km along the satellite ground track. First the altimeter data stream is divided into sequences of 30 individual neighbouring observations. Erroneous and suspicious individual observations are removed and the remaining data in each sequence are averaged to form a representative super-observation, provided that the sequence has at least 20 "good" individual observations. Then, further monitoring is performed with respect to these super-observations, which, for this purpose are collocated with ECMWF model and buoy data. The focus here is on URA backscatter, URA wind speed and URA significant wave height.

2.1. Data Coverage after June 2003

The loss of the global coverage due to the failure of the on-board low-bit rate tape recorders in June 2003 reduced the number of observations received at ECMWF to about 13% of the full coverage data volume as can be seen in Figure 1 which shows the daily rate of total number of the altimeter super-observations processed at ECMWF. The monthly data coverage of URA products for October 2010 can be seen in Figure 2. Apart from the usual coverage of the Northern Atlantic and the eastern parts of the North Pacific, several ground stations at various parts of the globe volunteered to receive and disseminate the product on the *best effort* basis. This led to the availability of the ERS-2 LBR products around Mexico (ground station at Miami), in the eastern parts of the Indian Ocean (ground station at Singapore) and in the Southern Ocean (ground stations at McMurdo and Hobart). The extra coverage around South Africa (ground station at Johannesburg) which was realised in the mid 2008 (see for example Figure 3 of Abdalla and Hersbach, 2008) did not last long. For the URA product, we will focus our attention on the quality of the altimeter products for the current coverage or specifically in the North Atlantic.

Assessment of the long-term quality of the product after the loss of the global coverage cannot be done by comparing it with statistics when there was full coverage. In order to avoid the reprocessing of the product over a rather long period for the exact area under current coverage, the readily available long-term statistics for the closest region is considered for comparison. The region covering the extra-tropical Northern Atlantic (north of latitude 20°N) is used as a common area with almost complete coverage before and after the loss of the global coverage. The 7-day running average of daily number of altimeter super-observations in the North Atlantic since the beginning of year 2000 is shown in Figure 3. It is clear that the current coverage in the North Atlantic is slightly lower than the usual coverage few years ago. The missing coverage is towards the southern edge of the region and in the area just southern of Greenland as can be seen in Figure 2.

2.2. Monitoring of URA Significant Wave Height in the North Atlantic

As usual, the quality of the URA significant wave heights (SWH) is rather stable and good, apart from the well-known ever-lasting overestimation of small SWH values. Figure 4 shows the time history of the 7- and 365-day running averages of the daily bias between the altimeter and the ECMWF operational wave model (ECWAM) SWH in the North Atlantic since the beginning of the year 2000. After excluding the apparent anomalous altimeter behaviour during March-April 2000 and February 2001, it is possible to distinguish a seasonal cycle of bias in Figure 4 with a minimum value taking place around April-May and a maximum value occurring around October-November before the loss of the global coverage. This seasonal cycle became stronger after the loss of the global coverage with the

minimum and maximum values shifted to cover the whole winter and summer, respectively. Although it is difficult to pinpoint the reason for the stronger cycle, later model changes like the unresolved bathymetry treatment introduced on 9 March 2004 and the change of wave model dissipation introduced on 5 April 2005 are possible candidates. Another possible reason could be related to the uncovered areas towards the tropical parts of the North Atlantic (see Figure 2) which usually show lower SWH variability compared to the higher latitudes. The 365-day running average in Figure 4 displays a clear general trend of reduced bias over the years until the beginning of 2008 when it became almost constant. The bias changed sign in mid 2005 indicating that the model wave heights became higher than the altimeter. These changes are mainly due to the model improvements. The bias between the altimeter and the model wave heights did not suffer any abrupt changes after the loss of the global coverage. The change in bias at the beginning of 2010 may be due to the model changes related to the swell damping (September 2009) and the bias correction (November 2009 and March 2010).

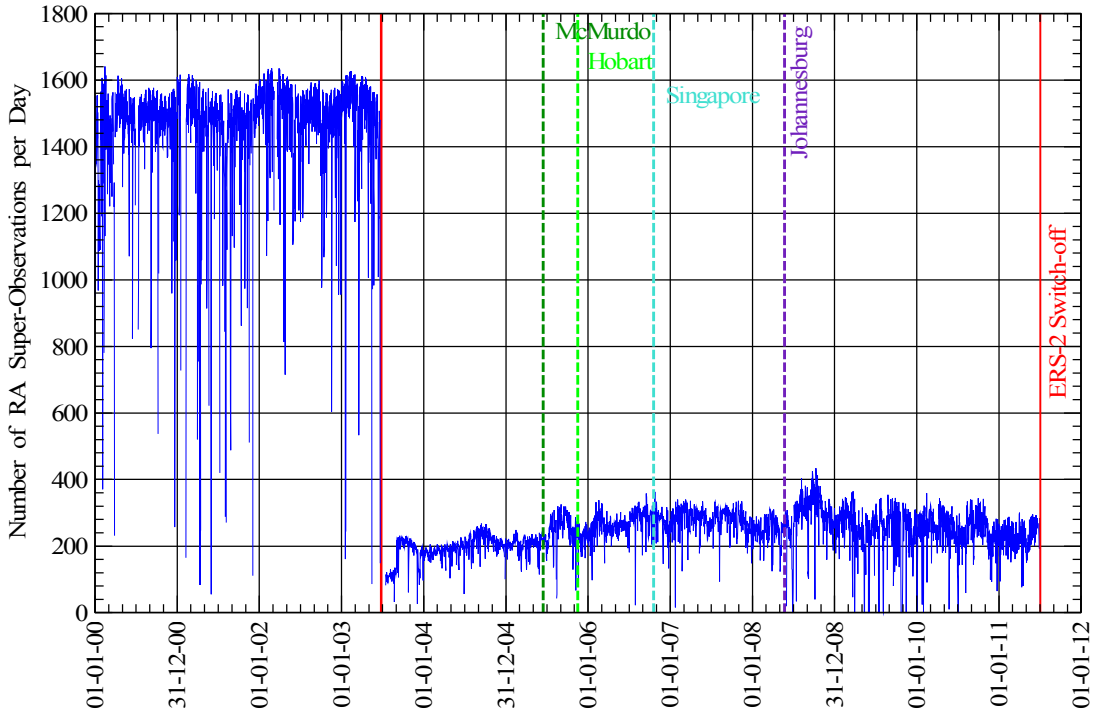

Figure 1: Time history of the total number of ERS-2 altimeter super-observations processed at ECMWF per day since 1 January 2000. Date of loss of global coverage is represented by a red thick vertical line.

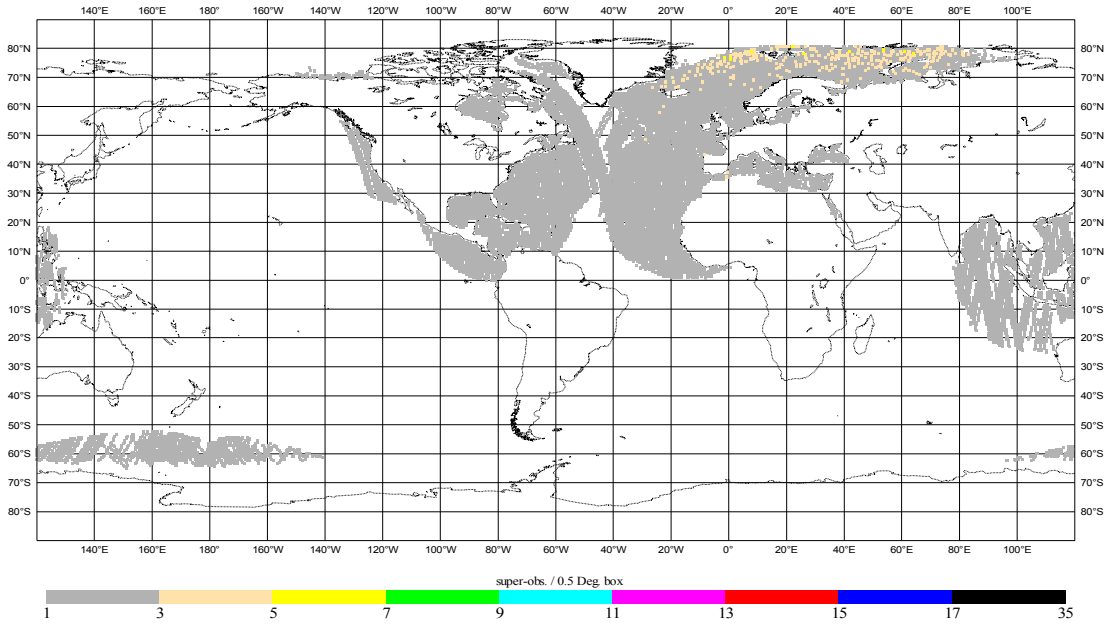

Figure 2: Typical ERS-2 radar altimeter monthly coverage (October 2010) after the loss of global coverage (June 2003) and before the change of orbit (February 2011), i.e. with the 35-day repeat cycle.

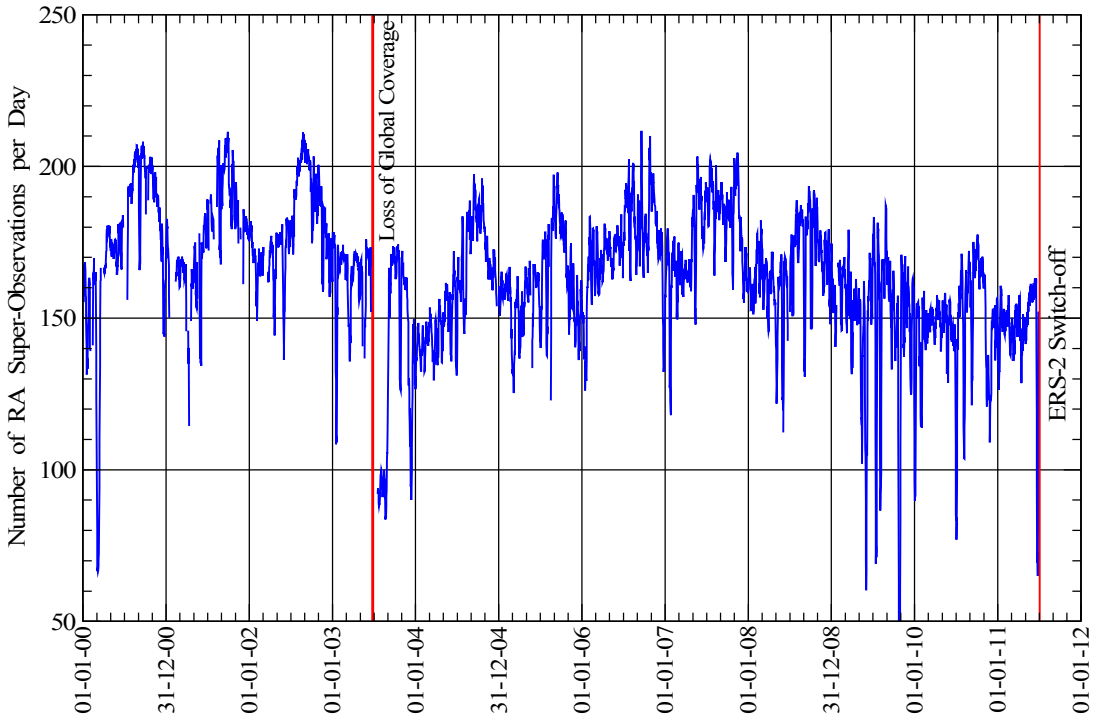

Figure 3: Time history of the 7-day running average of daily number of altimeter super-observations in the North Atlantic since 1 January 2000. Dates of loss of global coverage and switch-off are represented by red thick vertical line.

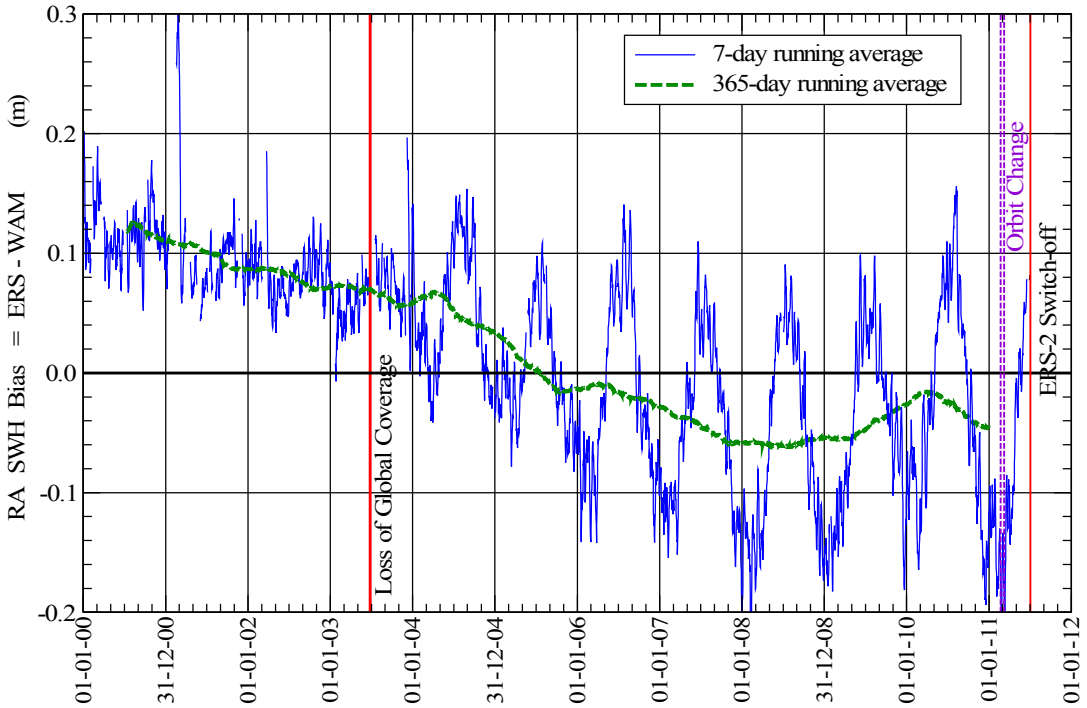

Figure 4: Time history of the 7- and 365-day running averages of daily bias of altimeter SWH with respect to wave model in the North Atlantic since 1 January 2000. The thick dashed line shows the bias trend (365-day running average).

Figure 5 shows the time history of the 7- and 365-day running averages of the daily scatter index (SI), which is defined as the standard deviation of the difference normalised by the mean value, of the altimeter significant wave height with respect to the ECWAM model in the North Atlantic since the beginning of year 2000. Both the seasonal variation (maximum during July-August and minimum during December-January) and the general trend of the reduction in the SI (the 365-day running average) can be seen. Again the seasonal variation seems to be stronger after the loss of global coverage. The higher SI values during July and August 2004 are due to a technical problem that prevented the ENVISAT RA-2 SWH product from being assimilated in the wave model causing a slight degradation in the model predictions. The continuous reduction of scatter index over the years until the beginning of 2008, as can be seen in Figure 5, is due to the model improvements, in particular the revised dissipation formulation in the wave model (April 2005), the high resolution atmospheric model of T799 and the assimilation of Jason-1 altimeter data (February 2006) and the use of model neutral winds to force the wave model. The slight increase of SI in 2010 may be due to the rejection of Jason-1 observations by the wave model assimilation scheme since April 2010 and due to a slight degradation of the small SWH values of EVNISAT RA-2 after the introduction of RA-2 processing chain IPF 6.02L04 in February 2010.

In summary, it is possible to say that the altimeter significant wave height product is as good as it used to be before the loss of the global coverage. Other statistics (not shown) deliver the same message. It is worth mentioning that the ERS-2 altimeter wave height product used to be assimilated in the ECMWF wave model until it was replaced by the corresponding product from ENVISAT on 21 October 2003.

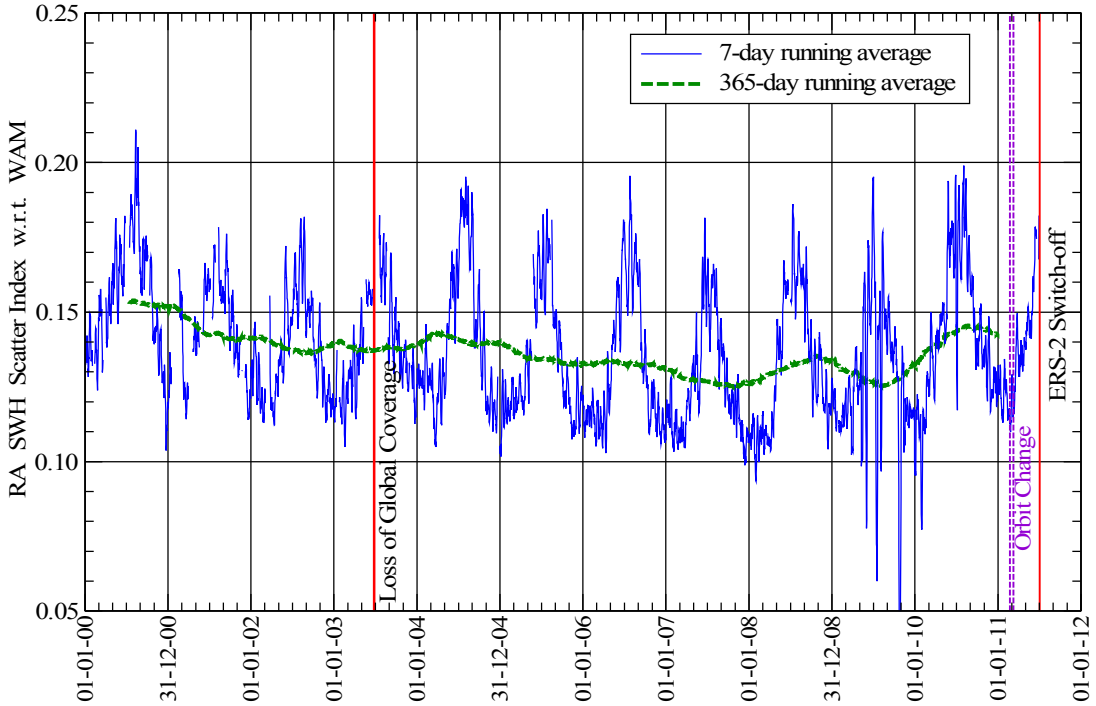

Figure 5: Time history of the 7- and 365-day running averages of daily scatter index of altimeter SWH with respect to the wave model in the North Atlantic since 1 January 2000. The thick dashed line shows the SI trend (365-day running average).

2.3. Monitoring of URA Surface Wind Speed in the North Atlantic

Before the loss of the global coverage, URA wind speed observations were not as good as the wave heights. They suffered several periods of degraded quality, especially after the start of the problems with the platform gyros in early 2000 (e.g. Abdalla and Hersbach, 2007). The "sun blinding effect" is responsible for most of the degradation in the Southern Hemisphere (SH) during the period from mid January to early March each year since year 2000.

Figure 6 shows the time history of the 7- and 365-day running averages of the daily bias of URA surface wind speed with respect to the ECMWF operational atmospheric model in the North Atlantic since 1 January 2000. The wind speed bias in the North Atlantic follows a seasonal cycle with positive bias (maximum) in the Northern Hemispheric (NH) winter and negative (minimum) in the NH summer as can be clearly seen in Figure 6. During the period between late 2000 and early 2005, the bias was fluctuation around zero. The same behaviour continued after the loss of the global coverage. A drop in bias (or increase in the model wind speed) is witnessed in the middle of 2005 when the model convection was changed on 28 June 2005.

On the other hand, Figure 7 shows the time history of the daily SI of surface wind speed with respect to the ECMWF operational atmospheric model in the North Atlantic since 1 January 2000. The SI follows a weak seasonal cycle with low values occurring during the NH winter and vice versa in summer. The exception to this cycle is the period from early January to early March each year since

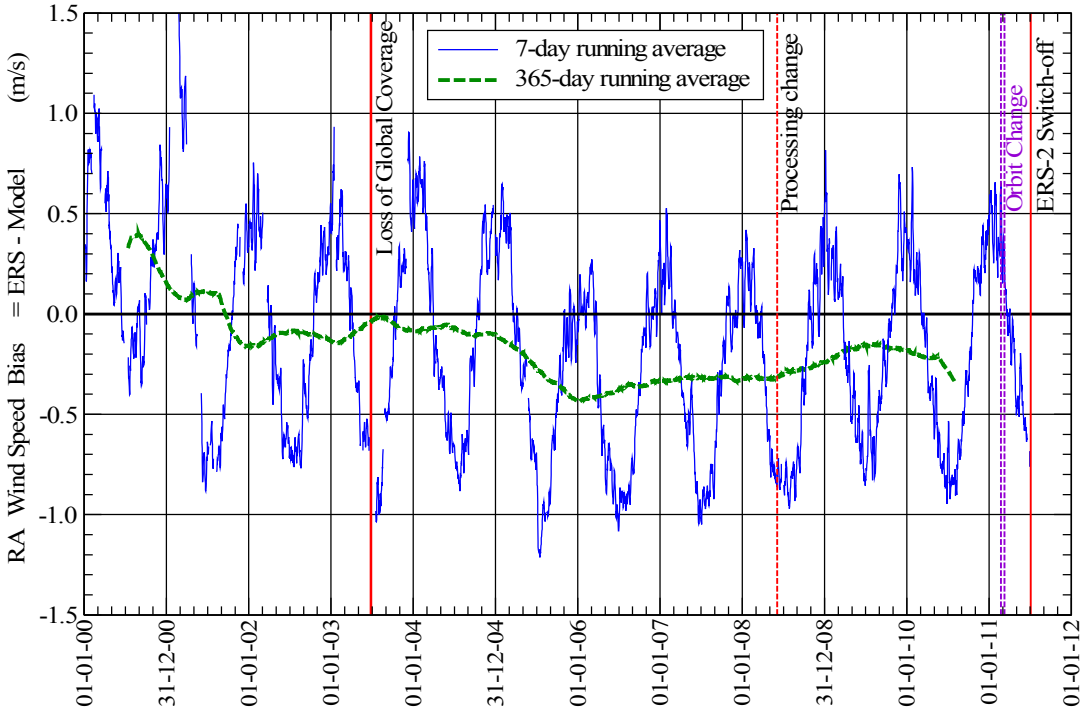

Figure 6: Time history of the 7- and 365-day running averages of daily bias of altimeter surface wind speed with respect to the ECMWF atm. model in the North Atlantic since 1 January 2000. The thick dashed line shows the bias trend (365-day running average).

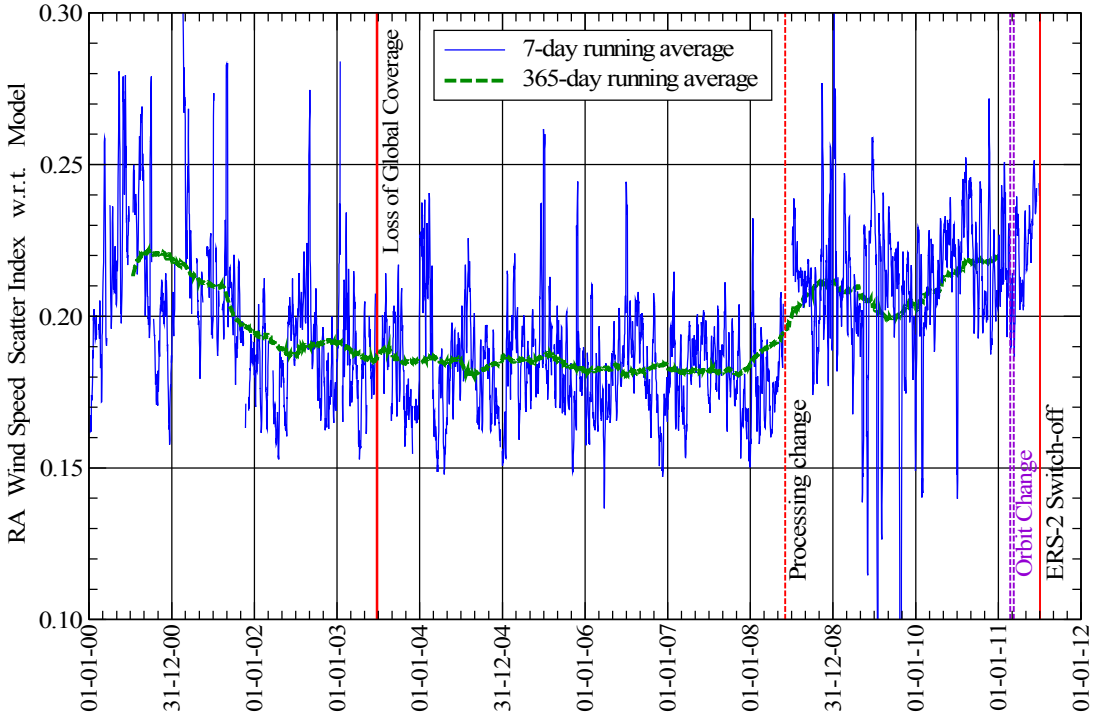

Figure 7: Time history of the 7- and 365-day running averages of daily scatter index of alt. surface wind speed with respect to the ECMWF atm. model in the North Atlantic since 1 January 2000. The thick dashed line shows the SI trend (365-day running average).

2001. This may be due the residual effect of the "sun blinding effect" which usually occur in the SH during the same period. Continuous improvements of the ECMWF operational atmospheric model result in lower wind speed scatter index values between this model and the altimeter. A drop in SI (and bias) in early 2002 can be clearly recognised. This coincides with a model change including the assimilation of QuikSCAT wind speeds. The usual trend of the SI reduction continued after the reduction of ERS-2 coverage. However, a change in the operational pre-processing of URA products at ECMWF by changing the number of 1-Hz observations involved to produce the super-observations (11 is used instead of 30) in June 2008. This caused the SI to increase as can be seen in Figure 7.

2.4. Monitoring of URA Altimeter Backscatter

Altimeter backscatter is the raw observation that is translated into the surface wind speed. Figure 8 displays the long-term monthly global mean backscatter coefficient values since December 1996. Before the loss of the global coverage, the monthly mean value used to be around 11.0 dB. However, the mean values used to increase to more than 11.4 dB for the month of July in years 1997 to 1999. Those peaks disappeared in year 2000 and later. Instead, the mean backscatter coefficient started to be rather low in the month of February (or March) each year from 2000. This is a direct result from the "sun blinding effect".

After the loss of the global coverage, the monthly mean started to have a strong seasonal cycle varies between 10.4 and 12.2 dB. This cycle has a peak during the NH summer (July-August) and a trough during winter (December-January). This is an expected behaviour in the NH. After the extension of the ERS-2 coverage by including more ground stations especially in the SH, the amplitude of the seasonal cycle of mean backscatter coefficient started to get smaller. The impact of including McMurdo, Hobart, Singapore, Johannesburg (even for a limited time) and Miami ground stations cannot be missed in Figure 8.

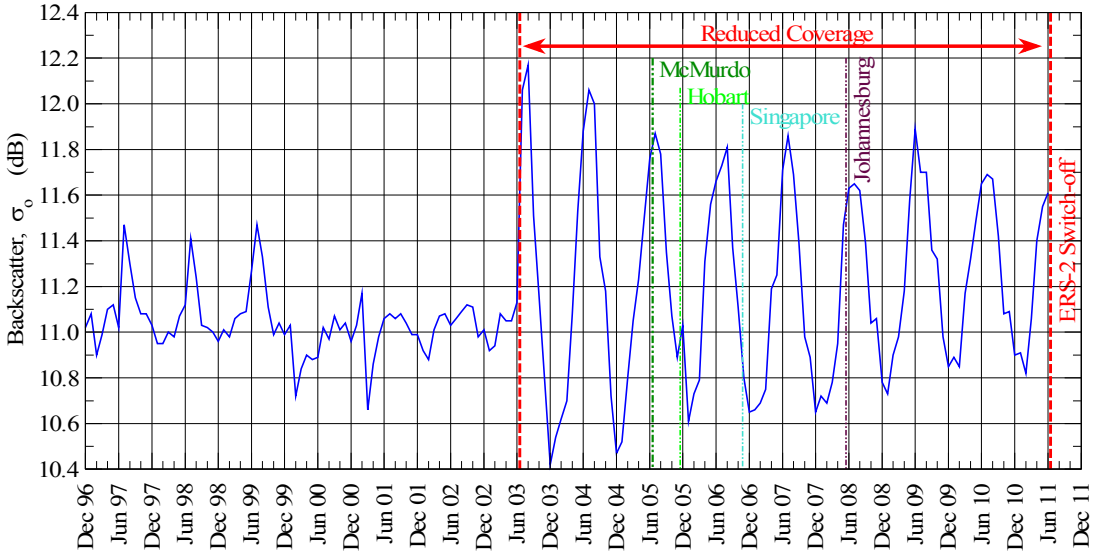

Figure 8: Time history of the monthly global mean of ERS-2 altimeter backscatter coefficient after QC since December 1996.

2.5. Recent Events: ERS-2 Orbit Change and Switch-off

ERS-2 mission was configured as a 35-day repeat orbit since the start of the mission. On 22 February 2011, manoeuvres started to change this orbit. The final orbit configuration of 3-day repeat cycle was reached on 10 March 2011. The typical monthly data coverage after the change of orbit can be seen in Figure 9 for June 2011. As expected, the almost continuous coverage with few visits per box (35-repeat cycle in Figure 2) is replaced with discrete tracks with more visits per grid box (3-day repeat cycle in Figure 9). There was no impact of the orbit change on the URA wind speed and SWH products. For example, the scatter plots comparing the altimeter wind speed against the ECMWF model product (as shown in Figure 10) and against buoy wind speed (as shown in Figure 11) for the month of April 2011, which was the first full calendar month after the change of orbit, do not show any anomaly. The same can be said about the SWH comparisons in Figure 12 for altimeter-model and in Figure 13 for altimeter-buoy.

Finally, ERS-2 was switched-off on 5 July 2011 after more than 16 years in orbit. The satellite was later put in a lower orbit of about 573 km before it was "neutralized" by disconnecting the batteries and depleting the fuel) on 5 September 2011.

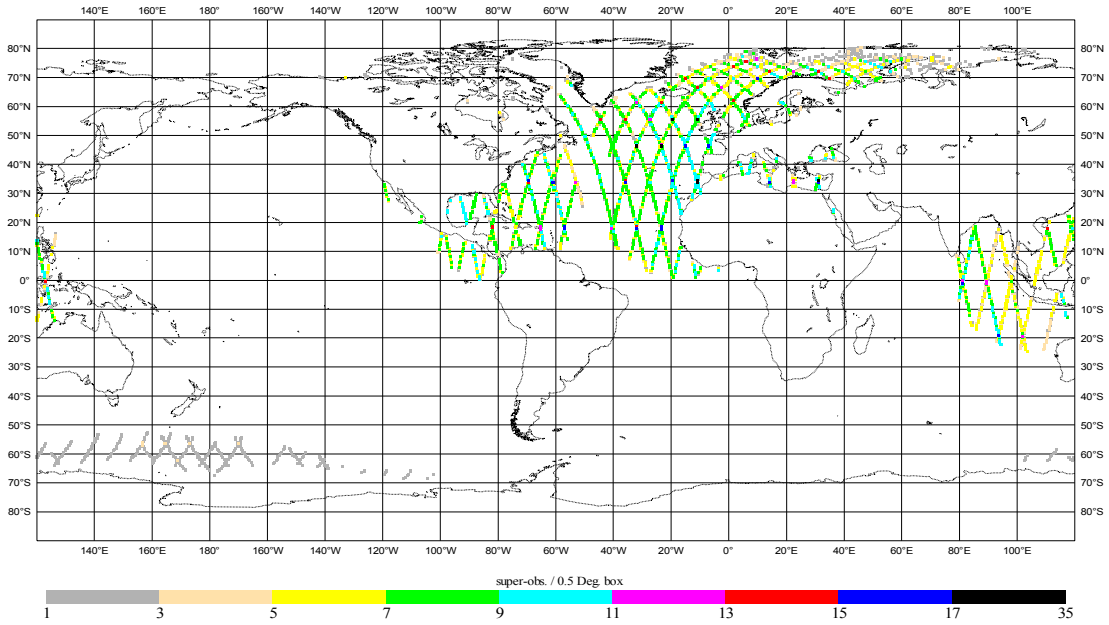

Figure 9: Typical ERS-2 radar altimeter monthly coverage (June 2011) after the change of orbit (February 2011) to the 3-day repeat cycle.

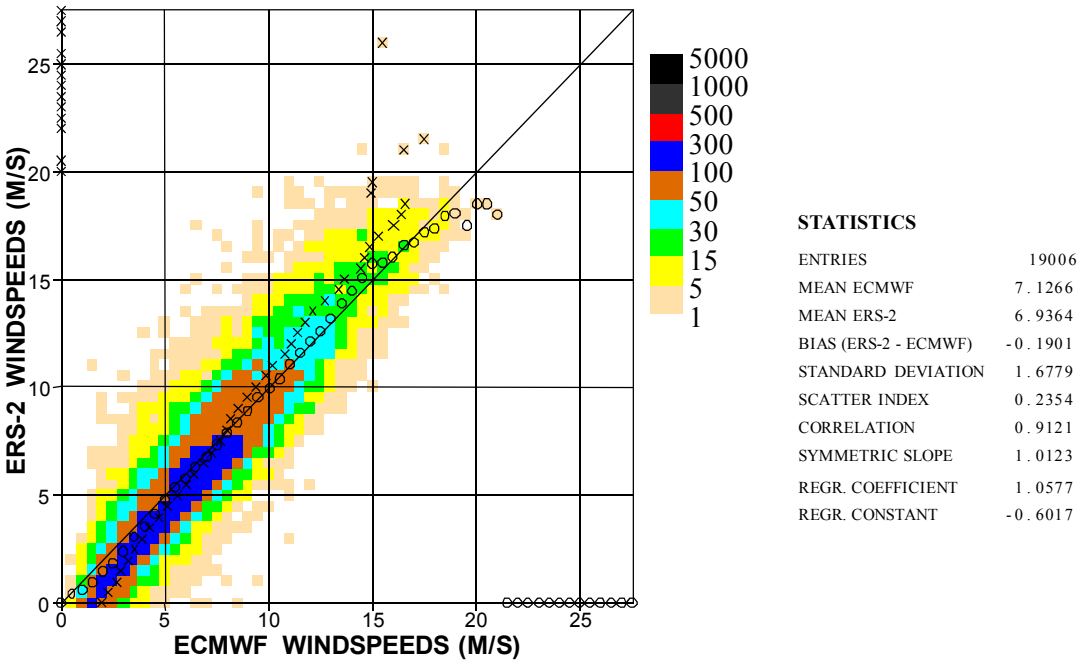

Figure 10: Comparison between ERS-2 altimeter and analyzed ECMWF model wind speed values for the month of April 2011.

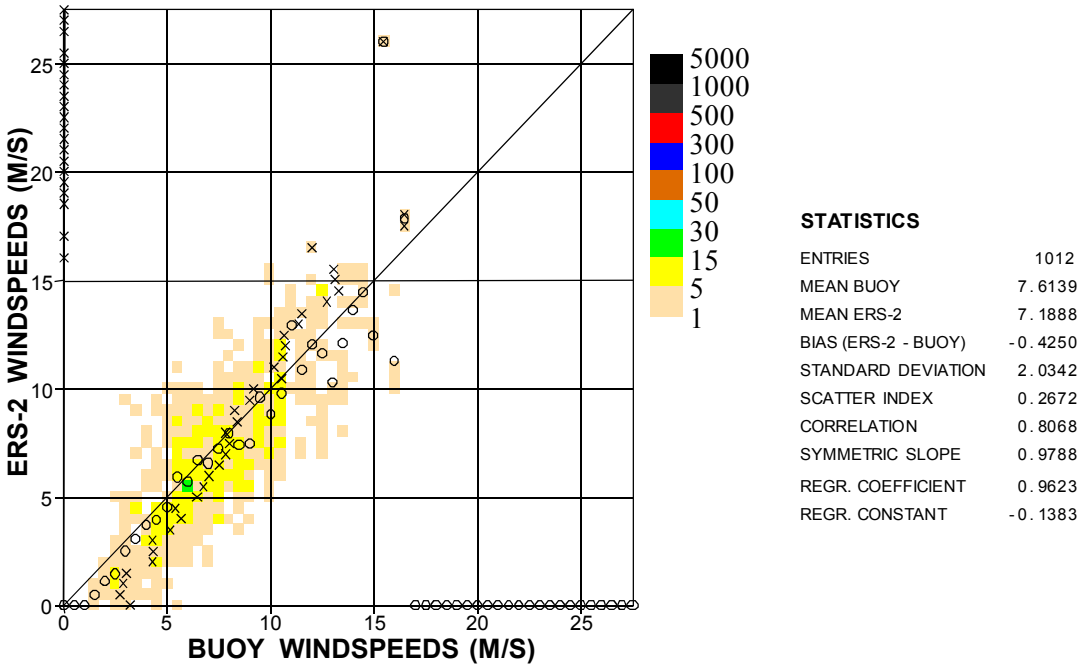

Figure 11: Comparison between ERS-2 altimeter and buoy wind speed values for the month of April 2011.

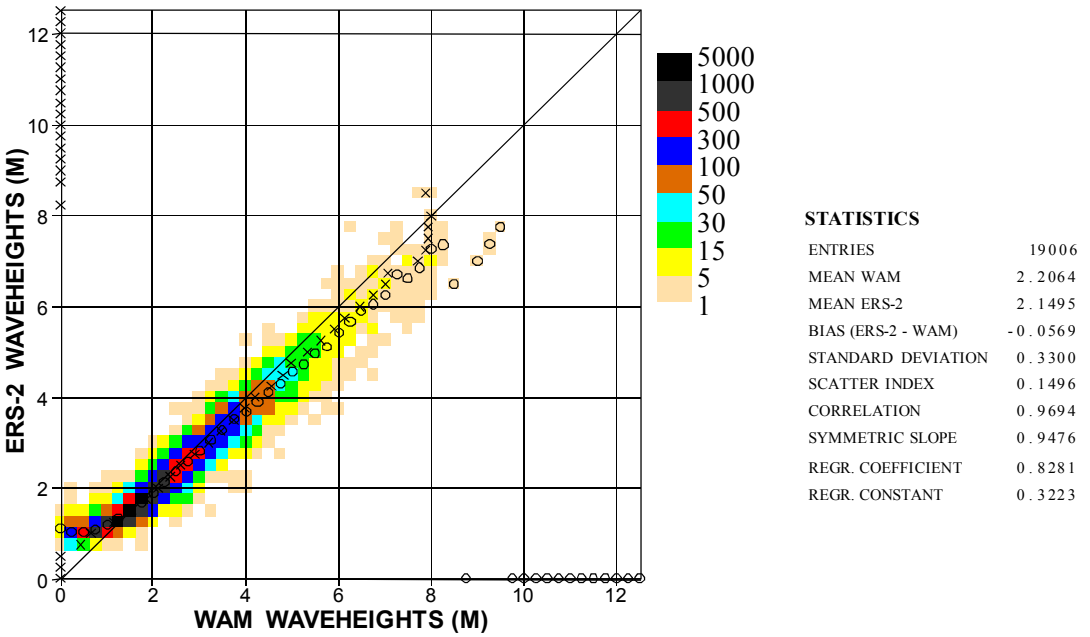

Figure 12: Comparison between ERS-2 Altimeter and FG wave model significant wave height values for the month of April 2011.

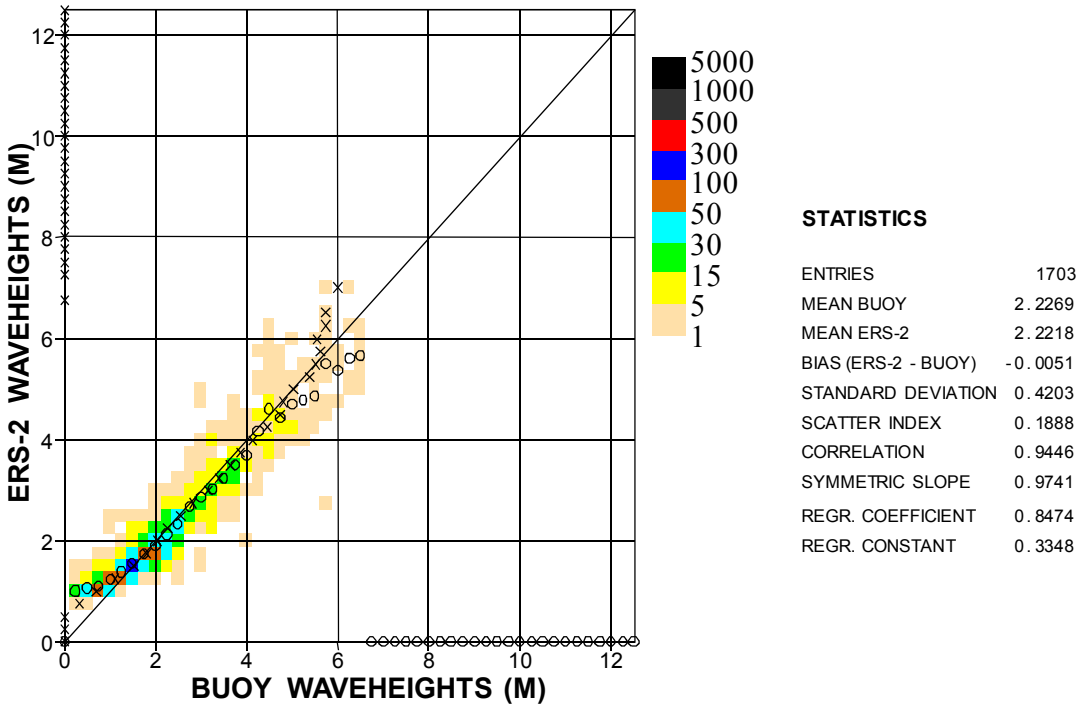

Figure 13: Comparison between ERS-2 Altimeter and buoy significant wave height values for the month of April 2011.

3. The Synthetic Aperture Radar (SAR) UWA product

For the UWA product, SAR records are provided at 200 km intervals, each containing an image spectrum for an area of about 5 km x 5 km. Records for which all parameters are within an acceptable range are collocated with ECWAM model spectra. The SAR image spectra are then transformed into corresponding ocean-wave spectra using an iterative inversion scheme based on the forward closed integral transformation (MPI scheme, Hasselmann and Hasselmann, 1991). For this procedure the collocated ECWAM model spectra serve as a first-guess. Depending on the outcome of the inversion process, further QC is applied. Long-term monitoring is based on integrated parameters such as the significant wave height, mean wave period and mean directional spread. Monitoring of the one-dimensional energy spectrum is performed as well.

3.1. ERS-2 SAR Data Coverage after June 2003

The loss of the global coverage due to the failure of the on-board low-bit rate tape recorders in June 2003 reduced the number of observations received at ECMWF to about 13% of the full coverage data volume as can be seen in Figure 14 which shows the global weekly number of SAR wave mode spectra processed at ECMWF. The coverage of ERS-2 SAR after the loss of the global coverage can be seen in Figure 15. Although, it is not as dense as the altimeter coverage (Figure 2), the coverage extends to almost the same areas.

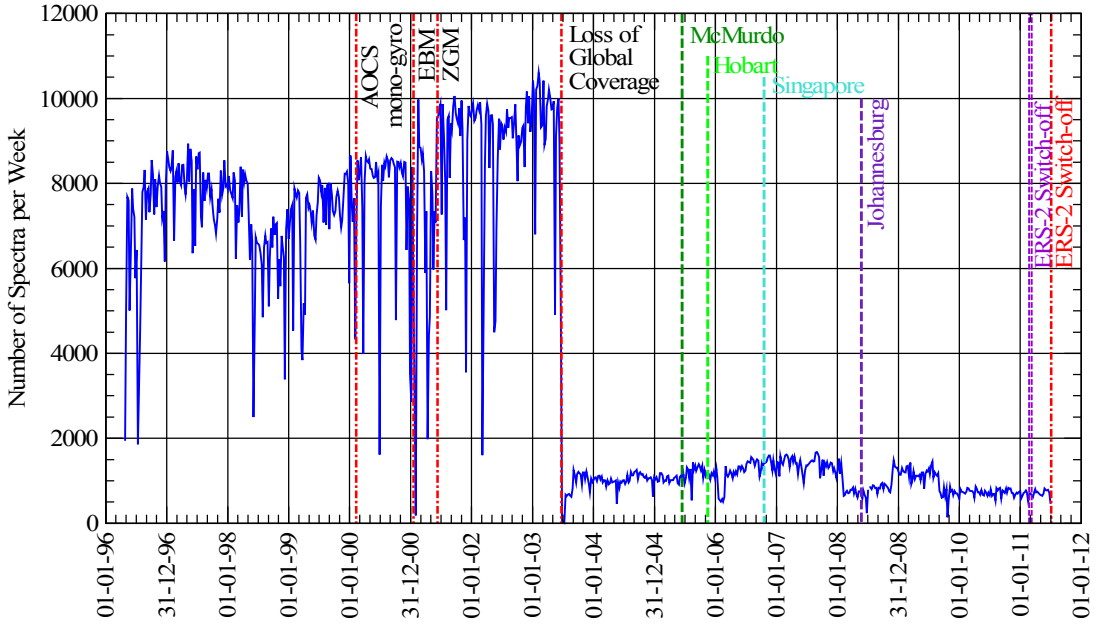

Figure 14: Time history of the global weekly number of ERS-2 UWA spectra during the period since April 1996. Important ERS-2 gyroscope related events are displayed.

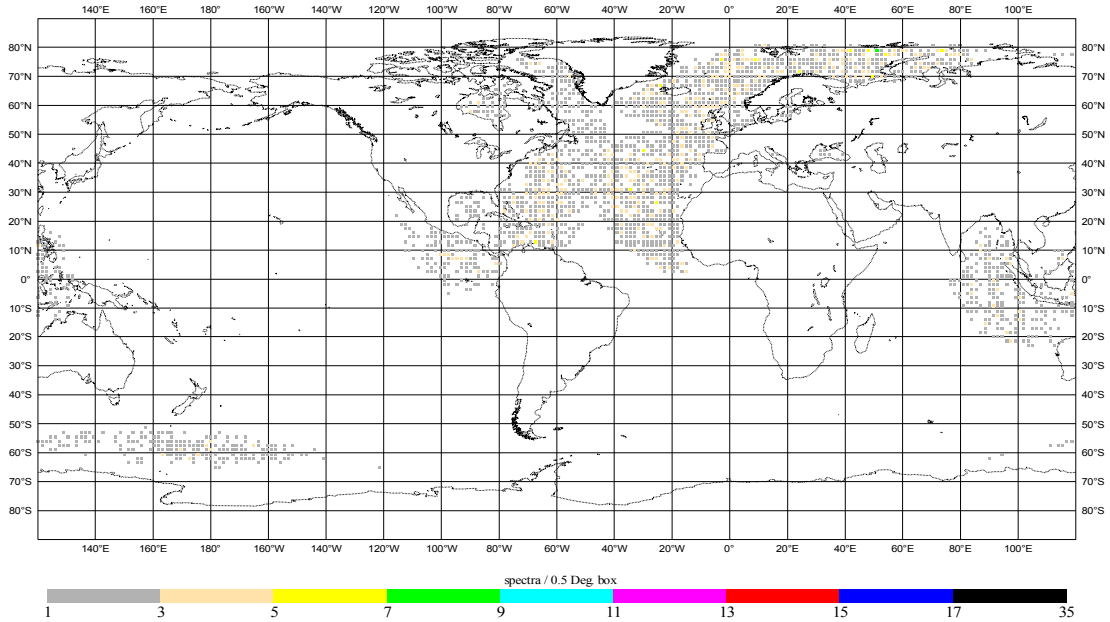

Figure 15: Typical ERS-2 SAR monthly coverage (October 2010) after the loss of global coverage (June 2003) and before the change of orbit (February 2011), i.e. with the 35-day repeat cycle.

As was done for the altimeter, the extra-tropical Northern Atlantic (north of latitude 20°N) is used for monitoring the Fast Delivery SAR wave mode UWA product. This is very close to the bulk of the current coverage. The weekly number of SAR wave mode spectra in the North Atlantic since the beginning of 1996 is shown in Figure 16. It is clear that the current coverage in the North Atlantic is slightly less than the nominal coverage. The difference is small and is due to the small gap at the southern edge of the North Atlantic. There was extra reduction of the amount of valid data between February and October 2008 and after August 2009. The quality of the UWA product in this area (i.e. North Atlantic) is investigated here.

3.2. ERS-2 SAR Wave Height in the North Atlantic

A long-term monitoring of the significant wave height computed from the inverted ERS-2 SAR spectra was performed. It is worthwhile mentioning that on 28 June 1998 the SAR inversion software was unable to properly handle the SAR data with the new calibration procedure introduced around that time. This was fixed with the implementation of the ECWAM model change on 20 November 2000. Furthermore, SAR wave mode data were assimilated in the wave model from 13 January 2003 to 31 January 2006. Other related events are summarised by Abdalla and Hersbach (2007). The most important events are those related to the situation of the gyroscopes. Those events are shown in Figure 14.

Figure 17 shows the time history of the weekly bias of the significant wave height computed from the inverted SAR wave mode spectrum with respect to the model wave height in the North Atlantic since April 1996. By ignoring the period with the inversion bug (from 28 June 1998 to 20 November 2000) and the period with EBM (from 17 January 2001 to mid June 2001), it is possible to recognise a

seasonal cyclic variation similar to the altimeter SWH (i.e. with minima during the NH winter and maxima during the summer). It is clear that the bias behaviour since the loss of the global coverage is similar to that of 2-3 years before. The statistics around the time of the orbit change between 22 February and 10 March 2011 should not be considered.

Figure 18 shows the time history of the daily scatter index of the SWH of the inverted SAR wave mode product with respect to the operational wave model in the North Atlantic since April 1996. The period with the inversion bug can be clearly recognised by the high SI values. There tends to be a kind of seasonal cycle (in phase with the bias cycle) of variation in SI after the recovery from the EBM using the ZGM. This seasonal cycle continued after the loss of the global coverage. Furthermore, the general trend of SI reduction continued over the period of limited coverage. Even the errors became smaller than ever; especially during the winter. This may be a consequence of assimilating the SAR wave mode product in the ECMWF operational wave model from 13 January 2003 to 31 January 2006. A step change in SI cannot be seen at these specific dates. However, the SI peak values started to be the lowest during the NH summer of 2003. In 2010, the SI started to increase again. A possible explanation for that is the blacklisting of Jason-1 observations as far as the data assimilation is concerned in April 2010 and due a slight degradation of small SWH values from EVNISAT RA-2 after the introduction of RA-2 processing chain IPF 6.02L04 in February 2010.

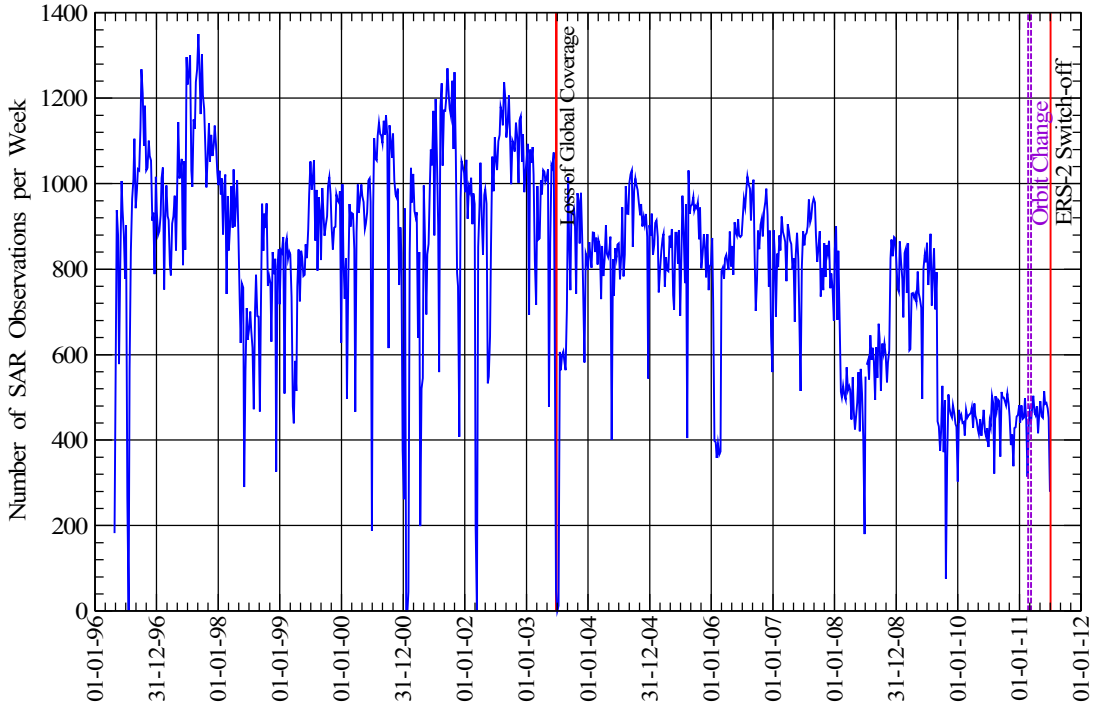

Figure 16: Time history of the weekly number of SAR wave mode spectra in the North Atlantic since 1 January 1996.

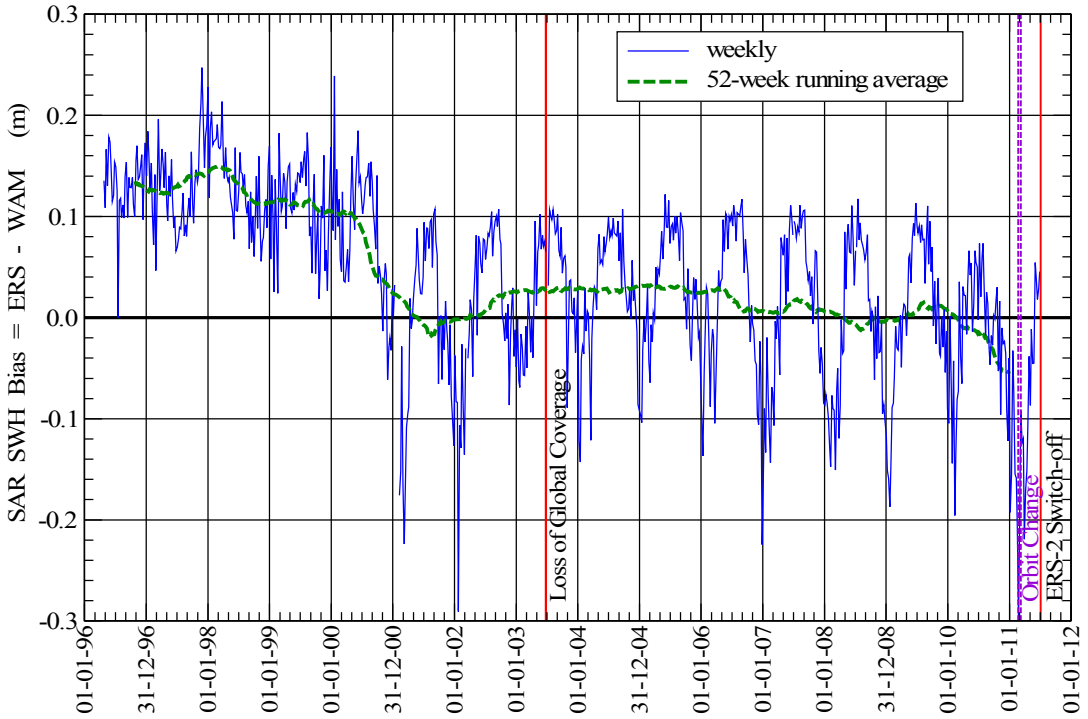

Figure 17: Time history of the weekly bias of SAR wave mode significant wave height with respect to wave model in the North Atlantic since April 1996. 52-week running average is shown by a thick dashed line.

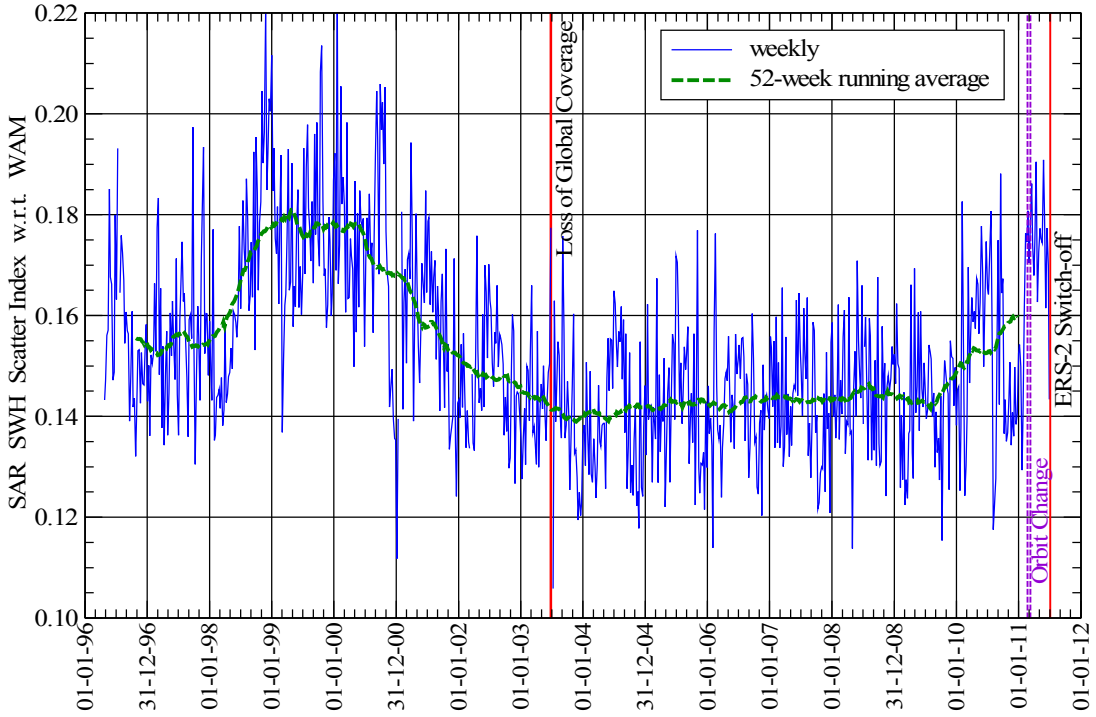

Figure 18: Time history of the weekly scatter index of SAR wave mode significant wave height with respect to wave model in the North Atlantic since April 1996. 52-week running average is shown by a thick dashed line.

3.3. Recent Events: ERS-2 Orbit Change and Switch-off

As already mentioned in Section 2.5, the orbit of ERS-2 was changed from 35-day repeat cycles to 3-day repeat cycles between 22 February and 10 March 2011. There was no valid SAR data available during the transition period. The typical monthly data coverage after the change of orbit (10 March 2011) can be seen in Figure 19 for June 2011. The observation locations became more spaced with more visits per box. Unlike the altimeter coverage map (Figure 9), discrete tracks cannot be easily distinguished.

The scatter plot comparing the SWH derived from the inverted SAR UWA products against the ECMWF wave model for April 2011 is shown in Figure 20. Although, one can conclude that there was no anomaly in Figure 20, the SI time series in Figure 18 suggests that it is highly possible that there is some degradation in the UWA product after the change of the orbit. Unfortunately, the 3-month lifetime of the 3-day repeat cycle configuration is not enough to make any solid conclusion regarding this issue.

Finally, ERS-2 was switched-off on 5 July 2011 after more than 16 years in orbit. The satellite was later put in a lower orbit of about 573 km before it was “neutralized” by disconnecting the batteries and depleting the fuel) on 5 September 2011.

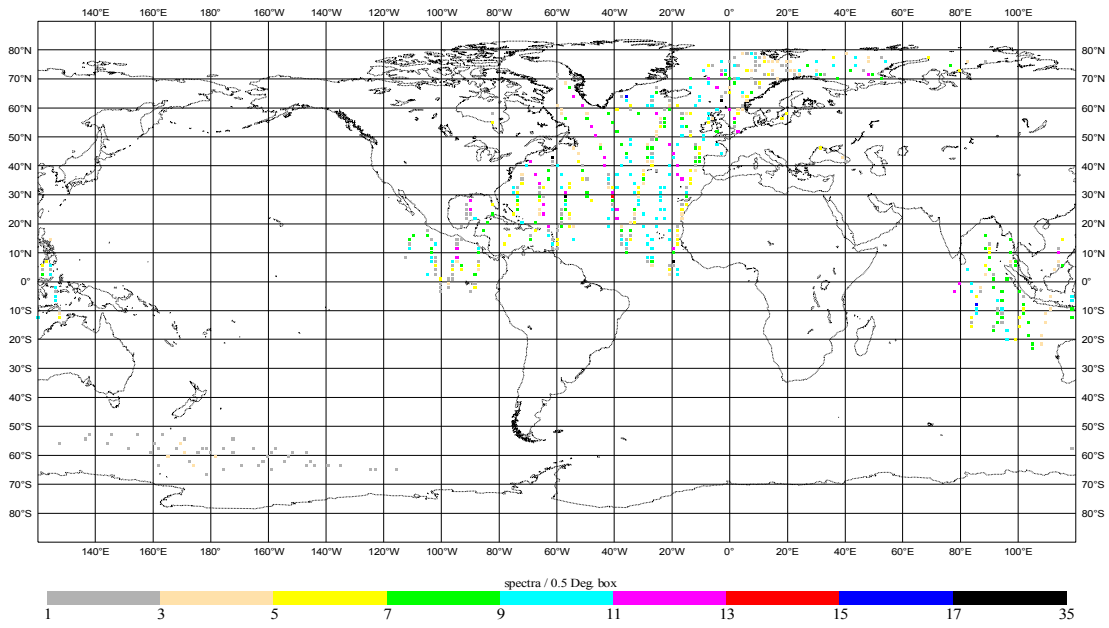

Figure 19: Typical ERS-2 SAR monthly coverage (June 2011) after the change of orbit (February 2011) to the 3-day repeat cycle.

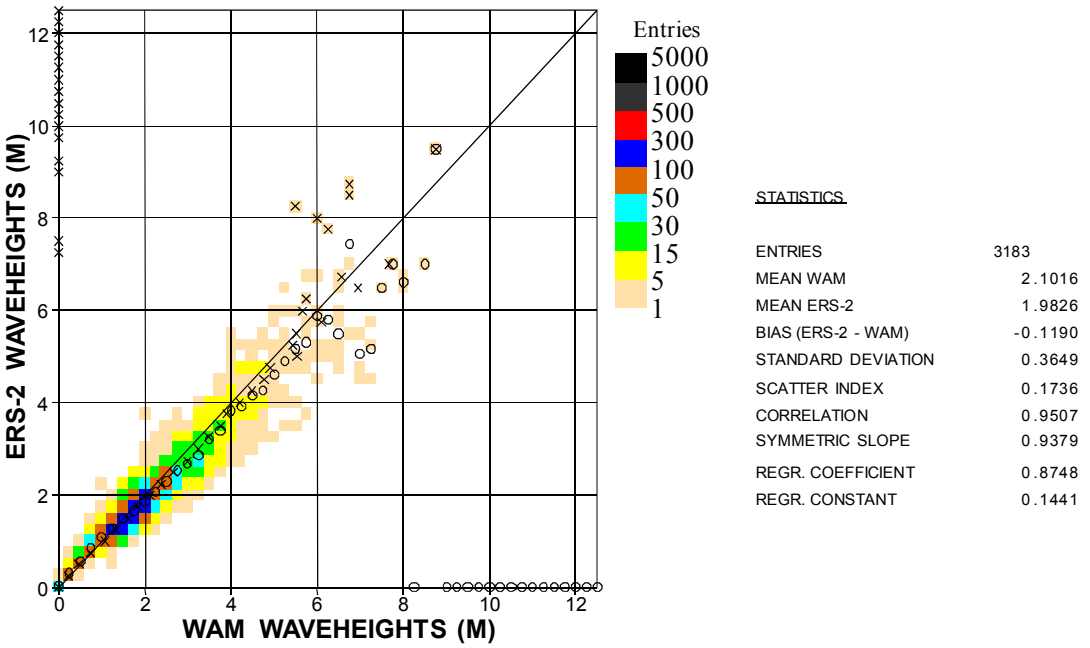

Figure 20: Comparison between ERS-2 SAR and AN wave model significant wave height values for the month of April 2011.

4. The Scatterometer UWI Product

4.1. Overview

The scatterometer on board ERS-2, as part of the AMI (Active Microwave Instrument), and previously ERS-1, obtains backscatter measurements from three antennas, illuminating a swath of 500 km, in which 19 nodes, or wind-vector cells (WVC), define a 25 km product (for details on configuration and geometry see Attema, 1986). From these backscatter triplets, two wind solutions are retrieved one of which is reported in a by ESA disseminated near-real time product, called UWI. For this the geophysical model function CMOD4 (Stoffelen and Anderson, 1997) is used.

ERS-1 was launched on 17 July 1991 and has provided scatterometer data from September 1991 until December 1999. ERS-2 was launched in April 1995. At ECMWF some preliminary data were received on 24 April 1995, while operational data flow started on 22 November 1995 (left-hand blue curve in Figure 21). Due to an on-board anomaly in January 2001, ESA was forced to suspend data dissemination between 18 February 2001 and 21 August 2003. However, off-line data were received from ESRIN covering the period from 12 December 2001 to 7 November 2003 (black curve in Figure 21). Two months before public re-dissemination, ERS-2 had lost its storage capacity of LBR data, including scatterometer data. After this event, data only remained available when in visual contact with a ground station. As a consequence, global coverage was lost for the newly disseminated stream, resulting in much lower data volumes (right-hand blue curve in Figure 21). The subsequent gradual increase in data volume is the result of the stepwise inclusion of new ground stations. In the last 2 years of mission few problems occurred to some ground stations leading to a decrease of data volume. For details see Section 4.3. ERS-2 was permanently switched off on 5 July 2011.

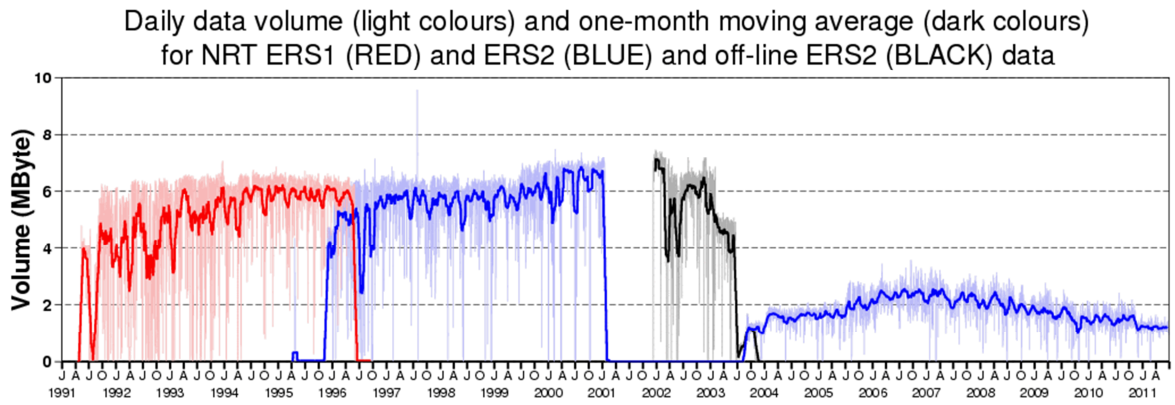

Figure 21: Volume of received ERS-1 and ERS-2 UWI data at ECMWF subject to the data cut-off time in Mbyte per day.

Within the framework of various contracts with ESA and ESRIN, ECMWF monitored UWI data for a number of years. By passing scatterometer winds to the ECMWF operational assimilation system an accurate comparison with model winds can be obtained. The findings of such comparison are, amongst other quality checks, recorded in cyclic reports on 5-weekly intervals. Elements of these reports are described in Section 4.2. A summary of the monitoring of the entire ERS-2 life will be presented in Section 4.3.

At ECMWF scatterometer data from ERS-1 and ERS-2 have been actively used in the operational integrated assimilation and forecast system (IFS) of ECMWF since January 1996. Before the ERS-2 anomaly in 2001, winds had been determined from CMOD4. However, since this geophysical model function exhibits biases that strongly depend on both incidence angle and wind speed, corrections had been applied (Isaksen and Janssen 2004). After the re-dissemination of the UWI product, scatterometer winds were re-introduced in IFS on 9 March 2004 (Hersbach et al., 2004). Winds were then based on the updated geophysical model function CMOD5 which resolves most of the incidence-angle and wind-speed dependent biases (Hersbach et al., 2007).

However, several collocation studies with buoy data (Portabella and Stoffelen, 2007; and Abdalla and Hersbach, 2007) indicated a residual overall bias of around -0.5 m/s. This bias was resolved by the development of CMOD5.4 (Hersbach et al., 2007), and winds based on this model function were introduced in IFS on 12 June 2007. Until the use of CMOD5.4 model, scatterometer winds have been assimilated at ECMWF as 10m wind. Therefore variations in stability, air density, ocean current and sea state were not accounted for. To take these effects into account at ECMWF it has been decided to assimilate scatterometer winds as equivalent neutral winds rather than 10m winds. A C-band geophysical model function for equivalent neutral winds, called CMOD5.N, has been developed (Hersbach, 2008). Winds based on this new model function were introduced in IFS on 9 November 2010 (Hersbach, 2010). ERS-2 switch off in July 2011 brings the assimilation of ERS scatterometer winds in IFS to an end after 20 years.

On 12 June 2007, data from the ASCAT scatterometer on-board MetOp-A were introduced in the operational assimilation suite at ECMWF. Winds were based first on CMOD5.4, and then, since November 2010, on CMOD5.N. Due to a difference in calibration between ERS-2 and ASCAT, bias

corrections in backscatter space and wind speed, respectively before and after wind inversion, are applied (Hersbach and Janssen, 2007).

4.2. Five-weekly cyclic UWI ERS-2 monitoring reports

The routine monitoring of the ERS-2 UWI product at ECMWF was summarized, until 7 March 2011 in the form of 5-weekly cyclic reports. As previously mentioned, the ERS-2 orbit was changed from 35 days to 3 days between 22 February and 10 March 2011. To highlight this new mission phase, the ERS-2 cycles counting was changed starting from 7 March 2011 (end of cycle 165). The first 3-day cycle was 301 resulting in a lack of continuity in the numbering (from 165 to 301). Following these modifications starting from cycle 301 the monitoring activity covered 12 cycles (36 days) in order to have a time span comparable to the previous reports (for practical reasons, in some plots, the old cycle numbering is used).

All the reports from Cycle 41 (start date 14 July 1998) up to 3D-Cycle 340 (end of mission on 5 July 2011) are available at http://earth.esa.int/pcs/ers/scatt/reports/ecmwf/. Up to Cycle 60 (nominal period) the UWI product has been compared with ECMWF first-guess winds as available within the assimilation system. These FGAT (first-guess at appropriate time) winds are well collocated with the scatterometer observation time and location.

From Cycle 69 onwards, e.g., with the start of the reception of offline data from ESRIN, collocation was performed with archived first-guess wind fields instead (available at 3-hourly resolution; and will be called FG winds). Despite the slightly higher collocation errors, this enables the monitoring of data that do not pass pre-screening quality control in the operational ECMWF assimilation system.The quality of winds inverted using the CMOD5 are monitored since cycle 69. At ECMWF, such retrieved ERS-2 scatterometer winds have been assimilated from 9 March 2004 until 5 June 2007, when CMOD5 was replaced by CMOD5.4 (see e.g. Section 4.4 of Abdalla and Hersbach, 2007).

The ECMWF scatterometer cyclic monitoring reports contain the following elements:

- An introduction, giving a general summary of the quality of the UWI data and trends w.r.t. previous cycles. Data coverage and interruptions in data reception are listed. Also, since Cycle 69 (12 November 2001) it is mentioned whether there was an enhancement of solar activity, and whether it could have affected the UWI wind product. Finally, it is informed whether the ECMWF assimilation system has changed and whether this had an anticipated impact on the quality of the ECMWF surface winds.

- A section giving a detailed description of performance during the cycle. It includes the following plots.

- Evolution of 5-weekly averaged performance of the cone distance, bias and standard deviation of UWI and CMOD4 wind speed and direction compared to ECMWF FG winds starting from Cycle 69. The plot covering up to the end of ERS-2 mission is given in Figure 22.

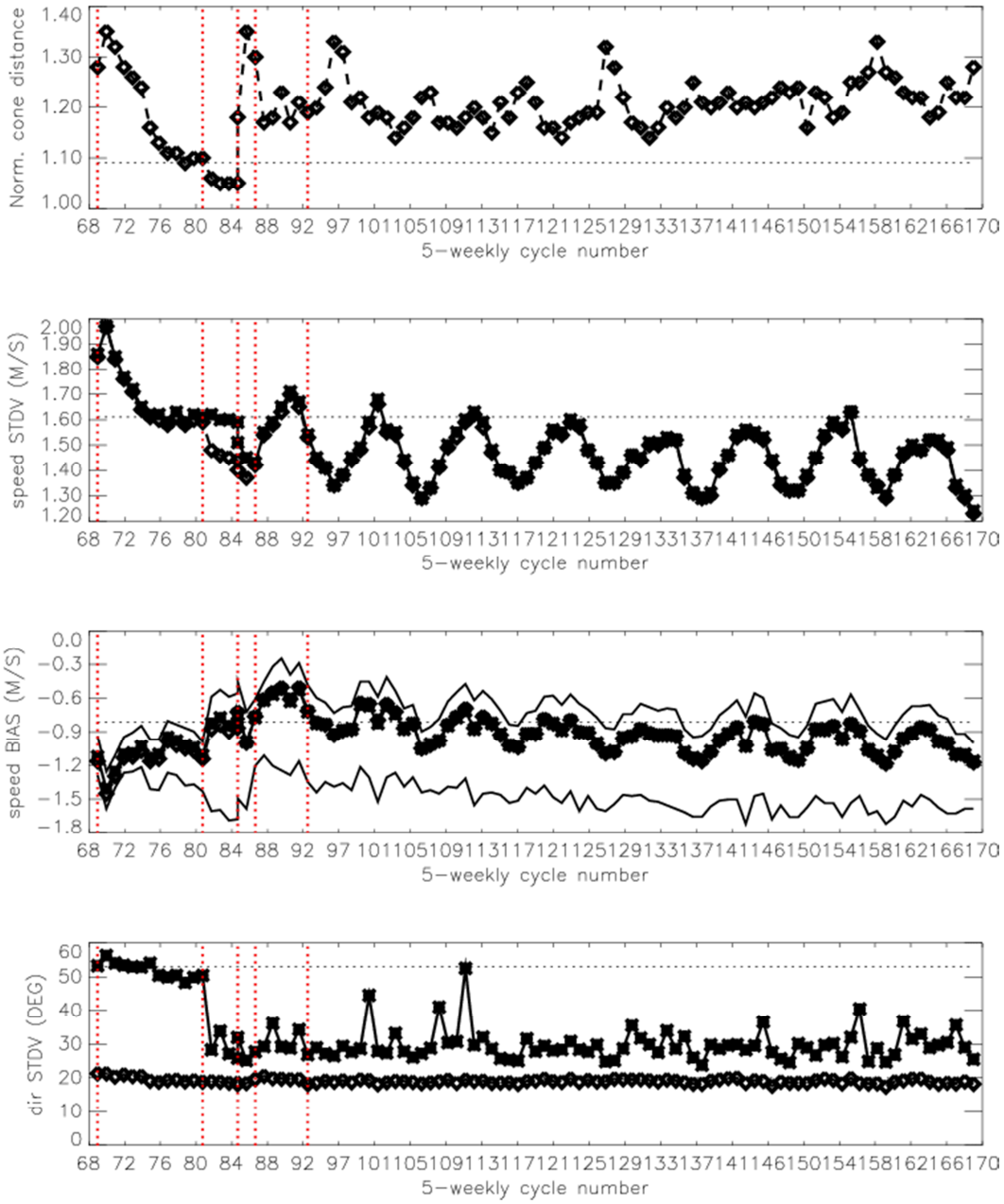

Figure 22: Evolution of the performance of the ERS-2 scatterometer averaged over 5-weekly cycles from 12 December 2001 (Cycle 69) to 4 July 2011 (end Cycle 170 according to the old cycle numbering) for the UWI product (solid, star) and de-aliased winds based on CMOD4 (dashed, diamond). Results are based on data that passed the UWI QC flags. For Cycle 85 two values are plotted; the first value for the global set, the second one for the regional set (see text for more details). Dotted lines represent values for Cycle 59 (5 December 2000 to 17 January 2001), i.e. the last stable cycle of the nominal period. From top to bottom panel are shown the normalized distance to the cone (CMOD4 only) the standard deviation of the wind speed compared to FG winds, the corresponding bias (for UWI winds the extreme inter-node averages are shown as well), and the standard deviation of wind direction compared to FG.

- Data coverage and geographical averages of UWI wind speed, and relative bias and standard deviation compared to ECMWF FG winds since Cycle 91. Figure 23 shows the coverage for 3D Cycles 324-336 (old numbering Cycle 168) while Figure 24 shows the coverage for the last year of the mission.

- Backscatter (σ^0) bias for the three antennas (fore, mid, aft) as function of WVC (1 to 19) and stratified with respect to ascending and descending tracks:

  $$dz=<z> /<zCMOD(\theta,FGAT)>,$$

  where $z=(\sigma^0)^{0.625}$, and θ is the WVC and antenna-dependent incidence angle. Note that the in this way estimated bias depends on the underlying model function. Results are produced on the basis of CMOD4. Trends in the inter-node and inter-antenna relationship indicate changes in the antenna patterns, because trends in the normalizing ECMWF winds would appear as integral shifts. Examples are provided in Figure 26, Figure 27 and Figure 28.

- Time series of the difference between the fore and aft incidence angle of node 10 (Cycle 81 onwards), and the UWI k -yaw quality flag (Cycle 88 onwards). Asymmetries indicate errors in yaw attitude control.

- Plots of time series of quantities averaged over 6-hourly data batches and stratified w.r.t. six classes of nodes (1-2, 3-4, 5-7, 8-10, 11-14 and 15-19) of:

  - The normalized distance to the cone, the fraction of rejected data on the basis of CMOD4 inversion, ESA flags or ECMWF land and sea-ice mask, and the total number of received data over sea.

  - Bias and standard deviation of UWI versus ECMWF first-guess winds for wind speed and direction.

  - The same for CMOD4 winds as inverted at ECMWF from level 1b.

- Global plots of locations where UWI winds were more than 8 m/s weaker or stronger than ECMWF FG winds (included from Cycle 79). Usually two specific cases are highlighted in a separate plot.

- Accumulated histograms (scatter plots) between UWI and ECMWF first-guess wind speed and direction. Scatter plots for FG winds versus de-aliased CMOD4 winds and CMOD5-based winds were produced from Cycle 74 onwards. Examples for a one-year accumulation period for the last 3 years of mission are presented in Figure 29, Figure 30 and Figure 31.

- Time series for at ECMWF assimilated ERS winds (based on CMOD5 or CMOD5.4, rather than CMOD4), and QuikSCAT winds relative to ECMWF FGAT winds for a region covering the North Atlantic and part of Europe (Cycle 94 onwards; for 3D Cycles 324-336 see Figure 25).

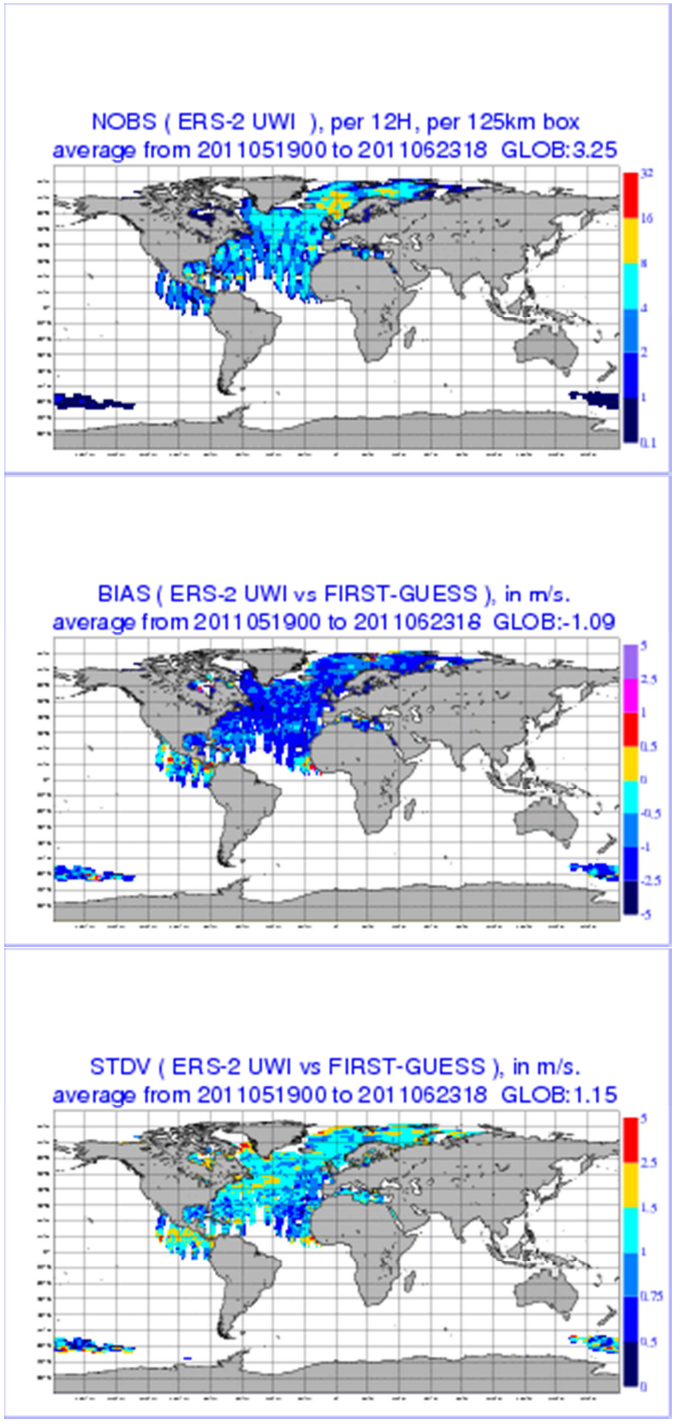

Figure 23: Average number (top) of observations per 12H and per N80 reduced Gaussian grid box (125 km), relative bias (middle) respectively standard deviation (lower panel) compared to ECMWF FG 10-meter winds, (125 km) of UWI winds that passed quality control at ECMWF for data in 3D Cycles 324-336 (old numbering Cycle 168- 18 May To 23 June 2011). Only data are plotted for grid cells that contained at least 5 observations.

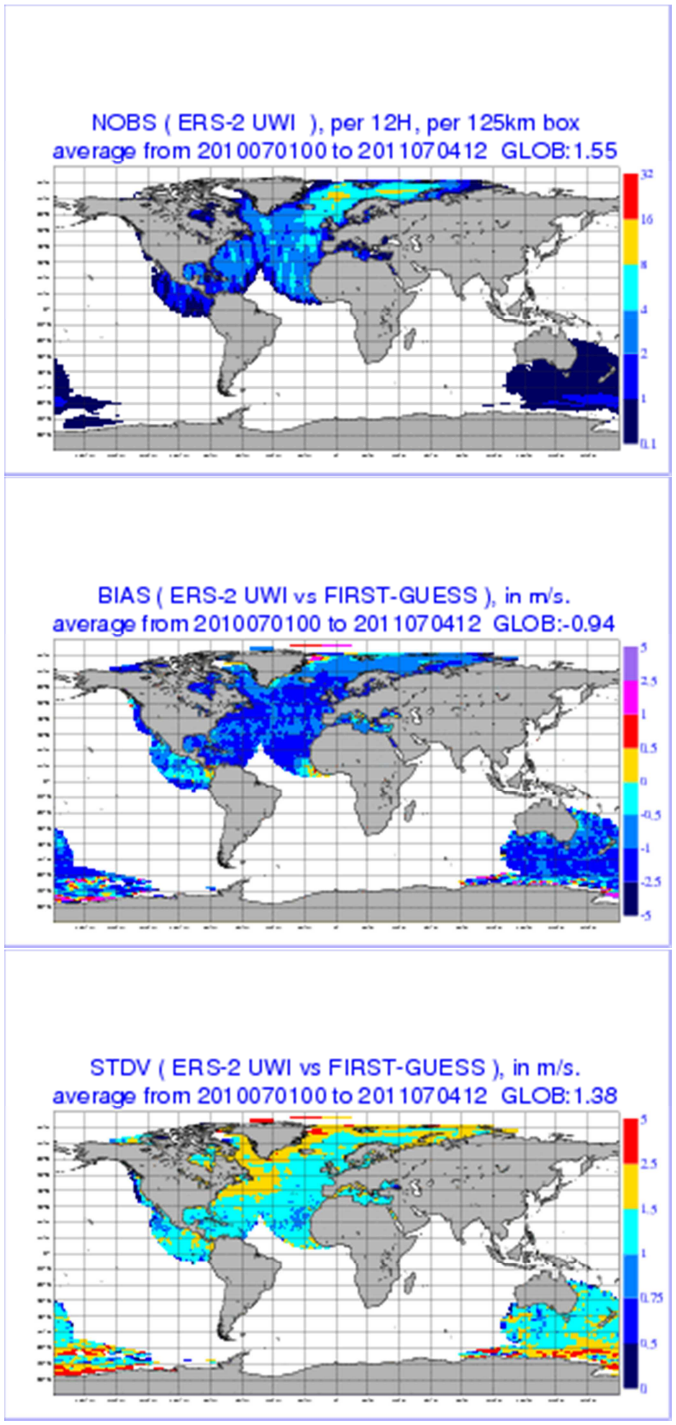

Figure 24: Average number (top) of observations per 12H and per N80 reduced Gaussian grid box(125 km) relative bias (middle) respectively standard deviation (lower panel) compared to ECMWF FG 10-meter winds, (125 km) of UWI winds that passed quality control at ECMWF for data over the last year of mission (1 July 2010 to 4 July 2011). Only data are plotted for grid cells that contained at least 5 observations.

4.3. General Overview for ERS-2

22 November 1995 - 19 March 1996

Pre-calibration phase. Large but constant σ^0 biases were encountered.

19 March 1996 - 6 August 1996

End of commissioning phase. A thorough calibration has resulted in revised look-up tables. Scatterometer data from ERS-2 (bias-corrected CMOD4 winds) are included in the ECMWF assimilation system on 1 June 1996, replacing the assimilation from ERS-1 that had been used from 30 January 1996. Details may be found in Isaksen and Janssen (2004).

6 August 1996 - 18 June 1997

Due to an erroneous switch to a redundant calibration subsystem σ^0 values decrease by 0.2 dB.

18 June 1997 - 17 January 2001 (Cycle 22 to Cycle 60)

Nominal period. Backscatter values return to old, well-calibrated levels. The performance of the UWI product is stable, although in the fall of 2000 there are some problems with the functioning of several of the six gyroscopes on-board the spacecraft. On average, backscatter levels are around 0.5 dB too low, leading to winds that are on average 0.7-0.8 m/s slower than FGAT winds. Although the inter-node and inter-antenna sigma biases are small, the UWI wind-speed bias does depend on node number (from -1.1 m/s for low to -0.6 m/s for high incidence angle). It is induced by imperfections in the CMOD4 model function (and do not appear for CMOD5). Standard deviation between UWI and FGAT winds are around 1.6 m/s. For Cycle 59, values of the average cone distance, (UWI - FGAT) and (CMOD4 - FGAT) statistics are displayed by the horizontal dotted lines in Figure 22.

17 January 2001 - July 2001 (Cycle 60 to 65)

As a result of the on-board failure there are no gyroscopes left for the platform's attitude control. The control system is switched to Extra Back-up Mode. The dissemination of scatterometer data is suspended after 2 February 2001; empty cyclic reports are made for Cycles 62 to 68.

July 2001 - 12 December 2001 (Cycle 65 to 69)

Introduction of the Zero-Gyro Mode (ZGM). Satellite pointing is achieved through payload data and the digital earth sensor. Although pitch and roll can be controlled accurately, large errors in the yaw attitude (several degrees) still occur. Such errors especially affect the quality of the scatterometer measurements. Dissemination of scatterometer data remains suspended.

12 December 2001 - 4 February 2003 (Cycle 69 to 81)

Restart of dissemination of UWI data, however, to a restricted group of users only. At ECMWF, the monitoring is resumed. Existing tools are updated where necessary.

Large errors in yaw, which especially seem to occur around periods of enhanced solar activity, have a large negative impact on the data quality. During these events, part of the backscatter signal

is destroyed, which, after inversion, results in far too low winds. Peaks of more than -3 m/s frequently occur, especially in January 2002 (Cycle 70), which marks a period of considerable solar activity. These incorrect data are also visible in the scatter diagrams of UWI versus FG wind speed as anomalously large numbers of collocations between strong ECMWF winds and weak UWI winds. For later cycles the situation improves.

Initially, also extremely large negative biases are observed in the backscatter levels, including data that were less affected by yaw errors. Large inter-node and inter-antenna differences induce large cone distances. The situation is worst for Cycle 70 but later slowly improves. However, the increasing negative bias towards higher nodes remains. In line with the average reduction in σ^0 bias, the cone distance and wind-speed biases gradually improve (see Figure 22).

For the random error of the UWI and CMOD4 wind speeds a similar trend is observed: worst for Cycle 70 (almost 2 m/s) and then first improving rapidly and later stabilizing. From Cycle 75 onwards its level is around the value obtained for the nominal period (see Figure 22). In general best results are obtained for winds inverted using CMOD5. Both the negative bias level and standard deviation are smaller for such derived winds.

The performance in wind direction is found to be much less affected. Although initially wind direction performs somewhat worse, at Cycle 72 it is on the level of the nominal period, and after Cycle 75 it has even become better (see lower panel of Figure 22).

4 February 2003 - 22 June 2003 (Cycle 81 to 85)

Start of the validation phase of ESACA, the new processor. Aim of this complete revision of the original LRDPF, was to bring the quality of the UWI product back to its nominal level. It is capable of the interpretation of on-board filter characteristics appropriately according to an estimation of the yaw attitude error. During the test phase, ESACA data are distributed for Kiruna station only, which leads to daily data gaps between approximately 21 UTC and 06 UTC.

The new de-aliasing algorithm, being part of ESACA, (and developed at DNMI) appears to perform well. The UWI winds agree considerably more often to the wind solution that is closest to the ECMWF FG wind direction. Values of standard deviations drop from 50 to less than 30 degrees (see Figure 22).

The UWI winds do not coincide anymore with one of the two solutions from the CMOD4 inversion at ECMWF. Inverted CMOD4 winds appear to be of much higher quality than the ESRIN disseminated UWI winds (see Figure 22). ESRIN tracked down quickly the cause for this non-ideal situation. Appropriate corrections to ESACA were implemented and since then UWI winds have been in line with CMOD4 again. The standard deviation w.r.t. FGAT winds are below 1.50 m/s, i.e., about 0.1 m/s better than it used to be during the nominal period.

Large fractions of high k_p values are found, especially for nodes at high incidence angles (more than 50%). Investigations by UK MetOffice and ESRIN revealed that there was a problem with the BUFR encoding algorithm. A solution was formulated and implemented.

In the near range the fore and aft antennas show large negative biases in the average backscatter levels. As a result, very large negative wind-speed biases are found for low nodes (-1.6 m/s). The cause was identified and resolved at ESRIN. Apart from the initially large near-range biases, the inter-node and inter-antenna differences in backscatter levels were small. Their level was comparable to that during the nominal period.

The incidence angles between the fore and aft antenna were not equal anymore. They showed a rapid variation in time and peaks up to 7 degrees were observed. This asymmetry was a direct result of errors in yaw attitude. A large anomaly on April 2003 (while the Earth was inside a gusty solar wind stream, source: www.spaceweather.com) resulted in low-quality winds. This event illustrated the potential usefulness of a yaw flag in the UWI product.

Along with improved quality of the CMOD4 winds, the normalized distance to the cone was below the level of the nominal period.

22 June 2003 - 21 August 2003 (Cycle 85 to 87)

On 22 June 2003 the second Low Bit-Rate recorder on-board ERS-2 failed, and was found to be beyond repair. As the first recorder had become unusable in December 2002, this meant that there was no facility left to store LBR data, which included scatterometer data. After a data-void period of three weeks, data flow was resumed on 16 July 2003, however, only for observations for which there was a direct contact with a ground station. For the Kiruna test data received at ECMWF, this meant that coverage was limited to the Atlantic north of 40°N, making statistics very sparse.

21 August 2003 - 7 March 2011 (Cycle 88 to 165)

On 21 August 2003, the public dissemination of UWI data restarted. This fortunate event made an end to the restricted distribution. From this date onwards data were received in the original manner (via the UK Met-Office), and were stored in the usual ECMWF analysis-input archives (the restricted data had been archived at a less accessible location). The original monitoring in the assimilation system (e.g., comparison with FGAT winds) was restored. However, cyclic reports were still based on the off-line monitoring (FG winds), since it included data rejected in an early stage of the assimilation system.

Besides Kiruna station, data were also received from Maspalomas, Gatineau and Prince Albert, which, bearing in mind the loss of the LBR recorders, resulted in a coverage over the North Atlantic, part of the Mediterranean, the Gulf of Mexico, and a small part of the Pacific north-west from the US and Canada. An initial gap in the North Atlantic was resolved on 15 January 2004, when a station at West Freugh (Scotland) was included. Coverage in the Caribbean was obtained by a station at Miami (February 2005), in the Chinese Sea by a station at Beijing (July 2005), and partial coverage over the Southern Hemisphere by the inclusion of McMurdo (Antarctica, June 2005) and Hobart (Tasmania, February 2006) stations, coverage over the Bay of Bengal and the North-Eastern part of the Indian Ocean by a station in Singapore (October 2006), and coverage of an area around South Africa by the inclusion of a station at Johannesburg on 23 May 2008 (This latter station has been into operation only until 16 December 2008 due to ground station hardware failure).

From Beijing, no data were received between 23 February and 15 May 2008, and since then coverage has been sporadic. From 27 June 2010 to 4 July 2011 no data at all have been received from Beijing due to ground station hardware failure. From 30 December 2009 to the end of the mission data have been missing from Singapore station due to a ground station facility problem. During the last year of the mission (July 2010-July2011), the data coverage of all available ground stations is shown in Figure 24.

7 March 2011 - 5 July 2011 (Cycle 3D-301 to 3D-340)

Following the request of the Cryosphere community, ESA decided to move ERS-2 to a 3-day repeat cycle to reproduce the ERS-1 Ice Phases of 1992 and 1994. The manoeuvre to move the satellite to the new orbit was performed in the so called transition period between 22 February 2011 and 10 March 2011. To highlight this new phase, the ERS-2 cycles counting has been changed starting from 7 March 2011 (end of cycle 165). The first 3D cycle was 301 resulting in a lack of continuity in the numbering (from 165 to 301).

The recording by separate ground stations means that in certain areas observations are reported more than once. For each ground station gridding into 25-km cells and de-aliasing is performed separately. It is found that overlapping cells may be dislocated (by 12.5 km), and that regularly not the same wind solution is selected for all ground stations.

The operational ESACA processor resolved all non-optimal features that had been detected during the validation period. Data quality was found to be high, although the cone distance increased and was 10% higher than for nominal data (see top panel of Figure 22). Assimilation experiments with winds inverted on the basis of CMOD5 showed a small positive impact in global forecast skill (Hersbach et al., 2004). This leaded to the re-introduction of ERS-2 scatterometer data in the ECMWF assimilation system on 8 March 2004.

An original flag for high k_p values was also set for yaw attitude errors exceeding 2 degrees. It appeared to work well and a close correlation with the asymmetry in incidence angle was observed. It was routinely checked whether peaks in attitude errors coincide with enhanced solar activity. Magnetic storms influence the outer part of the atmosphere, which in turn could affect the ERS-2 platform. Although sometimes collocations between anomalies and solar storms occur, the relation is not obvious. Besides, since mid 2006 the Sun resides near its minimum of its (chaotic) 11-year solar cycle, and, as a result, magnetic storms have been relatively sparse.

Since the loss of global coverage, a seasonal trend has been introduced in the now regional data set, making objective monitoring more difficult. A clear example of such a trend is observed for the relative standard deviation of the UWI wind speed compared to FG winds (see second panel of Figure 22; a more intense and volatile wind climate in winter time will naturally lead to an increased RMSE.

A seasonal trend also appears for bias levels of both wind speed and backscatter. For backscatter, bias patterns are found to be flat in winter time, but large asymmetries emerge during summer. Typical examples for this consistent yearly trend are given in Figure 26. The wind speed bias relative to ECMWF FG winds are found to be (like backscatter) most negative around July (1.1 m/s) and least

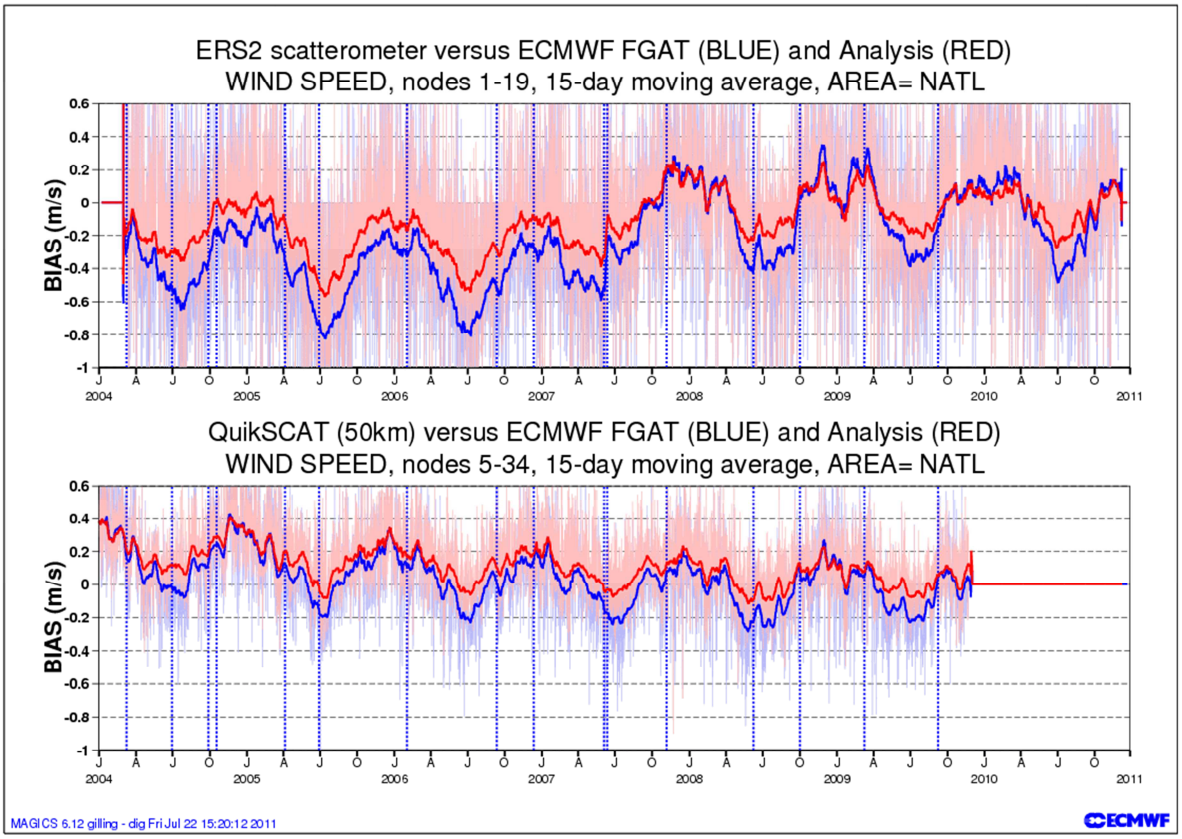

Figure 25: Wind-speed bias relative to FGAT winds for actively assimilated ERS-2 winds (based on CMOD5 before 7 June 2007; CMOD5.4 afterwards) for nodes 1-19 (top panel) and 50-km QuikSCAT (based on the QSCAT-1 model function and reduced by 4%) for nodes 5-34 (lower panel), averaged over the area (20°N-90°N, 80°W-20°E), and displayed for the period 01 January 2004 - 1 December 2010. Thick curves represent 15-day running means while thin curves represent 6-hourly periods values. Vertical dashed blue lines mark ECMWF model changes.

negative around February (0.8 m/s) as shown in Figure 22. The seasonal fluctuations are thought to be related to seasonal variations in the stability of the marine boundary layer. For a discussion, see Section5.4 of Abdalla and Hersbach (2006). The same trend is observed for ERS-2 winds as assimilated at ECMWF. These are not based on CMOD4 (as the UWI product) but are inverted by the usage of CMOD5 before 7 June 2007, CMOD5.4 afterwards until November 2010, CMOD5.N after November 2010.

A time series of active ERS-2 data restricted by an area in the North Atlantic is displayed in the top panel of Figure 25. The lower panel shows the evolution of the bias of active QuikSCAT data (subject to the same area) until the end of the mission in November 2009. It displays a similar yearly cycle, which confirms that the evolution in relative bias most likely has a geophysical nature, rather than being the result from a drift in the ERS-2 AMI instrument.

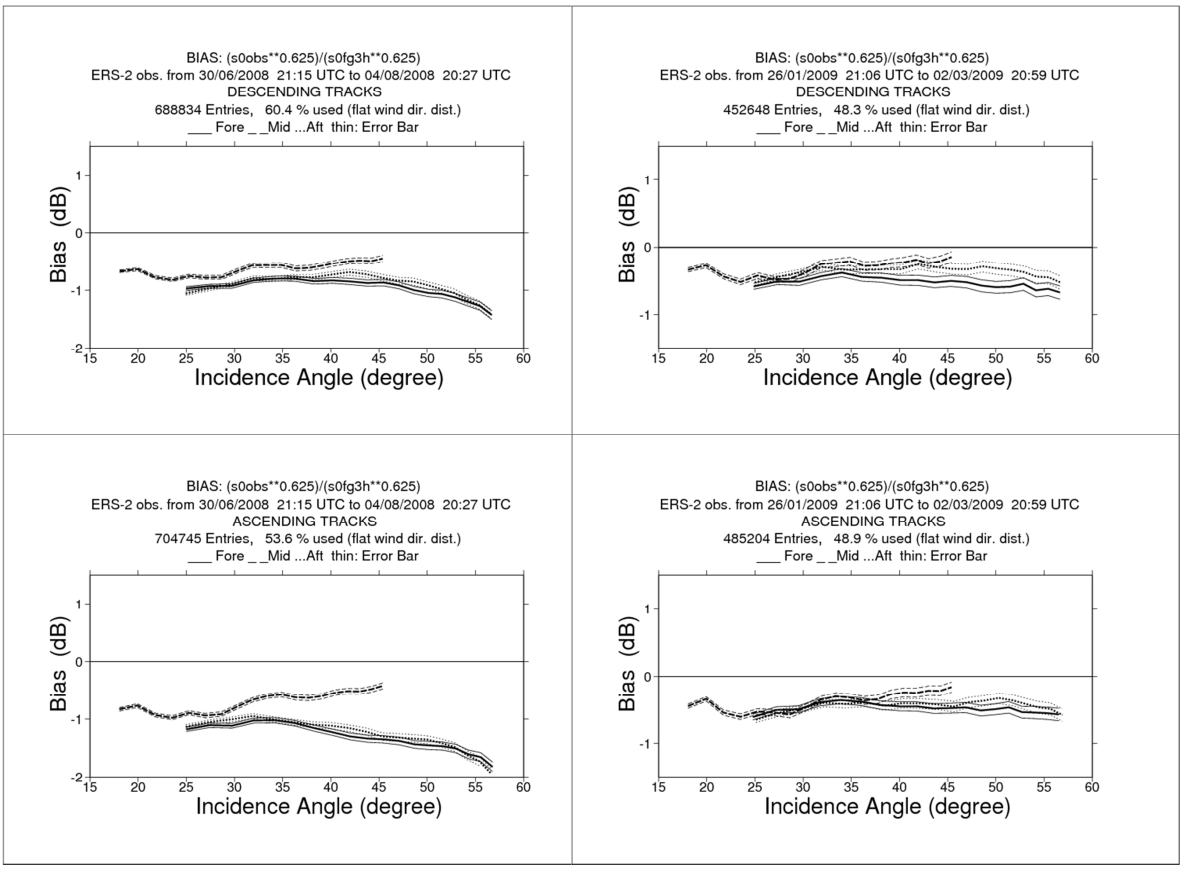

Figure 26: Ratio of $<\sigma_0^{0.625}/<CMOD4(FGAT)^{0.625}>$ converted in dB for the fore antenna (solid line), mid antenna (dashed line) and aft antenna (dotted line), as a function of incidence angle for descending (top panels) and ascending (lower panels) tracks of data within Cycles 138 (left panel) and 144 (right panel). These Cycles correspond to the most negative (-0.97 dB) and least negative (-0.42 dB) average ratio (between ascending and descending values) within the period July 2008 to July 2011. The thin lines indicate the error bars on the estimated mean.

In order to filter out seasonal effects, relative biases in backscatter space are presented in the right-hand panel of Figure 27 for the 1-year period from July 2008 to June 2009. For Cycle 59 (end 2000) similar plots are presented in the left-hand panels. Although accumulated over the limited 5-weekly period for this Cycle, seasonal effects are still filtered out by the fact that data were globally available (other cycles in 2000 display a similar pattern, not shown). Comparison between the two sets of plots shows that bias levels over the 1-year period is about 0.3 dB more negative than for nominal data. Same results are shown by comparing the one-year averages from 1 July 2009 to 30 June 2010 and from 1 July 2010 to 4 July 2011 to the nominal data in 2000. The main reason of this difference is the enhancement of ECMWF surface winds by about 0.3 m/s over the last decade. This trend emerges, e.g., from long term monitoring of QuikSCAT winds and buoy winds (not shown). The inter-antenna asymmetry has increased. For higher incidence angles the bias level of the mid antenna is less negative than for the side antennas especially for the ascending tracks. This asymmetry is most prominent during the summer as can e.g., be seen from the right-hand panel of Figure 26. Its origin is not completely known.

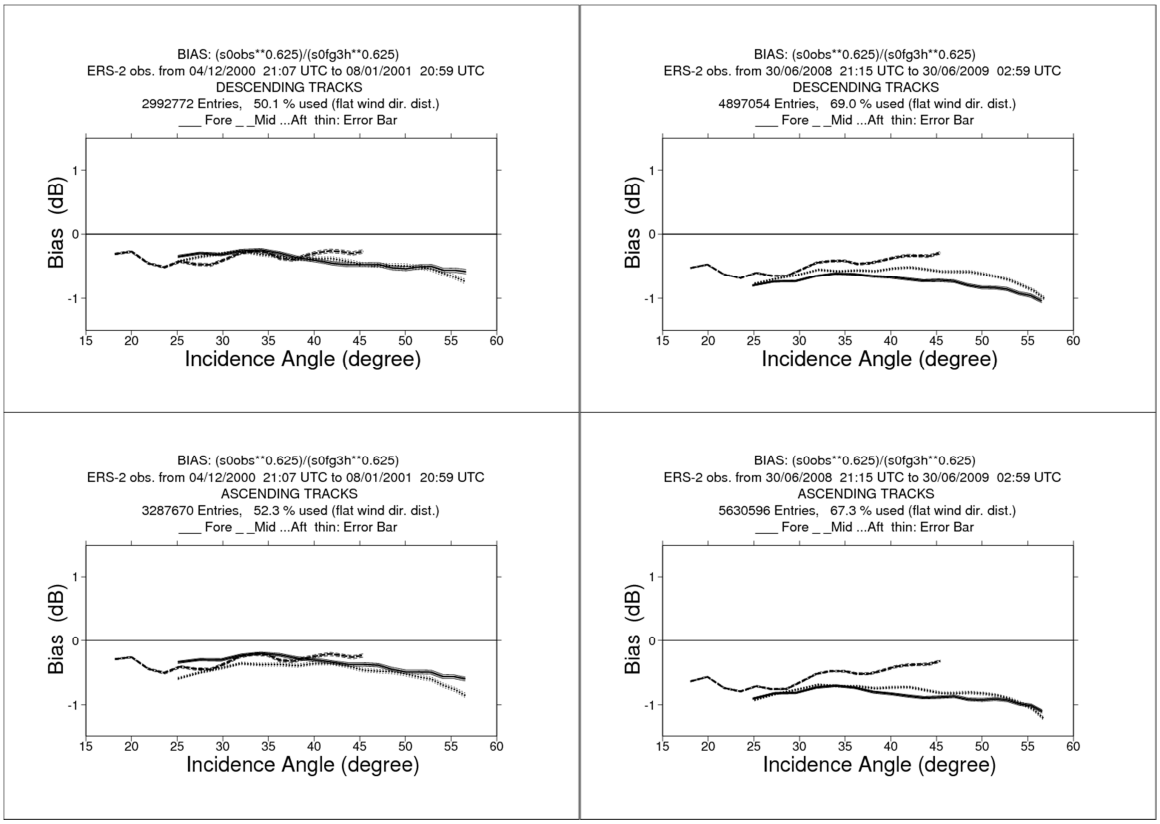

Figure 27: The same as Figure 26, but now on average over Cycle 59, the last cycle in nominal period (left panels) and the one-year period 1 July 2008 to 30 June 2009 (right panels) for descending (top panels) and respectively ascending (lower panels) track .

For wind the accumulation over the one-year period July 2008 - June 2009 (and all 19 nodes), indicates that UWI winds are on average 0.9-1.0 m/s biased low compared to ECMWF FG winds (top left-hand panels of Figure 29). This is slightly more negative than for nominal data (before January 2001), and matches the gradual increase (0.30 m/s) in average wind speed of the ECMWF first-guess winds since 2000 as mentioned above. Compared to a yearly average from July 2007 - June 2008 (see Abdalla and Hersbach, 2008), the situation is very stable (bias was on average -0.96 m/s). For both wind speed and wind direction, the scatter plots for the datasets 2009-2010 (Figure 30) and 2010-2011 (Figure 31) with respect to ECMWF FG winds are quite similar.

A similar picture holds for winds derived from CMOD5 (the analysis with CMOD5 is kept to compare results with previous reports). Scatter plots for 2008-2009 are similar to those for 2007-2008. Average relative wind bias of CMOD5 was around -0.45 m/s, which is on the level of the bias of CMOD5 compared to buoy data. Therefore with the introduction of the CMOD5.4 model, the ECMWF FG winds were nearly unbiased with respect to buoy data. Similar results for the one-year scatter plots for 2009-2010 and 2010-2011 are shown in Figure 30 and Figure 31.

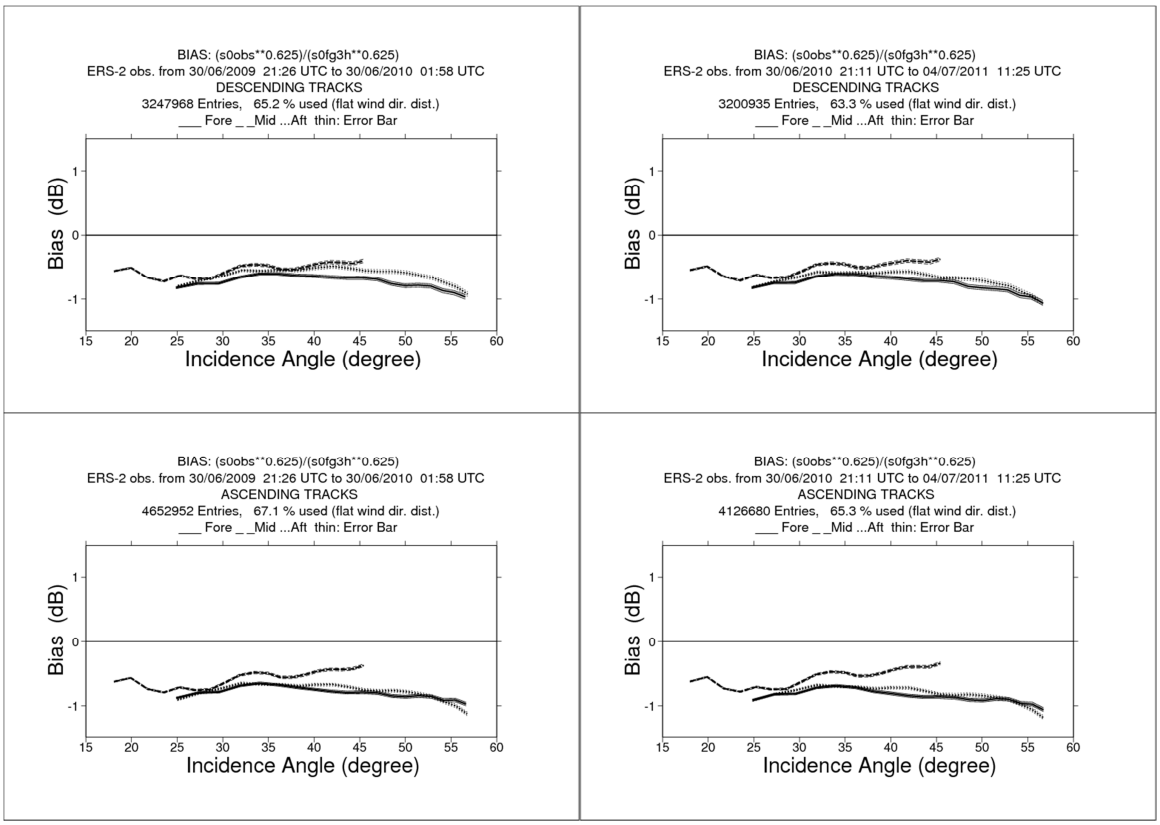

Figure 28: The same as Figure 26, but now on average from 1 July 2009 to 30 June 2010 (left panels) and from 1 July 2010 to 4 July 2011 (right panels).

Compared to the situation of nominal data (i.e., before 2001), the one-year accumulated relative standard deviation of UWI winds is about 0.1 m/s lower (1.5 m/s versus 1.6 m/s). This result is stable for the 3 one-year averages (2008-2009, 2009-2010, 2010-2011). As mentioned in the previous report, it is difficult to state whether the quality of the UWI product has improved, since part of the lower STDV should be the result of the current absence of strong winds in the Southern Hemispheric storm tracks, combined with a gradually improving quality of ECMWF winds.

As observed during the ESACA test phase, the quality of UWI wind direction is (as a result of the improved de-aliasing algorithm) superior to that of nominal data (see lower panel of Figure 22). Nevertheless, incorrect wind solutions are still frequently reported as can be seen from the lower-left panels of Figure 29, Figure 30 and Figure 31. Occasionally, peaks of degraded performance have occurred which usually can be traced back to temporarily missing input (model winds) in the ESACA de-aliasing software. Such peaks are not observed for the de-aliased CMOD5 winds.

A slight wind direction bias is still visible as observed in the previous reports. On average, (de-aliased) ERS-2 winds are found to be rotated by 2 to 3 degrees anticlockwise compared to ECMWF first-guess fields. One possible reason for this sustained bias is the lack of cross-isobar flow (Hollingsworth, 1994) at warm advection of ECMWF surface winds. A similar, but opposite in direction, effect is found in the Southern Hemisphere. The two biases compensate each other leading to globally unbiased wind direction. A study for QuikSCAT data versus model winds can be found in Brown et al. (2005).

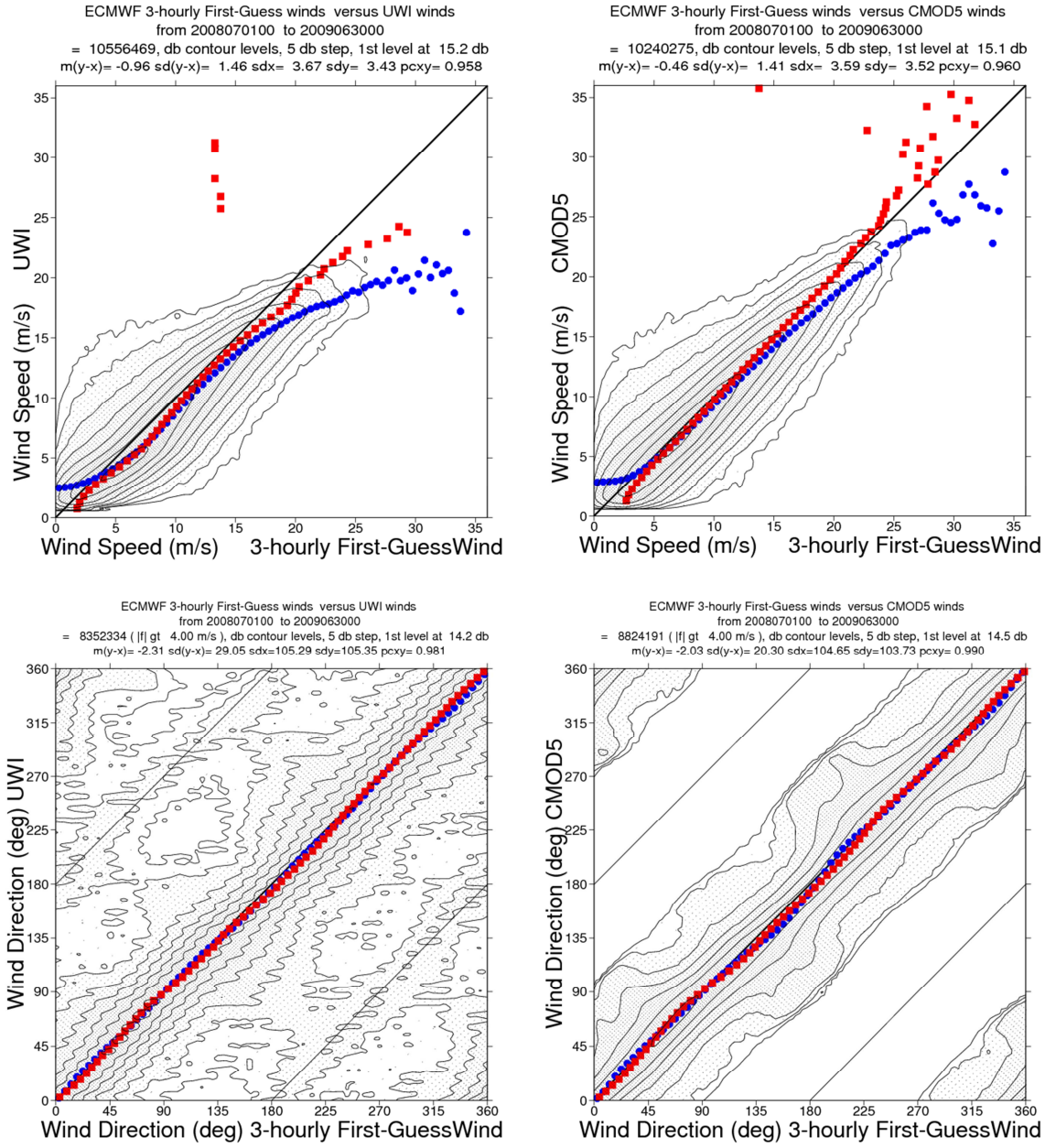

Figure 29: Two-dimensional histogram of UWI (left hand panes) and de-aliased CMOD5 (right hand panels) relative to ECMWF FG for wind speed (top panels) and wind direction (lower panels) over the one-year period from 1 July 2008 to 30 June 2009. Blue circles denote average for bins in the x-direction, and red squares averages for bins in the y-direction.

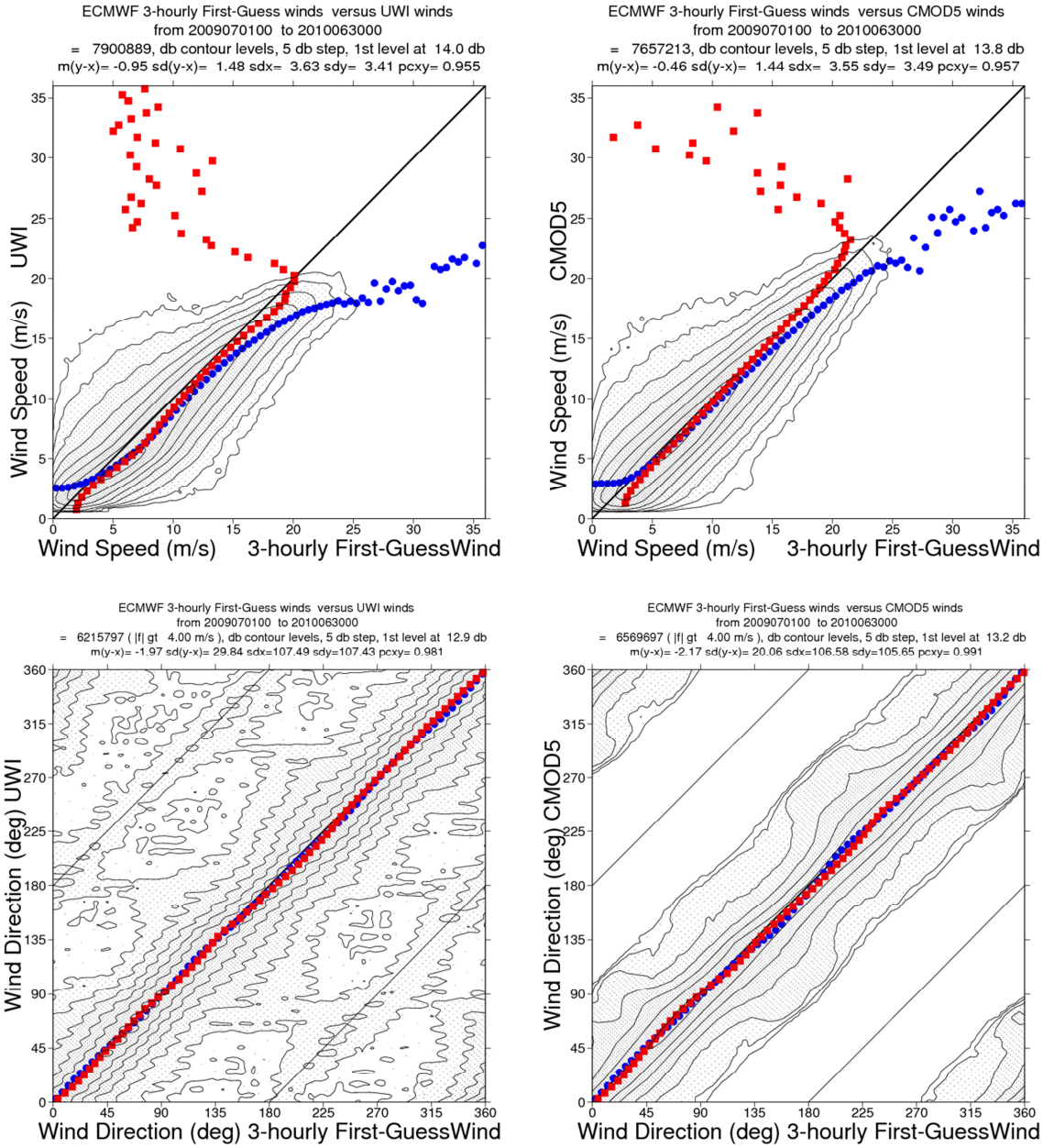

Figure 30: The same as Figure 29, but for the period from 1 July 2009 to 30 June 2010.

Locations of large differences between UWI (or CMOD5) and ECMWF FG winds are usually isolated. They often indicate meteorologically active regions, for which UWI data and ECMWF model field show reasonably small differences in phase and/or intensity. Tropical cyclones and frontal systems are typical candidates. One example (left-hand panel of Figure *32*) was the case of Hurricane Igor in the North Atlantic on 19 September 2010. ERS-2 scatterometer winds are not affected by the rain and are able to provide a detailed image of the wind in a hurricane. As shown in Figure *32*, ECMWF winds are too weak near the cyclone centre and also, as explained before, are affected by the problem of the lack of cross-isobar flow.

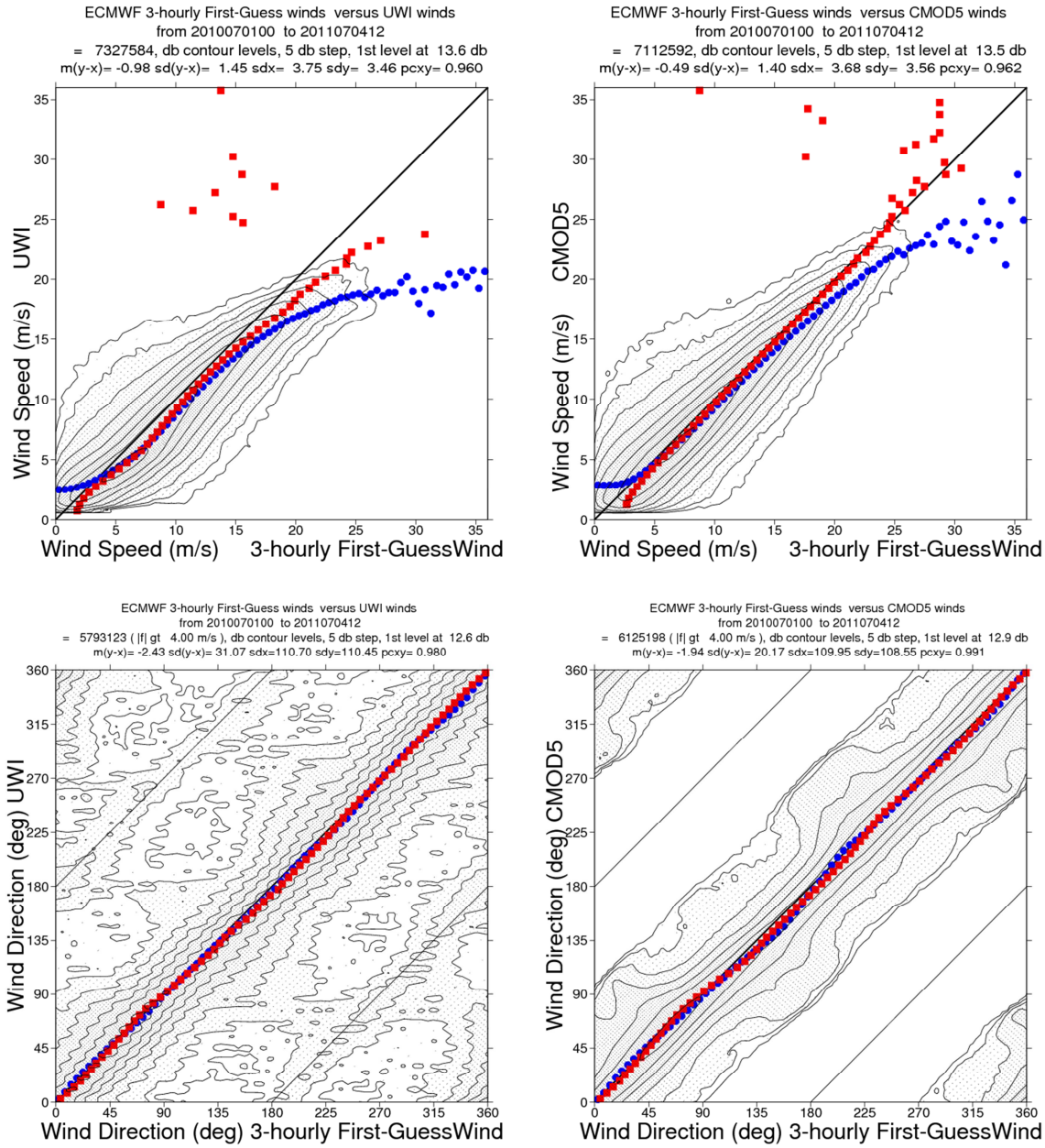

Figure 31: The same as Figure 29, but for the period from 1 July 2010 to 4 July 2011.

Sometimes large differences point to errors in the ECMWF first-guess fields. Occasionally there are cases where UWI winds are clearly incorrect. This is often manifested as odd patches within a surrounding wind field of presumably good quality. An example is shown in the right-hand panel of Figure *32*. These problems are found most likely to occur at light wind conditions relatively close to land and at lower incidence angles.

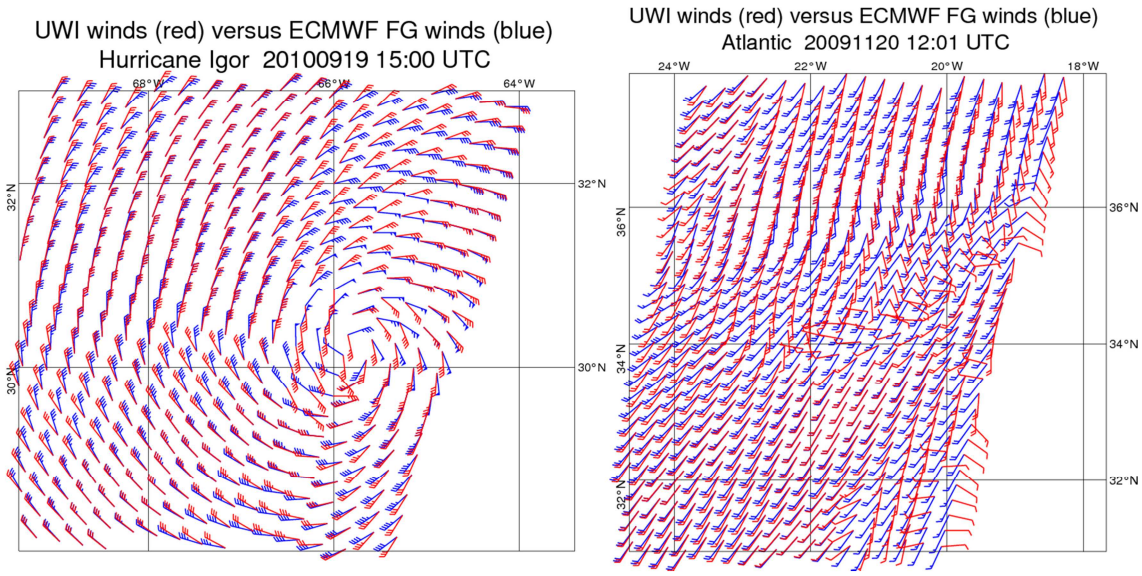

Figure 32: Two examples for situations where scatterometer and ECMWF winds differ significantly.

4.4. Validation of ERS Scatterometer Reprocessing Products (ASPS)

The ERS-2 scatterometer reprocessing project operationally started at ESRIN in July 2007 by using a dedicated processor called ASPS (Advanced Scatterometer Processing System). The aims of the ASPS project are:

- Reprocessing of the entire ERS1/2 scatterometer missions in order to provide a homogeneous data set;
- Reprocessing of ZGM data during the period 2001-2003;
- Provide yaw correction information;
- Enhance the spatial resolution: in addition to the L2.0 nominal resolution product (25 km), a 12.5-km product is also generated. They are named, respectively, as ASPS20N and ASPS20H;
- Provide sea-ice probability and detailed QC reports.

The radiometric quality of the ASPS reprocessed data has been improved through a detailed calibration analysis and computation of a refined antenna pattern. ASPS L2.0 product winds are based on the CMOD5.N model. They contain up to 4 wind solutions, in contrast to the single solution in the operational UWI products.

In support of the ERS reprocessing project, the quality of the new ASPS products, both the Nominal (25 km) and High Resolution (12.5 km), have been validated. Data from Cycle 30 (February 1998) to Cycle 81 (May 2003) have been received and analyzed. For the analysis some quality control steps have been applied to the data.

The ASPS20 product winds have been collocated with the ECMWF short-range forecast 10m wind fields. Then 0.2 m/s has been added to the ECMWF winds in order to adjust them to the equivalent 'neutral' winds. Furthermore the ASPS backscatter triplets have been inverted at ECMWF to CMOD5.N winds.

To identify the different datasets the following names have been used:

- ASPS20 is the solution selected in the ASPS product;
- ASPS20D is the ASPS solution closest to ECMWF wind;
- CMOD5.N is the CMOD5.N solution inverted at ECMWF that is closest to ECMWF wind.

As a first step the ASPS wind inversion (based on CMOD5.N) has been verified. ASPS20D winds have been compared to the CMOD5.N ones. For both products the solution closest to the ECMWF model wind has been selected. Results show that, apart from a small fraction of the data, the wind speed (Figure 33) and the wind direction (Figure 34) for both products are nearly identical. For this small amount of data where the products differ, differences arise in two separate populations in wind speed and in precise populations in wind direction (namely; 45°, 135°, 225° and 315°). When data with large directional difference are filtered out, the two populations in wind speed disappear as well (not shown). Similar differences were already observed in other products suggesting that they are most likely connected to small differences in the used inversion algorithm.

Also all winds from the three datasets have been compared to the ECMWF FG 'neutral' winds. The analysis has been done for both ASPS20N and ASPS20H products. Results for the Cycle 54 are shown in Figure 35 and Figure 36. All the three products show similar statistics in wind speed: ASPS winds are on average stronger than ECMWF 'neutral' ones. The bias ranges from 0.2 m/s (as shown in Figure 33 for Cycle 54) to 0.35 m/s for other cycles in 2003 (not shown here). This seems to be correct as ECMWF winds are known to be biased low for the periods analyzed. Also a wind vector cell dependent bias can be seen but this can be due to low data volume available for the analysis.

Some differences can be noticed for the wind direction standard deviation. ASPS20 winds are slightly worse than ASPS20D. This suggests that the ASPS de-aliasing is not perfect even if it shows better results than the operational ESACA de-aliasing (20-25° versus 27° of the operational ESACA). However, the de-aliased ASPS20 winds are of slightly higher quality than the CMOD5.N winds inverted at ECMWF.

Finally the bias between the ASPS20 backscatter triplets and the backscatter simulated from ECMWF 'neutral' wind subjected to CMOD5.N is shown in Figure 37 (ASPS20N product) and Figure 38 (ASPS20H product) for the case of Cycle 54. In general the ASPS20 winds are higher than ECMWF FG winds. This is a reflection of the underestimation of the ECMWF winds. All beams behave similarly in the mid range of WVC. Due to different geometry acquisition, the mid beam behaves slightly differently at the near and far range. The WVC dependency is also seen in the wind speed statistics. Same results have been found also for both the nominal and high resolution products of almost all cycles (not shown here).

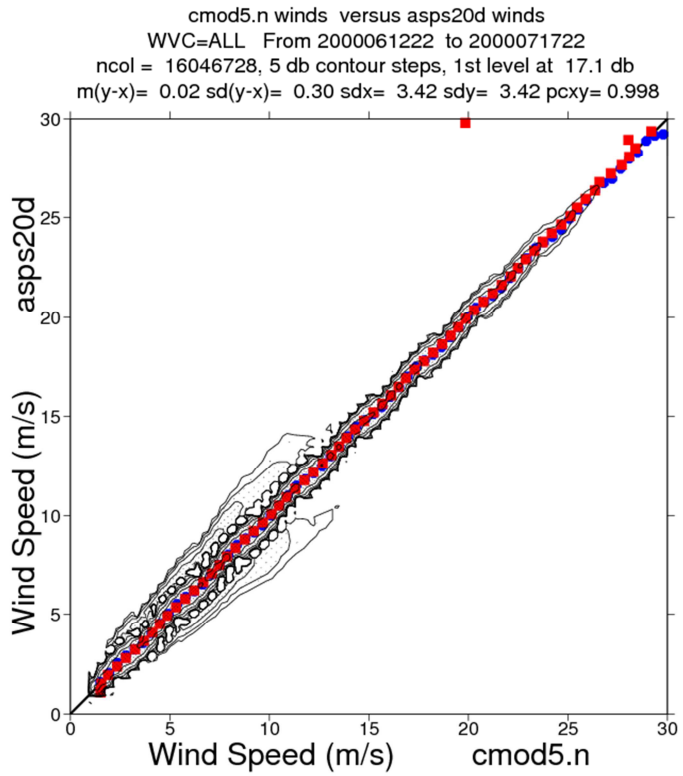

Figure 33: Comparison of ASPS wind solution closest to ECMWF model one versus ASPS winds inverted at ECMWF. Data from high resolution products winds: ERS-2 Cycle 54 (from 12 Jun 2000 to 17 July 2000).

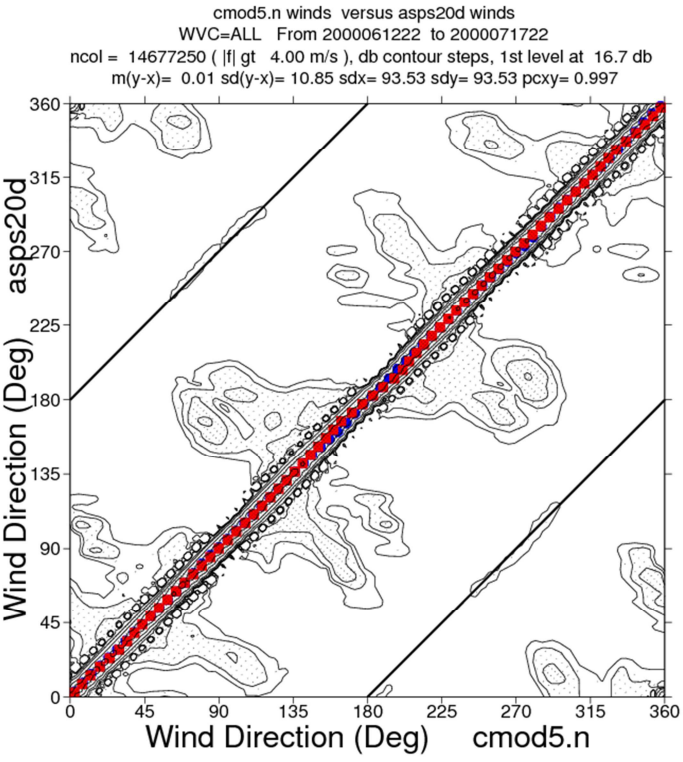

Figure 34: as in Figure 33 but for wind direction.

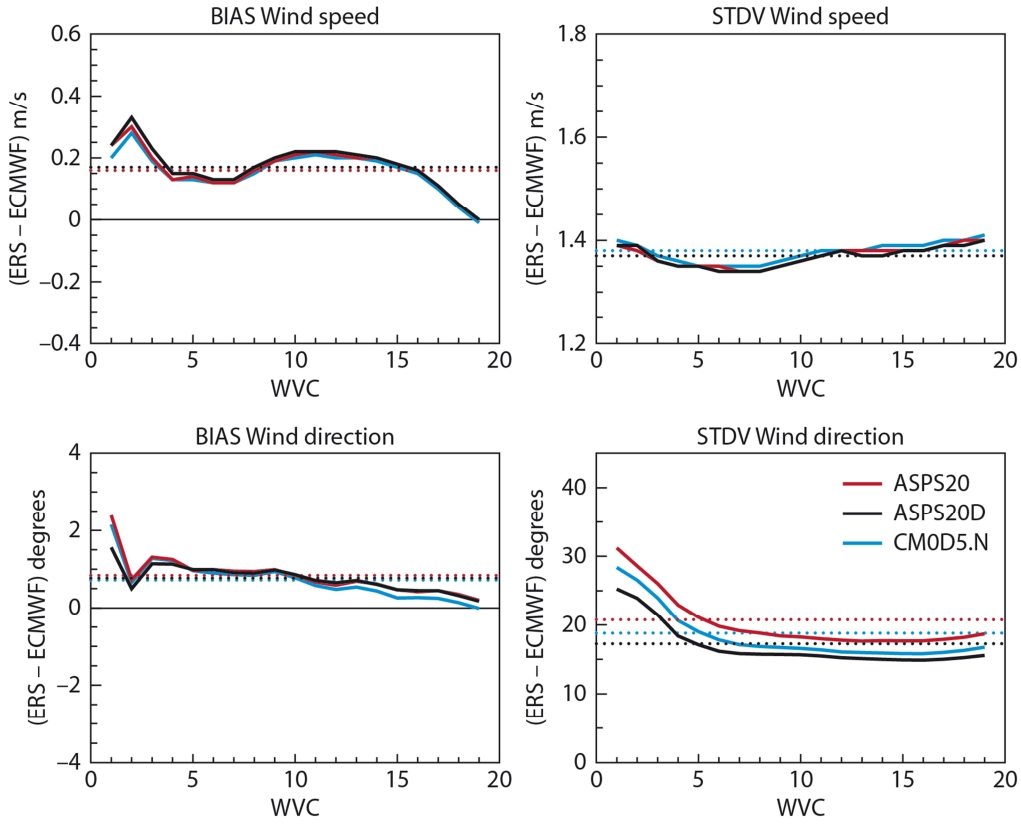

Figure 35: Wind speed and direction bias computed as Observations - ECMWF FG. Results are shown for ERS-2 Cycle 54 ASPS20N data (from 12 Jun 2000 to 17 July 2000).

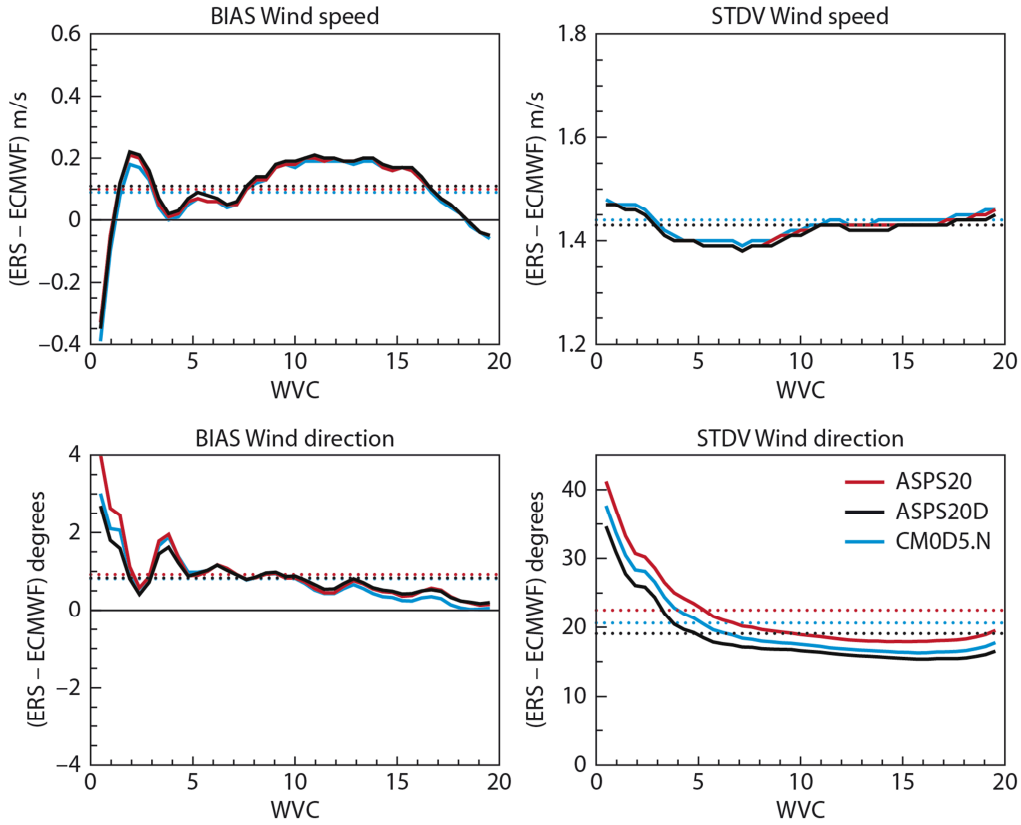

Figure 36: as Figure 35 but for ASPS20H products.

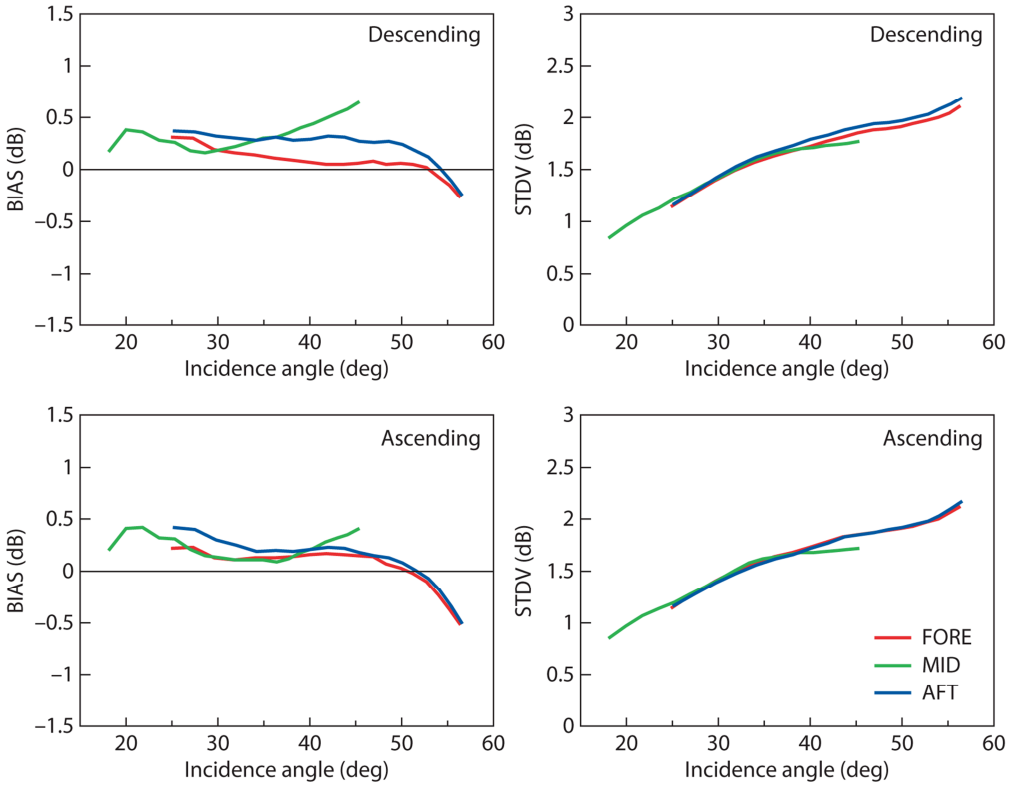

Figure 37: Bias (left hand panels) and Standard deviation (right hand panels) between ASPS sigma nought triplets and CMOD5N(ECMWF neutral) converted in dB for the fore antenna (red line), mid antenna (green lin0) and aft antenna (blue line), as a function of incidence angle for descending (top panels) and ascending (lower panels) tracks over Cycle 54 (ASPS20N).

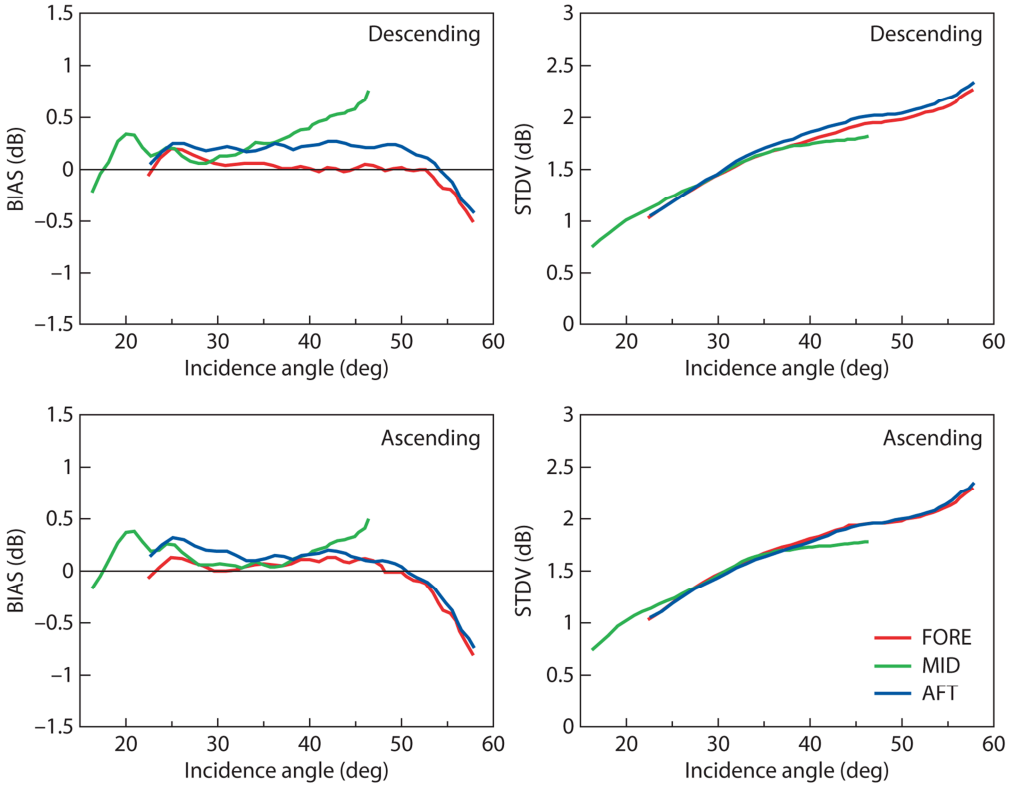

Figure 38: The same as Figure 37 but for the ASPS20H products.

The analysis of the ASPS reprocessed products highlighted some anomalies not identified in the first operational processing. In particular, the ocean calibration detected an issue for the aft beam for the cycles from 69 to 74. As can be seen in Figure 39, the aft beam bias has different performance compared to the fore and mid antennas. As a consequence, the wind retrieved by backscatter triplets affected by the aft beam issue show higher bias values in both speed and direction as shown in Figure 40. Actions have been taken at ESRIN to investigate the problem and to reprocess the cycles affected by this issue.

5. Long-Term Assessment of Ers-1/2 Products Using Era-Interim

5.1. Introduction

The wind and wave products from the ERS mission represent an invaluable data set. Hersbach et al. (2007b) and Abdalla and Hersbach (2007) have carried out a thorough verification of ERS wind and wave products against the consistent ECMWF 40-Year Reanalysis (ERA-40) for the winds and a model hindcast run forced by ERA-40 winds for wave heights. The availability of the latest ECMWF interim reanalysis (ERA-Interim), motivated the repetition of the same exercise with ERA-Interim. The performance of both ERS-1 and ERS-2 products compared to surface wind product from the ERA-Interim and the significant wave height product from two long-term stand-alone wave model

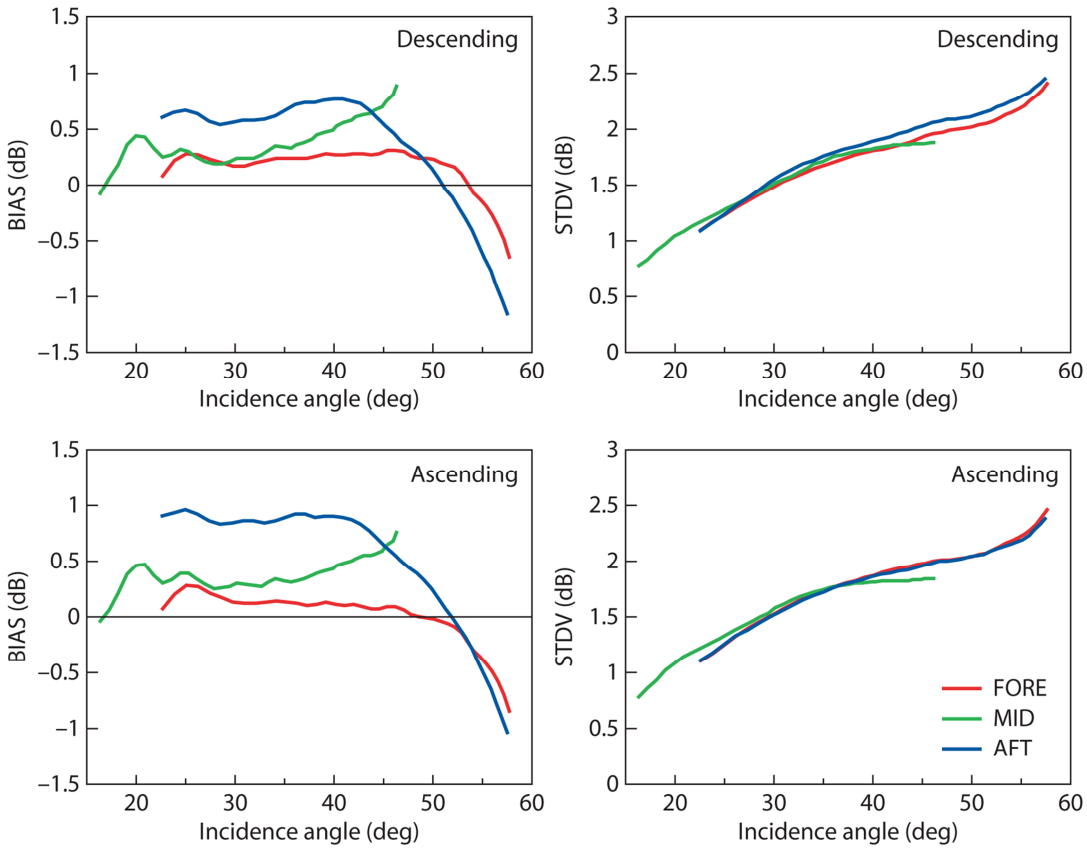

Figure 39: Bias (left hand panels) and Standard deviation (right hand panels) between ASPS sigma nought triplets and CMOD5N (ECMWF neutral) converted in dB for the fore antenna (red line), mid antenna (green line) and aft antenna (blue line), as a function of incidence angle for descending (top panels) and ascending (lower panels) tracks over Cycle 70 (ASPS20H).

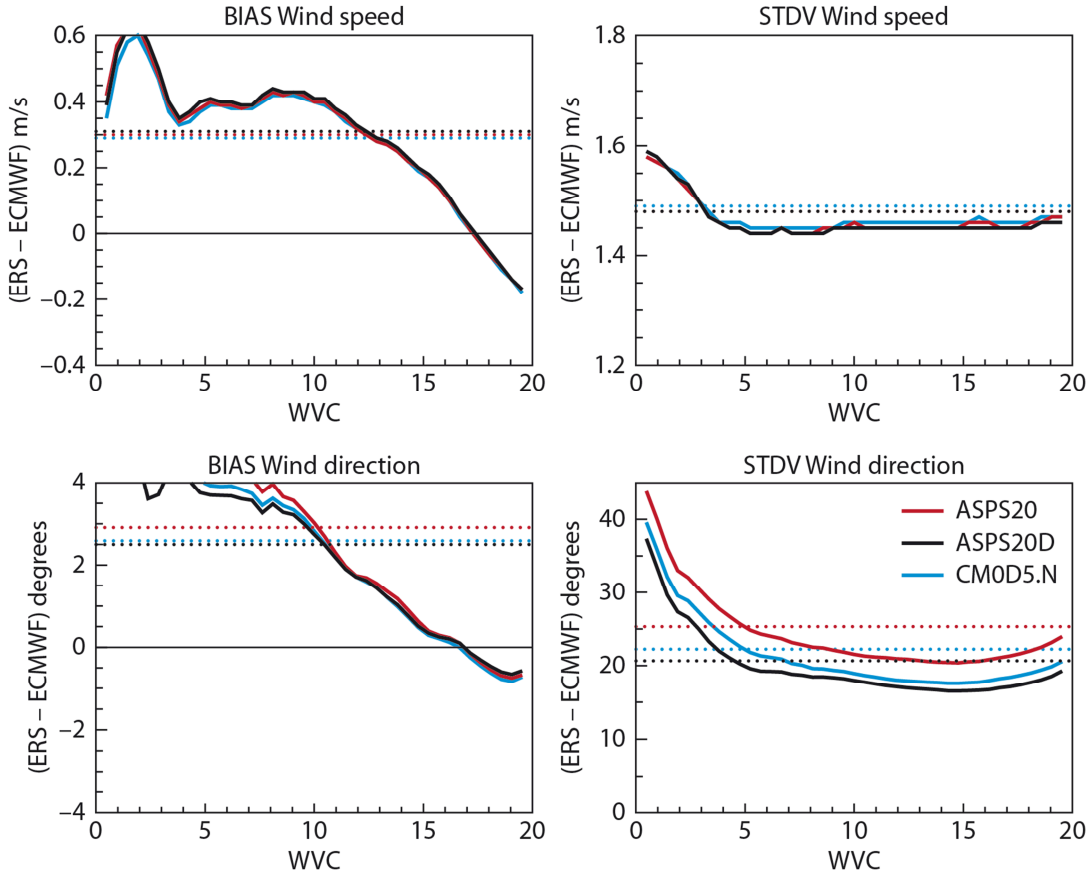

Figure 40: Wind speed and direction bias computed as Observations - ECMWF FG. Results are shown for ERS-2 Cycle 70 of ASPS20H products.

hindcast runs forced by ERA-Interim winds is presented here. The products involved here are the fast delivery (FD) Active Microwave Instrument (AMI) scatterometer wind (UWI) and the off-line OPR (Ocean Product) altimeter wind and wave products from ERS-1 and ERS-2.

The ERS missions started with the launch of ERS-1 (the first sun-synchronous polar-orbiting mission of ESA) on 17 July 1991. It was followed by ERS-2 which was launched on 21 April 1995. The Radar Altimeter (RA) and the Active Microwave Instrument (AMI) which consists of two separate radars; namely: the Synthetic-Aperture Radar (SAR) and the scatterometer are the instruments which are able to provide wind and wave data on-board both satellites.

According to ESA (2005), the launch and early orbit phase (LEOP) of ERS-1 began with the launch and ended with the satellite achieving nominal attitude and orbit. The duration of this initial phase was less than two weeks. A 3-day repeat cycle was adopted to provide frequent revisits to a number of dedicated sites for calibration purposes. The remaining effective life of the ERS-1 mission is sub-divided into the following phases (see also Table 1):

Table 1: ERS-1 Phases (Orbital Configurations).

Phase	A	B	R	C	D	E	F	G
	JUL DEC	MAR APR		DEC	APR	SEP	MAR	JUN
	1991	1992		1993	1994		1995	1996
Name	Comm. phase	1st Ice phase	Roll tilt	Multi-disciplinary phase	2nd Ice phase	Geodetic phase	Shifted geodetic phase	2nd Multi-disciplinary phase
Repeat cycle (days)	3	3	35	35	3	168	168	35
Purpose	Cal / Val	Arctic ice experi-ments	Sat. rotated by 9.5°	Nominal usage	Arctic ice experi-ments	Enables high density measure-ments	As phase E with 8 km shift	Nominal usage Tandem with ERS-2

Phase A - Commissioning Phase: 3-day repeat cycle. Lasted 138 days (from 25 July to 10 December 1991). Mainly to perform engineering calibration and geophysical validation.

Phase B - First Ice Phase: 3-day repeat cycle. Lasted 93 days (from 28 December 1991 to 31 March 1992). Optimised for the specific requirements of Arctic ice experiments.

Phase R - Experimental Roll Tilt Mode Campaign: 35-day repeat cycle. Lasted 12 days (from 2 to 14 April 1992). The satellite body was rotated by 9.5 degrees allowing operation of the SAR imaging mode at an incidence angle of 35 degrees. Performance of the RA Altimeter is slightly degraded because of the geocentric pointing instead of the local normal pointing.

Phase C - Multi-Disciplinary Phase: 35-day repeat cycle. Lasted 20 months (14 April 1992 to 23 December 1993). Mean sea surface determination, ocean variability studies and surface mappings are among various uses during this phase.

Phase D - Second Ice Phase: 3-day repeat cycle similar to the First Ice Phase (Phase B). Lasted 108 days (from 23 December 1993 to 10 April 1994).

Phase E - Geodetic Phase: 168-day repeat cycle. Lasted about 5 months (from 10 April 1994 to 28 September 1994). Enables high-density measurements to improve the determination of the geode using RA.

Phase F - Shifted Geodetic Phase: 168-day repeat cycle similar to the Geodetic Phase (Phase E) but with an 8 km spatial shift. Lasted about 6 months (from 28 September 1994 to 21 March 1995).

Phase G - Second Multi-Disciplinary Phase: 35-day repeat cycle similar to the first Multi-Disciplinary Phase (Phase C). Lasted about 14 months (from 21 March 1995 to 2 June 1996). Tandem mission with ERS-2 (from 17 August 1995 to 2 June 1996) was within this phase.

Phase G concluded the nominal ERS-1 mission. ERS-1 stayed in this configuration while serving as a backup for ERS-2. ERS-1 finally retired on 10 March 2000 after a failure in its on-board attitude control system.

On the other hand, ERS-2 was launched on 21 April 1995 and continued successful long life until it was switched-off and de-orbited on 5 July 2011. ERS-2 had only two phases of operations both with the same orbital configuration of 35-day repeat cycle:

Phase A - Commissioning Phase: Lasted from 2 May 1995 to 17 August 1995. Mainly to perform engineering calibration and geophysical validation.

Phase B - Routine Phase: Started on 17 August 1995 and still going on. Similar to ERS-1 Phases C and G. This phase started with the tandem mission from 17 August 1995 to 2 June 1996.

Nevertheless, ERS-2 was unfortunate to start losing its gyroscopes in early 2000. This led to the implementation of the Attitude and Orbit Control System (AOCS) mono-gyro attitude software early February 2000 (c.f. Femenias and Martini, 2000). Further loss of gyroscopes on 17 January 2001, which left a single working gyroscope, forced the piloting of the spacecraft without any gyroscopes in the Extra Back-up Mode (EBM). This led to degradation of some ERS-2 products. The implementation of the zero-gyro mode (ZGM) was fully introduced in June 2001 to assist the piloting of the spacecraft without any need for the frequent use of the only available gyroscope. Later on, the permanent failure of the ERS-2 low bit rate (LBR) tape recorders on 21 June 2003 prevented the continuation of the ERS-2 global coverage. ERS-2 LBR data coverage is limited within the vicinity of the ground stations. These events are summarised in Table 2.

Table 2: Main Events in ERS-2 Lifetime.

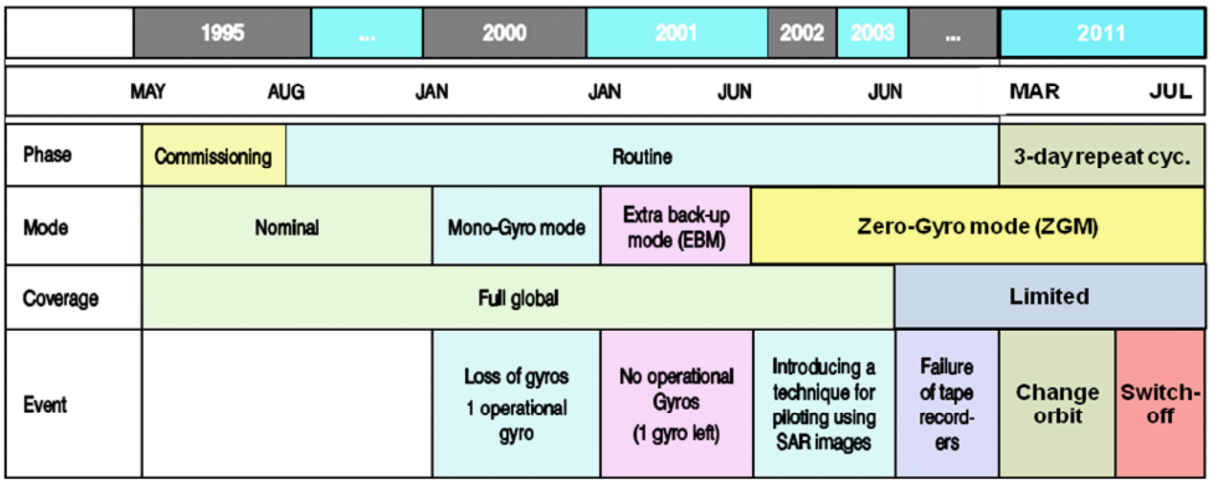

On 22 February 2011, manoeuvres started in order to change the 35-day repeat mission operated since the launch. It reached its final orbit configuration of 3-day repeat cycle on 10 March 2011. Finally, the satellite was switched-off on 5 July 2011. The de-orbiting of the satellite started on 6 July 2011 and has been successfully completed on 5 September 2011 after reaching its target circular orbit at about 573 km altitude. This will greatly reduce the risk of collision with other satellites or space debris. The re-entry of ERS-2 to the atmosphere is expected to take place in less than 15 years, in line with the latest guidelines of space debris management.

It should be noted that Altimeter product used in this evaluation is the offline OPR obtained from the French ERS Processing and Archiving Facility (CERSAT) of the French Research Institute for Exploitation of the Sea (IFREMER). The data were converted into BUFR format (see Abdalla and Hersbach, 2007). The same operational pre-processing and quality control procedures (c.f. Abdalla and Hersbach, 2004) were applied before the use of the data. The only exception is that the number of 1-Hz observations averaged to produce one super-observation was selected to be 11 (rather than the value of 30 used operationally for ERS-2).

5.2. ERA-Interim Wind and Wave Fields

As both operational atmospheric and wave models at the European Centre for Medium-Range Weather Forecasts (ECMWF) are changing frequently, the operational ECMWF data archive does not represent a consistent data set that can be used for the evaluation of the ERS products. The quality of both wind and wave fields are improving with time. In the past, ECMWF carried out two long-term reanalyses exercises (see Uppala et al., 2005): ERA-15 (15-year reanalysis) and ERA-40 (45-year reanalysis). While preparing for the future major reanalysis, which is planned to cover about 100 years, an interim reanalysis is currently being carried out (see Dee et al., 2011). It covers the period from the beginning of 1979 until the near real time (NRT). The results are made available for the users with a delay of a couple of months.

The ERA-Interim atmospheric model and reanalysis system uses Cycle 31R2 of ECMWF Integrated Forecasting System, IFS (Riddaway, 2009), which was introduced operationally in September 2006, configured for 60 levels in the vertical direction and a spatial horizontal resolution of about 79 km at the surface (T255 spherical harmonic representation). The atmospheric model is coupled to an ocean-wave model resolving 30 wave frequencies and 24 wave directions with a horizontal resolution of about 110 km. (see Berrisford, 2009).

One needs to keep in mind that although the model version is frozen, the data usage changes with time due to the availability of data for assimilation. Therefore, the reanalysis fields do not represent a 100% consistent data set but they are, however, the best in terms of consistency.

ERS-1, ERS-2 and QuikSCAT scatterometer surface wind-vector data produced using an improved geophysical model function (GMF), as will be explained later, are assimilated. On the other hand, ERS-1, ERS-2, Envisat, Jason-1 and (since 1 February 2010) Jason-2 altimeter wave height data are assimilated. The altimeter data are corrected to remove the bias based on altimeter-buoy collocation. Unfortunately, the ERA-Interim system implemented a “non-optimal” bias correction file which was produced temporarily during the development instead of the final version.

Due to the use of improper bias correction files in ERA-Interim and to the fact that the resolution of the ERA-Interim wave model is rather coarse, it was decided not to use the wave heights directly from ERA-Interim. Two long-term stand-alone wave model runs forced by ERA-Interim wind fields were carried out. One run uses the proper wave bias correction file while the other run is a hindcast that does not use any wave data. Both model runs have a resolution of about 40 km. The wave fields produced from these two model runs were used for the evaluation of ERS RA OPR wave products.

5.3. UWI: The Scatterometer Product

Space-borne scatterometers provide surface vector-wind information over the global oceans on 25-km intervals in polar orbits with swath's between 550 km and 1,800 km wide. A geophysical model function (GMF) is required to convert sets of observed backscatter values into a wind vector. In ERA-40 scatterometer data had been used from the European Remote sensing Satellites ERS-1 and ERS-2. Wind inversion was based on CMOD4 (Stoffelen and Anderson, 1997), where known biases of this GMF were corrected in wind-speed domain (Isaksen and Janssen, 2004). Prior to wind inversion, corrections in backscatter had been applied to counteract on known changes in calibration levels in the product as received from ESA over time. A close examination of the ERS wind product as used in ERA-40 did, however, show significant residual dependencies as function of time and swath position. For this reason a thorough re-calibration was repeated for ERA-interim, while an improved GMF (CMOD5.4) had removed most of the necessity for speed bias correction after wind inversion (Abdalla and Hersbach, 2007). A small difference in calibration between ERS-1 and ERS-2 was observed and absorbed, and suitable corrections allowed for the extension of assimilation of good-quality ERS-1 data from 1 January 2003 (ERA-40) back to 16 April 1992. ERA interim uses data from ERS-2 starting from 22 November 1995 until the end of the mission in July 2011. Due to a major on-board anomaly, data have not been available between 17 January 2001 and 21 August 2003, after which coverage is limited to predominantly the Northern Atlantic.

In contrast to ERA-40, ERA-interim also uses scatterometer data from the NASA QuikSCAT satellite. The same setup is used as in the ECMWF operational suite (Riddaway, 2009), although the start date has been brought forward from 22 January 2001 to 24 February 2000. This is the first date for which the product provides a flag that is essential for quality control on contamination by rain from which QuikSCAT suffers. ERA-interim does not assimilate data from the ASCAT scatterometer on the EUMETSAT Metop-A satellite (available from February 2007). The relevant code, as used in operations, was developed after the definition of the ERA interim suite.

The usage of scatterometer data in ERA interim is summarized in Figure 41. Top and middle panels show the STDV and mean, respectively, of globally-averaged first-guess departures. The bottom panel relates to the number of assimilated wind vectors (see the remark in the caption of Figure 41). Note that due to the regional coverage since August 2003, results from ERS-2 cannot be directly compared to those of QuikSCAT and the pre-2001 global ERS sets. Locally large seasonal oscillations average out considerably over the global sets, but not over the regional ERS-2 set.

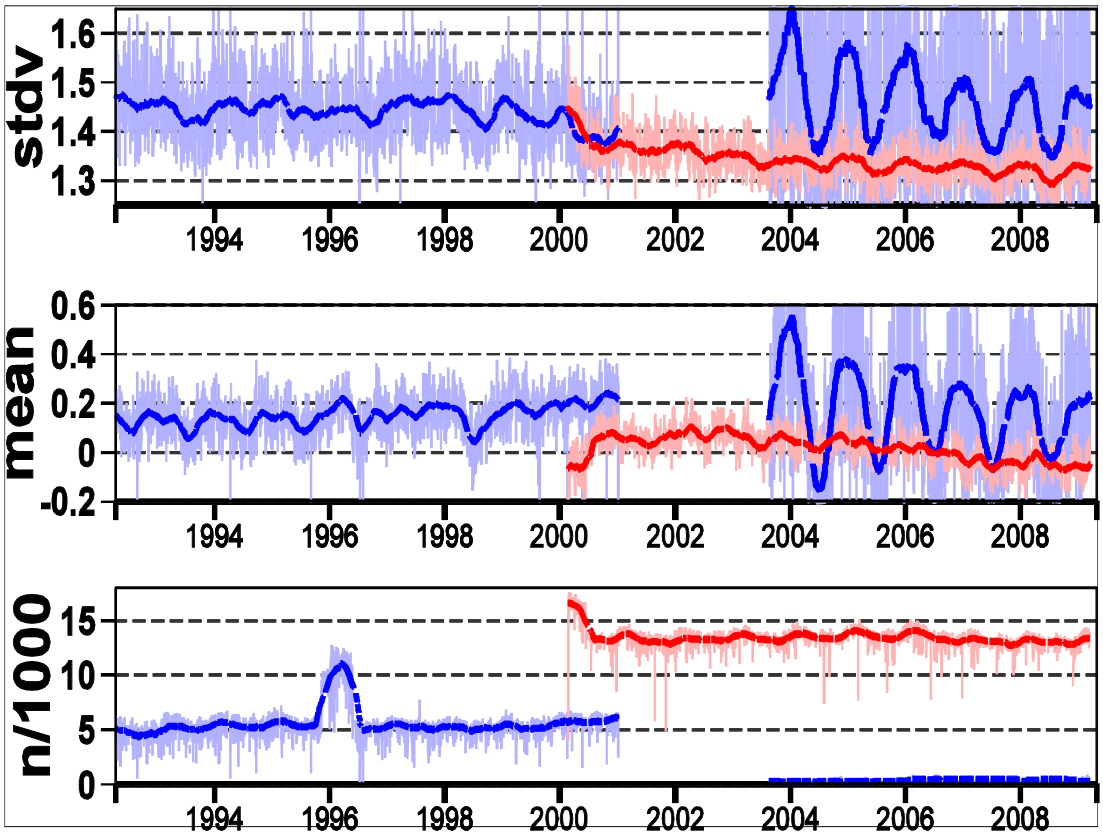

Figure 41: Time series for the STDV (top) and mean (middle) of global-average FG departures in wind speed, and the daily number of used wind vectors (bottom) for ERS-1 and ERS-2 (blue) and for QuikSCAT (red). Dark and light colours represent three-monthly and daily moving averages, respectively. To represent a lower weight in the assimilation system on 50 km non-thinned QuikSCAT cells compared to 100-km thinned 25 km ERS cells (Riddaway, 2009), for QuikSCAT, the number of observations has been divided by four.

Compared to ERA-40, the long-term global average of STDV for first-guess departures has improved considerably from 1.62 m/s (Isaksen and Janssen, 2004) to 1.45 m/s. Statistics for ERS-1, ERS-2 and QuikSCAT overlap well. Around 1999, an initially rapid, but later slower reduction in STDV emerges, which reaches a level of 1.32 m/s near the end of 2008. This remarkable trend indicates an improvement in the quality of the ERA interim surface wind over time.

For the analysis departures (not shown), larger values are found for ERA interim than for ERA-40 (STDV of 1.10 m/s versus 0.97 m/s). In addition, for QuikSCAT a very small trend towards higher STDV emerges, which might be a reflection of the increasing competition with other satellite data in the 4D-Var cost function.

For ERS-1 and ERS-2 the combined departure statistics shows a smooth behaviour. Neither jumps, nor a change around the transition from ERS-1 to ERS-2 (reflected by an increased combined data volume around 1996) is visible. A difference of around 0.15 (0.08) m/s does emerge between first-guess (analysis) departures for ERS and QuikSCAT. A direct collocation study between QuikSCAT and

ERS data during the almost one-year overlap period does confirm a small wind-speed dependent bias between both scatterometers (not shown). Although the mismatch only represents 2% of the global-average wind speed, the issue of inter-calibration between ERS and QuikSCAT should require more attention in a future re-analysis. Also, the small change in behaviour of QuikSCAT near the end of 2000 is to be further investigated.

Between the start of assimilation (April 1992) and 2002, the long-term behaviour of the global average first-guess departure indicates a small decrease in the ERA-interim surface wind speed compared to ERS and QuikSCAT. After 2002, the trend (of around 0.1 m/s) is reversed. This latter trend had previously been observed in the ECMWF operational model, where it was ascribed to changes in model resolution and physics. It now emerges, that it is more likely related to the evolution of the observation system.

5.4. Altimeter OPR Wind Speed Product

Figure 42 shows the time series of the mean difference between the ERS OPR surface wind speed and the corresponding ERA-Interim model analysis values (i.e. bias) in the top panel and the standard deviation of the difference (SDD) between them in the bottom panel. It is clear that in general the altimeter OPR wind product is quite good apart from some of the issues summarised below. On a global scale, the surface wind speed from both ERS-1 and ERS-2 altimeters compared to ERA-Interim was virtually unbiased during most of the ERS mission life when they were operating nominally (i.e. apart from the periods with the issues below). This is quite an interesting result as ERA-Interim does not assimilate altimeter winds. The SDD for both ERS-1 and ERS-2 is about 1.45 m/s. The same value was found from the comparison between the scatterometer UWI product and ERA-Interim values (see Figure 41 and Section 5.3) although the latter comparison uses the model first-guess winds while Fig. 4 uses the model analysis. There is a weak global seasonal cycle in both bias and SDD statistics following the Northern Hemispheric cycle with peaks during November-February.

As reported earlier by Hersbach et al. (2007b) and Abdalla and Hersbach (2007), ERS-1 OPR wind speed suffered abrupt changes coinciding with orbit configuration changes such that Phases C and G, both of 35-day repeat cycles, are with a bias of about +0.2 m/s while other phases, which do not have 35-day repeat cycles, have a bias of about -0.2 m/s. It is most probable that this is due to processing configuration rather than an instrumental issue.

There were two abrupt changes in ERS-2 winds in early 2000 and early 2001 coinciding with the loss of gyros events. However, it seems that the former happened few days before the gyro problem. The large error in ERS-2 winds in January 2001 was due to a processing issue combined with the fact that the platform was piloted in the “Extra Backup Mode (EBM)” without any gyros. The processing issue lasted few days while the EBM piloting extended till the implementation of the “Zero-Gyro Mode (ZGM) in June 2001. There was a slight degradation in the wind speed product after the implementation of the ZGM. After the loss of the global coverage due to the failure of the onboard tape recorders, there is clear seasonal cycle of differences (not shown).

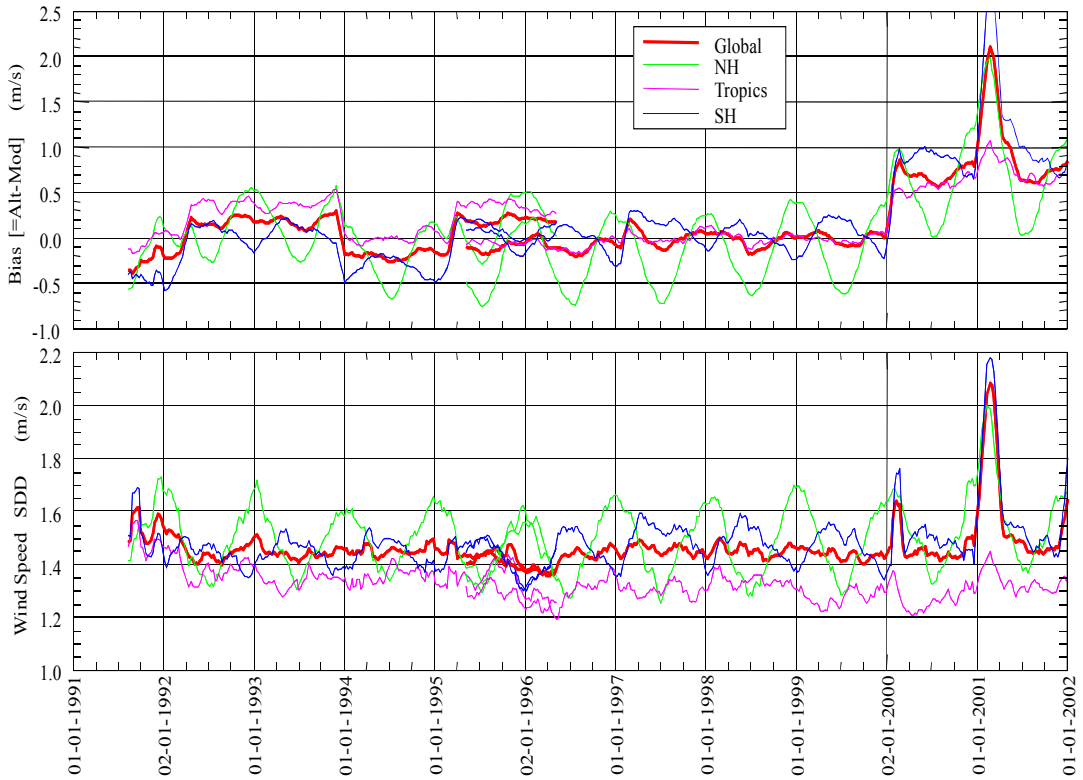

Figure 42: Time series for the bias, defined as bias = satellite – model, (top panel) and the standard deviation of difference, SDD, (bottom panel) between ERS altimeter OPR and ERA-Interim model winds.

5.5. Altimeter OPR SWH Product

Figure 43 shows the time history of the bias (upper panel) and the SDD (lower panel) of the ERS SWH compared to the model hindcast (i.e. without any wave data assimilation) forced by ERA-Interim surface winds. Figure 44 shows the statistics computed from the comparison between ERS products and the wave model run with (bias-corrected) wave data assimilation. It is important to mention that although the altimeter wave height data were corrected to bring them to the level of the wave heights from the buoys, this procedure was not carried out for the altimeter data used in the comparisons shown in Figure 43 and Figure 44.

From both Figure 43 and Figure 44, it is clear that ERS-2 SWH product is on average about 0.30 m higher than the corresponding product from ERS-1, as was reported by Hersbach et al. (2007b) and Abdalla and Hersbach (2007). There is also a clear seasonal cycle in the bias and the SDD statistics for products from both satellites. Those cycles get smaller due to data assimilation. The global bias cycle is in phase with (i.e. dominated by) the Southern-Hemispheric one which has peaks during July-October. On the other hand, the global SDD cycle follows the Northern Hemispheric cycle with peaks during November-February. Normalising with the mean model SWH (not shown) does not totally eliminate those seasonal cycles. Compared to the model, ERS-1 OPR SWH is in general lower by about 0.18 m and 0.35 m compared to the model values without and with data, respectively. The ERS-2 SWH is higher by about 0.12 m compared to the model run without data but lower by about 0.06 m compared to the model with data. It is important to note that during the early days of ERS-1 and the

period after the loss of ERS-2 gyros, the OPR SWH was higher than usual. In case of ERS-1 this may be an indication of a decreasing drift.

For both satellites, the global SWH SDD fluctuated around a mean value of about 0.32 m compared to the hindcast and about 0.28 m compared to the model run with data. However, it seems that the fluctuations in case of ERS-1 have lower amplitude compared to those of ERS-2.

It is quite clear that the SWH product is rather robust. The ERS-1 orbit configuration changes (phases) and the he loss of the ERS-2 gyroscopes had a minor impact on the quality of SWH product

Finally, Figure 45 shows the impact of ERS wave height data assimilation on model results. The error reduction is simply the difference between the SDD from the comparisons against the wave model run without any data and the run with data assimilation normalised by the SDD from the run without data. As can be seen in Figure 45, assimilation of ERS altimeter SWH reduces the model error by about 5-18%. The lower values correspond to periods when wave data were not used; for example the period from late January and early February 2001 data were black listed following the loss of the ERS-2 gyros.

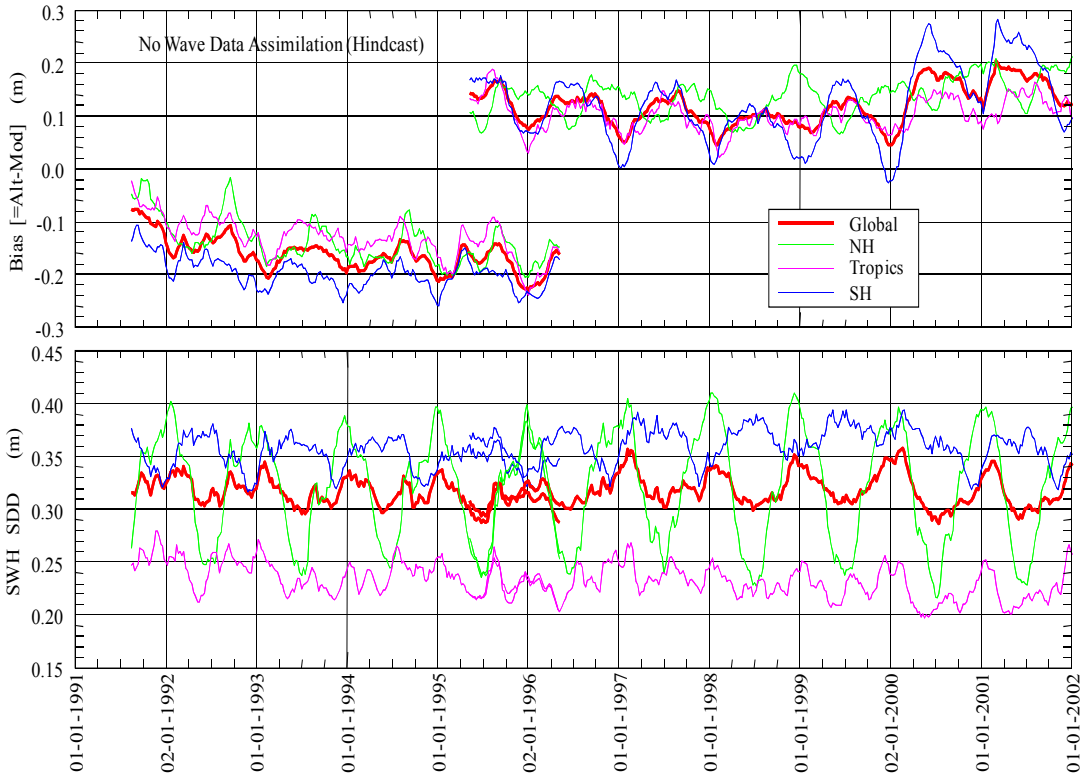

Figure 43: Time series for the SWH bias, defined as: satellite – model, (top panel) and SDD (bottom panel) between ERS altimeter OPR and the model hindcast run (i.e. without wave data assimilation) forced by ERA-Interim winds.

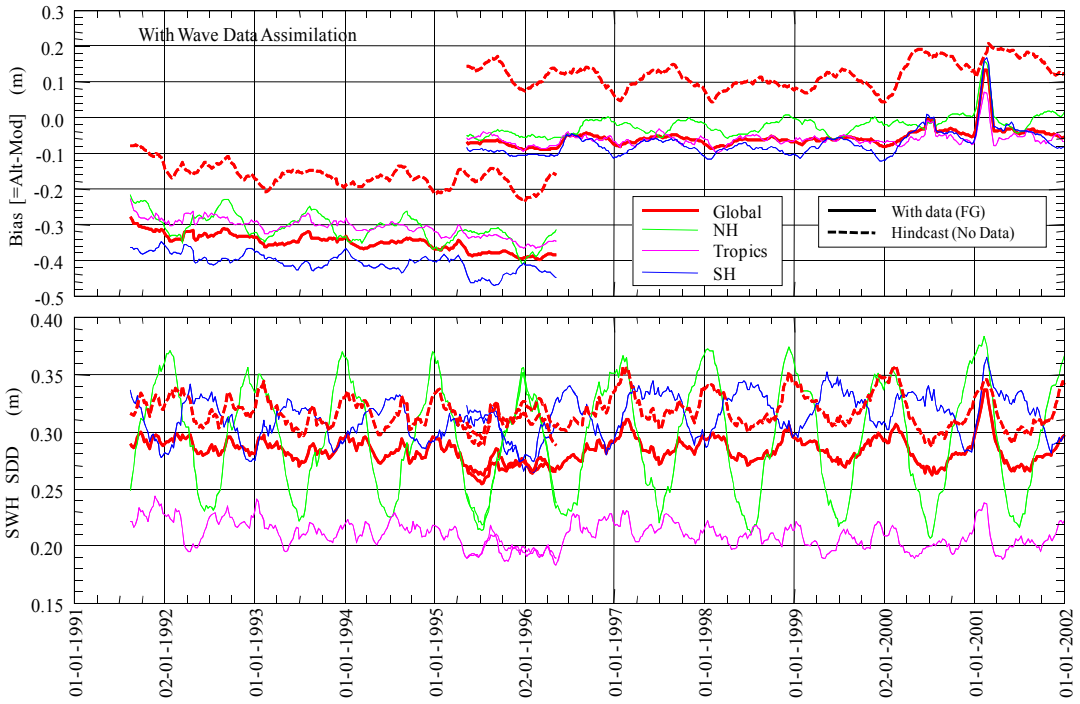

Figure 44: Same as Figure 43 except for the use of first-guess from the model run with wave data assimilation. The global statistics from the hindcast run (i.e. Figure 43) are shown as dashed lines for comparison.

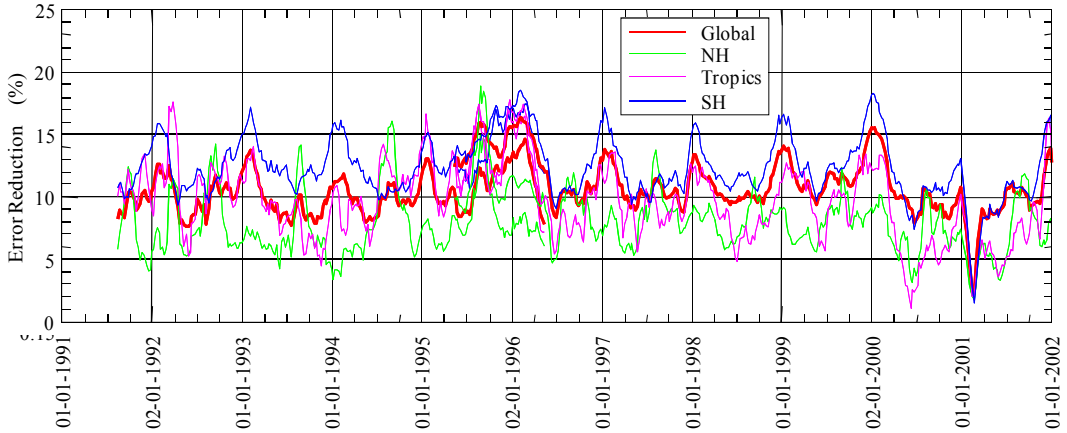

Figure 45: Time series of the error reduction due to ERS OPR wave height data assimilation in wave model.

6. Concluding Remarks

Continuous monitoring and verification of the ERS-2 fast delivery wind and wave products from RA (URA), SAR (UWA) and scatterometer (UWI) have been carried out routinely at ECMWF until the end of the ERS mission. Data from ECMWF atmospheric (IFS) and wave (ECWAM) models and from in-situ buoy observations were used for this purpose.

As a result of the loss of gyros in early 2001, several products were degraded. The main victim was the UWI product, which became of poor quality forcing ESA to halt its dissemination. ESA managed to improve the quality of the UWI product which culminated in the public re-dissemination on 21 August 2003. The quality of the UWI product has been closely monitored at ECMWF since 12 December 2001. On 8 March 2004 ERS-2 scatterometer data were reintroduced at the ECMWF assimilation system. The degradation impact of zero-gyro mode was less pronounced on the URA and UWA products.

Since the failure of the ERS-2 low bit rate (LBR) tape recorders on 22 June 2003, data coverage was restricted within the visibility of ground stations covering the North Atlantic and western coasts of North America. More ground stations were later utilized to extend the coverage to the Southern Ocean, the eastern coasts of China, the north eastern parts of the Indian Ocean and the southern coasts of Africa.

Despite the lack of the global coverage of LBR ERS-2 data, the remaining coverage represented an important area for many applications. Even positive impact on global forecast skill was found in several assimilation experiments (Hersbach, 2004), which led to the re-introduction of the usage of ERS-2 scatterometer data at ECMWF on 8 March 2004. Since then, the validation of the UWI products showed quite stable performance of the instrument until the end of the mission in July 2011.

About 5 years (1998-2003) of ERS-2 scatterometer reprocessed products (ASPS) have been validated and compared to ECMWF operational first-guess winds. It is found that the quality of ASPS wind is good. ASPS winds are stronger by about 0.2-0.35 m/s compared to ECMWF neutral model winds. This is a realistic result since the ECMWF surface winds are known to be biased low. Also ASPS winds have lower direction standard deviation than the UWI ones when compared to ECMWF winds.

The change in orbit which happened in February/March 2011 did not have any impact on the altimeter and scatterometer products. However, there is some degradation in the SAR UWA products.

Long-term evaluation of ERS wind and wave products was carried out for the whole lifetimes of both ERS-1 and ERS-2 missions. Offline altimeter ocean product (OPR) and fast delivery products from SAR (UWA) and scatterometer (UWI) were evaluated against ERA-40 (Abdalla and Hersbach, 2006 and 2007) and against ERA-Interim (Section 5) and the following results were obtained:

OPR SWH products from both satellites are of good quality. ERS-2 SWH product is about 30 cm higher than ERS-1. It seems, however, that ERS-1 SWH product is slightly better than ERS-2 product.

The OPR wind speed product had several problems by time. ERS-1 OPR wind product suffered significant abrupt changes in bias at least 3 times. On the other hand, ERS-2 OPR wind speed product

was rather stable for the first 4.5 years before it started to degrade (especially in the Southern Hemisphere) after the gyro problems started in early 2000. Therefore, one should handle the altimeter wind speed product with care especially for climate studies.

SWH from ERS-1 UWA product is too high with respect to the wave model with at least two significant jumps in bias. The product seems to be degraded during Phase G (after March 1995). On the other hand, ERS-2 UWA product seems to be much better with lower bias and standard difference with respect to the wave model. However, a calibration bug (July 1998-November 2000) and the loss of the gyros (January-June 2001) degraded the product (or its inversion) during most of ERS-2 lifetime.

A re-calibration of the ERS archive from the start until January 2001 on the basis of a collocation with ERA-40 winds suggests that there is a small difference in calibration between ERS-1 and ERS-2 (Abdalla and Hersbach, 2007). Backscatter levels of ERS-1 are around 0.2 dB higher than for ERS-2, which translates to a difference in wind speed of approximately 0.2 m/s.

In general (apart from known issues), the global standard deviation of difference values between ERS products and the corresponding (ERA-Interim) model parameters are: about 1.45 m/s for both scatterometer UWI and altimeter OPR winds and about 0.28 m (0.32 in case of the comparison against the hindcast run) for altimeter OPR wave height. ERS-1 OPR wave heights are about 0.30 m lower than ERS-2.

Assimilation of ERS altimeter OPR wave heights reduces the model error by about 5-18% with an average value of about 12%.

The use of the currently available ERS wind and wave data for climate studies should be done with care due to the various abrupt changes. Therefore, there is a need for a consistent ERS full data set which is being done through several efforts like the ASPS project for the scatterometer (De Chiara, 2010) and the REAPER project (Baker et al., 2010). In general, the re-processing of satellite data would benefit the re-analysis efforts towards the production of a more consistent output. This in turn is needed for re-processing of the data to produce more consistent observation records.

Monthly or cyclic monitoring reports can be found at:

- **URA** (monthly): http://earth.esa.int/pcs/ers/ra/reports/ecmwf
- **UWA** (monthly): http://earth.esa.int/pcs/ers/sar/reports/ecmwf (password protected)
- **UWI** (5-weekly): http://earth.esa.int/pcs/ers/scatt/reports/ecmwf

Acknowledgements

We would like to thank Peter Janssen, Jean-Raymond Bidlot and Raffaele Crapolicchio for support and valuable discussions.

Appendix A: Related Model Changes

Note: All changes were introduced for the 6-hour time-window centred at 18:00 UTC. For further details, use the following link:

http://www.ecmwf.int/products/data/operational_system/evolution/

21 Jun. 1992 Operational implementation of the global model on a 3-degree latitude-longitude grid (63°S to 72°N). The wave spectrum is discretized using 12 directions and 25 frequencies (from 0.041772Hz).

15 Aug. 1993 Assimilation of ERS-1 RA wave heights in global model.

3 Jul. 1994 The global model horizontal resolution was increased to 1.5 degree (from 81°N to 81°S).

19 Sep. 1995 New windsea/swell separation scheme.

30 Jan. 1996 Changes to IFS (e.g. 3DVAR operational).

1 May 1996 Assimilation switch from ERS-1 to ERS-2 RA wave heights.

1 Jun. 1996 Changes to IFS to switch the assimilation of scatterometer winds from ERS-1 to ERS-2.

4 Dec. 1996 The global model horizontal resolution was changed to a 0.5 irregular latitude-longitude grid, with an effective resolution of about 55 km (from 81°N to 81°S). Change the wave-model integration scheme to accommodate Hersbach and Janssen new limiter.

13 May 1997 Modification of the advection scheme by defining the first direction as half the directional bin.

27 Aug. 1997 Changes to IFS (e.g. scatterometer winds are no longer blacklisted for speeds above 20 m/s and modification to the scatterometer bias).

11 Nov. 1997 Changes to IFS (e.g. modification of the scatterometer QC).

25 Nov. 1997 Changes to IFS to implement the 4D-Var assimilation scheme.

1 Apr. 1998 Changes to IFS model (e.g. change horizontal resolution to T319).

28 Jun. 1998 Operational implementation of the coupling between WAM and IFS.

9 Mar. 1999 10 m winds are used in coupled model. IFS changes (e.g. change vertical resolution to 50 levels, and modification of the scatterometer QC).

13 Jul. 1999 RA wave height correction based on non-Gaussianity of the sea surface elevation. Change to the frequency cut-off in the integration scheme. IFS changes (new physics/dynamics coupling).

12 Oct. 1999 Changes to IFS model (e.g. change vertical resolution to 60 levels, and new orography).

11 Apr. 2000 RA data quality control based on peakiness factor. Penalization of low altimeter wave heights in data assimilation. An extra iterative loop to determine the surface stress.

27 Jun. 2000 Sea ice fraction is used for the ice mask. The buoy validation software was upgraded to use the proper anemometer height.

11 Sep. 2000 Assimilation scheme in IFS changed to 12 hour 4D-Var.

20 Nov. 2000 Increase the horizontal resolution of the atmospheric model to T511 (around 40 km). Increase spectral resolution in the global deterministic WAM model to 24 directions and 30 frequencies. Improved advection scheme on irregular grids. New empirical growth curves in the RA data assimilation. Bug fix of the SAR inversion software to properly use SAR data with the new calibration procedure (the bug was effective since June 1998).

11 Jun. 2001 IFS modifications.

21 Jan. 2002 Modified scheme for the time integration of the source terms. Assimilation of QuikSCAT data in IFS model.

8 Apr. 2002 Inclusion of wind gustiness and air density effect. Removal of spurious values for the Charnock parameter. Blacklisting procedure for wave data.

16 Apr. 2002 Extra quality control for QuikSCAT.

13 Jan. 2003 Assimilation of ERS-2 SAR data. Background check for altimeter data during assimilation. Significant changes to IFS model, including a new minimisation scheme and improved background error in the assimilation part.

22 Oct. 2003 Assimilation of ENVISAT Radar Altimeter-2 Ku-Band significant wave heights. ERS-2 RA wave height assimilation was discontinued. (This change was introduced at 6-hour time-window centred at 00:00 UTC.)

8 Mar. 2004 Use of unresolved bathymetry in wave model. Wave model is now driven by neutral 10-metre wind. Re-introduction of ERS-2 scatterometer data based on CMOD5.

28 Jun. 2004 The implementation of the early delivery system.

27 Sep. 2004 Proper treatment of the initialisation of wave fields for time windows 06 and 18 UTC.

5 Oct. 2004 Stop erroneously discarding some ENVISAT altimeter data in wave analysis.

5 Apr. 2005 Use of a revised formulation for ocean wave dissipation due to wave breaking.

1 Feb. 2006 Implementation of the high resolution atmospheric (T799) and wave (0.36°) models. ENVISAT ASAR Level 1b Wave Mode spectra replaced ERS-2 SAR in assimilation. Jason altimeter wave height data are assimilated.

12 Sep. 2006 Revised cloud scheme, including treatment of ice super-saturation and new numerics; implicit computation of convective transports.

5 Jun. 2007 Three outer loops for 4D-Var (T95/159/255).

12 Jun. 2007 Active use of IASI and ASCAT from METOP.

6 Nov. 2007 Atmospheric model changes including a new formulation of convective entrainment and relaxation timescale.

3 Jun. 2008 Atmospheric model changes. Improved advection scheme for wave model. Use of 4 wind solutions for QuikSCAT rather than 2 previously.

1 Oct. 2008 Atmospheric model changes. OSTIA sea surface temperature and sea ice analysis. Conserving interpolation scheme for trajectory fields in 4D-Var.

24 Oct.2008 Use of NCEP SST analysis over Great Lakes, minor fixes to OSTIA SST and sea ice analysis.

10 Mar. 2009 Atmospheric model changes. Revised snow scheme, including diagnostic liquid water storage and a new density formulation. Extend wave model domain from 81°N to 90°N.

8 Sep. 2009 Atmospheric model changes. Non-orographic gravity wave scheme. Wave damping in wind input source term for ocean waves. Routine monitoring of soil moisture observations from Metop-A ASCAT.

30 Sep. 2009 Modification to non-orographic gravity wave drag scheme.

10 Nov. 2009 Change of the altimeter significant wave height bias correction for data assimilation.

26 Jan. 2010 Atmospheric and wave model changes (high horizontal resolution).

22 Mar. 2010 Change of the altimeter significant wave height bias correction for data assimilation following the change of ENVISAT RA-2 processing chain in February 2010.

22 Jun. 2010 Atmospheric model changes. Ensemble Data Assimilation provides initial-time perturbations for EPS. GRIB API library used to process GRIB data.

9 Nov. 2010 Atmospheric model changes. Adaptation to neutral wind of the observation operator for scatterometer data. Five species prognostic microphysics scheme, including cloud rain water content and cloud ice water content as new model variables. Retuning of subgrid-scale orographic gravity wave drag. Adjustment to diffusion in stable boundary layers near surface.

15 Feb. 2011 Use NCEP sea ice over Caspian and Sea of Azov.

18 May 2011 Atmospheric model changes. GRIB2 model level data. Background error variances from EDA used by deterministic 4D-Var.

References

Abdalla S. and Hersbach H. (2004). The technical support for global validation of ERS Wind and Wave Products at ECMWF, *Final report for ESA contract* 15988/02/I-LG, ECMWF, Shinfield Park, Reading.
http://www.ecmwf.int/publications/library/ecpublications/_pdf/esa/ESA_abdalla_hersbach.pdf

Abdalla S. and Hersbach H. (2006). The technical support for global validation of ERS Wind and Wave Products at ECMWF (April 2004 - June 2006), *Final report for ESA contract* 18212/04/I-LG, ECMWF, Shinfield Park, Reading.
http://www.ecmwf.int/publications/library/ecpublications/_pdf/esa/ESA_abdalla_hersbach_18212.pdf

Abdalla S. and Hersbach H. (2007). The technical support for global validation of ERS Wind and Wave Products at ECMWF (April 2004 - June 2007), *Final report for ESA contract* 18212/04/I-OL, ECMWF, Shinfield Park, Reading.
http://www.ecmwf.int/publications/library/ecpublications/_pdf/esa/ESA_abdalla_hersbach_18212-2007.pdf

Abdalla S. and Hersbach H. (2008). The technical support for global validation of ERS Wind and Wave Products at ECMWF (July 2007 - June 2008), *Final report for ESA contract* 20901/07/I-EC, ECMWF, Shinfield Park, Reading.
http://www.ecmwf.int/publications/library/ecpublications/_pdf/esa/ESA_abdalla_hersbach_20901-2008.pdf

Attema, E.,P.,W. (1986). An experimental campaign for the determination of the radar signature of the ocean at C-band, *Proc. Third International Colloquium on Spectral Signatures of Objects in Remote Sensing*, Les Arcs, France, ESA, SP-247, 791-799, 1986.

Baker, S., Massmann, F.-H., Otten, M., Roca, M., Scharroo, R., Soussi, B. and Visser, P. (2010). Reprocessing of Altimeter Products for ERS: The Reaper Project. *Proc. "ESA Living Planet Symposium 2010"*, Bergen, Norway, 28 June – 2 July 2010.

Berrisford, P., D. Dee, K. Fielding, M. Fuentes, P. Kallberg, S. Kobayashi and S. Uppala (2009). The ERA-Interim archive. *ERA Report Series* No. 1, ECMWF, Reading, UK. Available from:
http://www.ecmwf.int/publications/

Bidlot, J. R., D.J. Holmes, P.A. Wittmann, R. Lalbeharry, H.. Chen (2002). Intercomparison of the performance of operational ocean wave forecasting systems with buoy data. *Wea. Forecasting*, **17**, 287-310.

Bidlot, J.R., Janssen, P.A.E.M., Abdalla, S. (2007). A revised formulation of ocean wave dissipation and its model impact. *ECMWF Technical Memorandum* 509, Available from:
http://www.ecmwf.int/publications/

Brown, A.R., Beljaars, A.C.M., Hersbach, H., Hollingsworth, A., Miller, M., Vasiljevic, D.(2005). Wind turning across the marine atmospheric boundary layer. *Quart. J. Roy. Meteor. Soc*. **607**, 233-1250.

Crapolicchio, R., Lecomte, P., Neyt, X., (2004). The Advanced Scatterometer Processing System for ERS data: design, products and performance. *Proceedings of the ENVISAT and ERS Symposium*, Salzburg, Austria, 6-10 September 2004.

Crapolicchio, R., De Chiara, G., Elyouncha, A., Lecomte, P., Neyt, X., Paciucci, A., and Talone, M. (2012). ERS-2 Scatterometer: Mission Performances and Current Reprocessing Achievements Accepted IEEE Transactions on Geoscience and Remote Sensing - Recent Advances in C-Band Scatterometery Special Issue (*In press*).

De Chiara, G., Crapolicchio, R., and Lecomte, P. (2010). The ERS-2 scatterometer Mission: Instrument Performances, Data Quality Control and Reprocessing Status, *Procedings of the ESA Living Planet Symposium*, Bergen, Norway, 28 June-2 July 2010.

Dee, D.P., S. M. Uppala, A. J. Simmons, P. Berrisford, P. Poli, S. Kobayashi, U. Andrae, M. A. Balmaseda, G. Balsamo, P. Bauer, P. Bechtold, A. C. M. Beljaars, L. van de Berg, J. Bidlot, N. Bormann, C. Delsol, R. Dragani, M. Fuentes, A. J. Geer, L. Haimberger, S. Healy, H. Hersbach, E. V. Hólm, L. Isaksen, P. Kållberg, M. Köhler, M. Matricardi, A. P. McNally, B. M. Monge-Sanz, J.-J. Morcrette, B.K. Park, C. Peubey, P. de Rosnay, C. Tavolato, J.-N. Thépaut, F. Vitart, (2011). The ERA-Interim reanalysis: Configuration and performance of the data assimilation system, *Quart. J. Roy. Meteor. Soc*. **137**, 553-597.

ESA (2005). ERS-1 Mission Phases (from 1991 onwards). An Internet web page accessible from: http://earth.esa.int/rootcollection/eeo/ERS1.1.7.html

Féménias P., and Martini A. (2000). ERS-2 AOCS mono-gyro attitude software Qualification Period - Radar Altimeter Data Analysis. *ESA-ESRIN Technical Note*, accessible from: http://earth.esa.int/pcs/ers/ra/events/monogyro/

Hersbach, H. (2003). CMOD5. An improved geophysical model function. *ECMWF Technical memorandum* 395, Available from: http://www.ecmwf.int/publications/

Hersbach, H. (2008). CMOD5.N: A C-band geophysical model function for equivalent wind, ECMWF Technical Memorandum 554, UK. Available from: http://www.ecmwf.int/publications/

Hersbach, H., (2010). Assimilation of scatterometer data as equivalent-neutral wind, ECMWF Technical Memorandum 629. Available from: http://www.ecmwf.int/publications/

Hersbach, H., Janssen P.A.E.M., Isaksen, L. (2004). Re-introduction of ERS-2 scatterometer data in the operational ECMWF assimilation system. *Proceedings of the ENVISAT and ERS Symposum*, Salzburg, Austria, 6-10 September 2004.

Hersbach, H., Stoffelen A., and Haan de S., (2007). An improved C-band scatterometer ocean geophysical model function: CMOD5, *J. Geophys. Res*., **112** (C3) C03006.

Hersbach, H., Abdalla, S. and Bidlot, J.-R., (2007b). Long Term Assessment of ERS-1 and ERS-2 Wind and Wave Products. *Proc. "Envisat Symposium 2007"*, Montreux, Switzerland, 23–27 April 2007 (ESA SP-636, July 2007), Paper 463341.

Hersbach, H. and Janssen, P. (2007). Preparation for assimilation of surface-wind data from ASCAT at ECMWF. *ECMWF Research Department Memorandum* R60.9/HH/0750. Available from ECMWF on request.

Isaksen, L., and Janssen P.A.E.M. (2004). The benefit of ERS scatterometer Winds in ECMWF's variational assimilation system. *Q. J. R. Meteorol. Soc*. **130** 1793-1814.

Janssen, P.A.E.M. (2004). *The interaction of ocean waves and wind*. Cambridge Univ. Press, 300p.

Janssen, P.A.E.M., Hansen, B. and Bidlot J.R. (1997). Verification of the ECMWF wave forecasting system against buoy and altimeter data, *Wea. Forecasting*, **12**, 763-784.

Janssen, P., Bidlot, J.R., Abdalla, S., Hersbach H. (2005). Progress in Ocean Wave Forecasting at ECMWF. ECMWF Technical Memorandum 478. Available from: http://www.ecmwf.int/publications/

Portabella M., and Stoffelen A., (2007). Development of a global scatterometer Validation and Monitoring, to appear at: http://www.knmi.nl/publications/

Riddaway, B. (*Ed.*), (2009). Integrated Forecasting System (IFS) Documentation. ECMWF, Reading, UK. Available from: http://www.ecmwf.int/research/ifsdocs/

Simmons A., Uppala S., Dee D., and Kobayashi S., (2007). ERA-Interim: New ECMWF reanalysis products from 1989 onwards, *ECMWF Newsletter*, 110, 25-35.

Stoffelen, A.C.M., and Anderson D.L.T. (1997). Scatterometer Data Interpretation: Derivation of the Transfer Function CMOD4*, J. Geophys. Res*., **102** (C3) 5,767-5,780.

Uppala, S.M., Kållberg, P.W., Simmons, A.J., Andrae, U., Da Costa Bechtold, V., Fiorino, M., Gibson, J.K., Haseler, J., Hernandez, A., Kelly, G.A., Li, X., Onogi, K., Saarinen, S., Sokka, N., Allan, R.P., Andersson, E., Arpe, K., Balmaseda, M.A., Beljaars, A.C.M., Van De Berg, L., Bidlot, J., Bormann, N., Caires, S., Chevallier, F., Dethof, A., Dragosavac, M., Fisher, M., Fuentes, M., Hagemann, S.; H\'olm, E., Hoskins, B.J., Isaksen, L., Janssen, P.A.E.M., Jenne, R., McNally, A.P., Mahfouf, J.F., Morcrette, J.J., Rayner, N.A., Saunders, R.W., Simon, P., Sterl, A., Trenberth, K.E., Untch, A., Vasiljevic, D., Viterbo, P., Woollen, J. (2005). The ERA-40 re-analysis *Quart. J. Roy. Meteor. Soc*. **131**, 2961-3012.